UNIVERSITY OF GENOA

PHD PROGRAM IN BIOENGINEERING AND ROBOTICS

Bound by the past: Serial dependence in multisensory perception across domains and modalities

Jessica Bertolasi

Doctoral School in Bioengineering and Robotics (XXXVIII cycle)

Thesis submitted for the degree of *Doctor of Philosophy*

June 2026

Monica Gori	Supervisor
Davide Esposito	Co-supervisor
Paolo Massobrio	Head of the PhD program

Thesis Jury:

Mauro Manassi, *University of Aberdeen*	External examiner
Eli Brenner, *Vrije Universiteit*	External examiner

Dibris

Department of Informatics, Bioengineering, Robotics and Systems Engineering

Bound by the past: Serial dependence in multisensory perception across domains and modalities

Jessica Bertolasi

DIBRIS
University of Genoa

This dissertation is submitted for the degree of

Doctor of Philosophy

June 2026

Life is not easy for any of us. But what of that? We must have perseverance and above all confidence in ourselves. We must believe that we are gifted for something and that this thing must be attained.

Marie Salomea Skłodowska-Curie

Declaration

I hereby declare that except where specific reference is made to the work of others, the contents of this dissertation are original and have not been submitted in whole or in part for consideration for any other degree or qualification in this, or any other university. This dissertation is my own work and contains nothing which is the outcome of work done in collaboration with others, except as specified in the text and Acknowledgements. This dissertation contains fewer than 65,000 words including appendices, bibliography, footnotes, tables and equations and has fewer than 150 figures.

Jessica Bertolasi

June 2026

Acknowledgment

This PhD journey has been long and exhausting, filled with challenges, unexpected turns, and countless moments of doubt. Yet, despite everything, I have finally reached the end.

First, I would like to express my gratitude to my principal investigator, Dr. Monica Gori, for her supervising role throughout my doctoral journey. I am also sincerely thankful to Dr. Davide Esposito for his constant support, insightful discussions, and patience throughout the many stages of this work. I would also like to extend my thanks to Professor Nadia Vanessa Garcia Hernandez for accompanying me in an extraordinary transoceanic collaboration and for her valuable advice, as well as for the constant support she has always shown me. I finally want to thank Professor David Pascucci for giving me the opportunity to spend a research period abroad in his laboratory in Switzerland, and for generously mentoring and teaching me both during my time in his lab and continuing to provide invaluable and stimulating discussions.

A heartfelt thank you goes to all my colleagues in the UVIP lab for creating such a crazy, collaborative, and dynamic research environment. To my dearest colleagues, affectionately known as the *bulle* – Marta, Stefania, Gloria, and Anna – thank you for your unwavering friendship, laughter, and shared strength: you made even the hardest days lighter and the joyful ones unforgettable.

Scientific Production

Journal papers

- Amadeo, M.B., Escelsior, A., Esposito, D., Inuggi, A., Versaggi, S., Marenco, G., Massalha, Y., Bertolasi, J., Pereira da Silva, B., Amore, M., Serafini, G., Gori, M. (2024). Multisensory temporal processing in schizophrenia and bipolar disorder: implications for psychosis. Schizophrenia, 10, 98. https://doi.org/10.1038/s41537-024-00502-z
- Bertolasi, J., Esposito, D., Vitale, A., Gori, M. (2025). Exploring the role of serial dependence in visual time perception. Journal of Vision, 25(8):7. https://doi.org/10.1167/jov.25.8.7
- Bertolasi, J.†, Garcia-Hernandez, N.V.†, Memeo, M., Guarischi, M., Gori, M. (2025). Evaluation of HoloLens 2 for Hand Tracking and Kinematic Features Assessment. Virtual Worlds, 4(3), 31. https://doi.org/10.3390/virtualworlds4030031
- Esposito, D.†, Bertolasi, J.†, Escelsior, A., Amedeo, M.B., Inuggi, A., Perucco, M., Alvano, A., Marcenaro, M., Zizzi, A., Pereira Da Silva, B., Serafini, G., Amore, M., Gori, M. (2026). Differentiating Bipolar Disorder From Schizophrenia: The Role Of The Induced Roelofs Illusion. i-Perception, 17(2), 1–22. https://doi.org/10.1177/20416695251394612
- Gori, M.†, Amadeo, M.B.†, Sturlese, M., Riberto, M., Vitale, A., Bertolasi, J., Tovar, D.A., Lewkowicz, D.J., Murray, M.M., Wallace, M.T., Vitali, H. (2026). The role of movement on the development of the audiotactile temporal binding window. Developmental Science29, no. 3: e70191. https://doi.org/10.1111/desc.70191

- Bertolasi, J., Esposito, D., Domenici, N., Gori, M. (2026). Serial dependence in auditory temporal perception is influenced by temporal proximity but not stimulus type. Acta Psychologica, 266, 106997. https://doi.org/10.1016/j.actpsy.2026.106997

- Lotto, C., Bertolasi, J., Bernardocchi, A., Javier Fernandez, I., Anschuetz, L., Molinari, G. Intraoperative and postoperative management in endoscopic ear surgery: perspectives from a worldwide survey. *Under review*
- Domenici, N., Tonelli, A., Bertolasi, J., Ponente, C., Gori, M. Saccadic compression of time and space in developmental dyslexia. *Under review*

Conference papers

- Bertolasi, J., Garcia-Hernandez, N.V., Gori, M. Assessing Human Size Perception in Real and Mixed-Reality Environments, 2025 IEEE Medical Measurements & Applications (MeMeA), Chania, Greece, 2025, pp. 1-5, doi: 10.1109/MeMeA65319.2025.11066289
- Vitale, A.†, Bertolasi, J.†, Orciari, L., Lorini, C., Parmiggiani, A., Murray, M. M., Wallace, M.T., Gori, M. TaK: a Tactile Knob to Investigate Orientation Perception, 2025 IEEE Medical Measurements & Applications (MeMeA), Chania, Greece, 2025, pp. 1-6, doi: 10.1109/MeMeA65319.2025.11068010
- Bertolasi, J., Garcia-Hernandez, N.V., Caroglio, E., Petri, S., Gori, M. Isolating haptic feedback from visual feedback using mixed reality technology: a case study on serial dependence experiment, 2025 IEEE International Symposium on Mixed and Augmented Reality (ISMAR), Daejeon, Korea (South), 2025, pp. 779-780, doi: 10.1109/ISMAR-Adjunct68609.2025.00186
- Vitale, A., Bertolasi, J., Esposito, D., Parmiggiani, A., Gori, M. Just noticeable difference in motion direction perception: assessing the effect of blindness onset and orientation, 15th International Conference on Human Haptic Sensing and Touch Enabled Computer Applications (EuroHaptics), Siena, Italy, 2026. *Accepted*

Posters

- Bertolasi J.†, Vitale A.†, Esposito D., Gori M. (2023). Investigating serial dependence in visual time perception. 21st International Multisensory Research Forum

- Bertolasi J., Esposito D., Vitale A., Burr D.C., Gori M. (2024). Temporal Continuity in Visual Perception: Exploring Serial Dependence in Time Perception and its Relationship with Working Memory Capacity. 31st European Conference on Visual Perception
- Bertolasi J., Garcia-Hernandez N.V., Gori M. (2025). Assessing Human Size Perception in Real and Mixed-Reality Environments. 20th edition of the IEEE International Workshop on Medical Measurements and Applications
- Vitale A.†, Bertolasi J.†, Orciari L., Lorini C., Parmiggiani A., Murray M.M., Wallace M., Gori M. (2025). TaK: a Tactile Knob to Investigate Orientation Perception. 20th edition of the IEEE International Workshop on Medical Measurements and Applications
- Bertolasi J., Garcia-Hernandez N.V., Caroglio E., Petri S., Gori M. (2025). Isolating haptic feedback from visual feedback using mixed reality technology: a case study on serial dependence experiment. 24th IEEE International Symposium on Mixed and Augmented Reality

† Authors contributed equally to this work.

Dataset

- Esposito D., Bertolasi J. (2024). Dataset and analysis code for the Roelofs test on psychiatric population. OSF 10.17605/OSF.IO/NH5XD
- Bertolasi J. (2024). Dataset for Exploring the Role of Serial Dependence in Visual Time Perception. OSF 10.17605/OSF.IO/ETRU3
- Bertolasi J. (2025). Dataset for Serial Dependence in Auditory Temporal Perception: The Role of ISI and the Nature of the Stimuli. OSF 10.17605/OSF.IO/RUJ84
- Bertolasi J. (2025). Supplementary materials and dataset for the experiment of Isolating haptic feedback from visual feedback via HoloLens 2. OSF 10.17605/OSF.IO/7XJ26
- Bertolasi J. (2025). Dataset for Evaluation of HoloLens 2 for Hand Tracking and Kinematic Features Assessment. OSF 10.17605/OSF.IO/6YZQJ
- Bertolasi J. (2025). Dataset for just noticeable difference in motion direction perception. OSF https://doi.org/10.17605/OSF.IO/CBHJ2
- Bertolasi J. (2026). Dataset for Serial dependence in touch: results on tactile motion direction perception in sighted and visually impaired populations. *Private project*

– Bertolasi J., Esposito D., Domenici N. (2026). Preliminary dataset for the study of cross-sensory visuo-haptic serial dependence, currently in the data collection and consolidation phase. *Private project*

Abstract

Serial dependence refers to the tendency of perceptual judgments to be systematically biased toward or away from recently encountered stimuli. This mechanism is believed to promote perceptual stability in a dynamic and often noisy environment. Over the past decade, serial dependence has become a central topic in perceptual neuroscience, with extensive evidence demonstrating its influence on a wide range of visual features, from low-level attributes such as orientation and position to higher-level judgments such as attractiveness. However, comparatively little is known about how serial dependence operates in temporal perception and across sensory modalities.

The primary objective of this doctoral project was to investigate whether serial dependence extends to the perception of temporal duration in vision and audition, to examine its manifestation in tactile perception, and to assess the role of visual experience in shaping multisensory serial dependence. In particular, this work aimed to determine whether serial dependence reflects a general computational principle of perception or whether it is modulated by modality-specific constraints and sensory history.

To address these questions, a series of psychophysical experiments was conducted using discrimination and reproduction paradigms. Serial dependence was examined in visual and auditory temporal perception, as well as in tactile motion perception. To investigate the contribution of visual experience, experiments were performed both in sighted participants and in individuals with visual impairment. In addition, mixed reality technology was adopted

to enable precise experimental control and to isolate visual contributions in visuo-haptic tasks, allowing the study of serial dependence in controlled multisensory environments.

The results provide converging evidence that serial dependence extends beyond classical visual features to temporal perception in both vision and audition, although its expression depends on temporal context and task demands. In auditory temporal perception, serial dependence emerged under specific temporal conditions, suggesting a dependence on the temporal proximity of successive stimuli. In the tactile domain, serial dependence effects were more selective and appeared to depend on visual experience, as they were absent in visually impaired participants. Multisensory experiments further indicated that vision plays a critical role in shaping serial dependence in haptic judgments, highlighting the importance of cross-modal calibration processes.

Overall, these findings suggest that serial dependence is a flexible perceptual mechanism whose expression varies across sensory modalities and depends on both stimulus characteristics and sensory experience. By demonstrating modality-specific constraints and a critical role of visual experience in multisensory serial dependence, the findings provide new insights into the computational principles underlying perceptual stability.

Additionally, these results have direct implications for the design of human-robot interaction systems, multisensory interfaces, and rehabilitation technologies, where adaptive integration of sensory information over time is essential. Moreover, the experimental paradigms and mixed-reality methodologies developed in this project offer robust tools for studying perception in controlled multisensory environments, with potential applications in device calibration, sensory substitution, and computational models of human perception.

Table of Contents

List of Figures

List of Tables

List of Acronyms

2AFC	Two-Alternative Forced Choice
AIC	Akaike Information Criterion
ANOVA	Analysis of Variance
BF	Bayes Factor
CI	Confidence Interval
CSV	Comma-Separated Value
DF	Degree of Freedom
DIP	Distal Interphalangeal
DoG	Derivative of Gaussian
EEG	Electroencephalography
HMD	Head-Mounted Display
HL2	HoloLens 2
ICP	Iterative Closest Point
IMU	Inertial Measurement Unit
IQR	Interquartile Range
ISI	Inter-Stimulus Interval
JND	Just Noticeable Difference
LMEM	Linear Mixed-Effects Model
MAD	Median Absolute Deviation
MCP	Metacarpophalangeal
MEG	Magnetoencephalography

MRTK	Mixed Reality Toolkit
MR	Mixed Reality
NLMEM	Non-Linear Mixed-Effects Model
PIP	Proximal Interphalangeal
PSE	Point of Subjective Equality
RMSE	Root Mean Square Error
RoMAT	Robot for Multisensory Analysis and Testing
RGB	Red, Green, Blue
SD	Standard Deviation
SE	Standard Error
TAE	Tilt After-Effect
TaK	Tactile Knob
VIF	Variance Inflation Factor
VM	Vicon Motion Capture System

Chapter 1

The Concept of Serial Dependence

In our daily lives, we perceive events as continuous. For instance, when we see a car next to us on the street, we perceive it as the same car we saw moments earlier, regardless of our movement or any temporary obstructions. Despite changes in the scene, our perception of it remains stable. The phenomenon of how past experiences shape our perception of the present has been studied in various forms for centuries. However, the term "serial dependence" was introduced about a decade ago to describe the bias in perceiving a current stimulus in relation to previously encountered stimuli. In other words, the perception of the present moment can be influenced by recent experiences, leading to a sense of temporal continuity in subjective experience. While serial dependence has been extensively studied in visual perception, its relationship with time, other sensory modalities, and multimodal interactions remains largely unexplored. The limited number of studies addressing these aspects often do so in a fragmented or preliminary way, leaving significant gaps in our understanding of how perceptual continuity operates across different cross-sensory and temporal dimensions.

The research presented in this dissertation has the primary objective of further investigating serial dependence across different perceptual modalities and, additionally, to propose a novel technological methodology for studying perceptual phenomena. This chapter will provide an

overview of the research by outlining its theoretical background and its specific aims and scope.

1.1 Theoretical background

1.1.1 How does the brain maintain temporal coherence in what it sees?

A fundamental challenge in perceptual neuroscience is to understand how the brain maintains a coherent and stable representation of the world despite constant changes in sensory input. Our sensory information is often limited and ambiguous: for example, when observing a small bird hanging on a branch while walking, it may temporarily become occluded by leaves from another branch or appear from a slightly different perspective due to our movement. Since the surrounding environment exhibits a certain degree of temporal stability, one way to reduce sensory ambiguity is by integrating information from the recent past (Trapp et al., 2021). The temporal regularity of the external world makes recent events a valuable source of plausible hypotheses about the current state of reality, which can help guide perceptual interpretation in the present moment. To achieve this, it has been proposed that the brain engages in an inferential process, combining sensory input with internal expectations and predictions about perceived stimuli (Clark, 2013). This integration transforms raw sensory data into the rich and stable percepts that characterize conscious experience.

Psychophysical studies on the perception of ambiguous stimuli have shown that human perceptual interpretation is strongly influenced by immediately preceding experience (Fecteau & Munoz, 2003). This influence of experience operates through two main mechanisms, which act in opposite yet complementary ways: hysteresis and adaptation.

The term hysteresis refers to the phenomenon whereby perception tends to preserve a previous interpretation of a stimulus, even when changes in the sensory signal would make an alternative interpretation plausible. This phenomenon manifests as a persistence effect, in which a stimulus is perceived as more similar to the previously experienced percept than it actually is. Such perceptual inertia has been observed in various domains, including binocular

rivalry (Buckthought et al., 2008), apparent motion (Hock et al., 1993), and emotion recognition (Sacharin et al., 2012), and appears to serve a functional purpose – namely, to ensure perceptual stability and coherence within an inherently noisy and dynamic sensory environment.

In contrast, the phenomenon of adaptation represents an opposite process: prolonged exposure to a particular feature of a stimulus (such as motion direction) produces a repulsive effect, whereby a subsequent stimulus appears oriented in the opposite direction, as illustrated by the classic waterfall illusion (Purkinje, 1820). This process, attributed to neural habituation mechanisms (Anstis et al., 1998), serves the functional role of enhancing sensitivity to novel information, thus promoting change detection rather than stability.

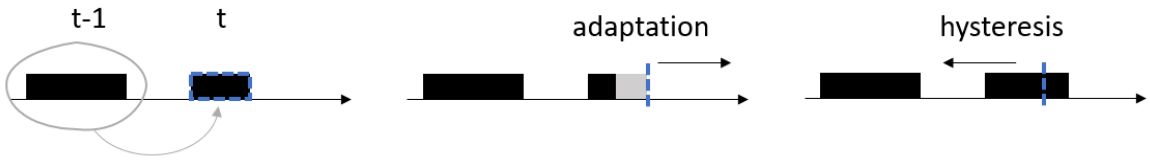

Figure 1.1 – Illustration of how past information (t-1) interacts with present input (t). In adaptation, previous experience induces a repulsive effect on current perception, whereas in hysteresis, it exerts an attractive influence, stabilizing the ongoing percept.

The two dynamics thus reflect complementary perceptual strategies: hysteresis acts to preserve perceptual coherence, while adaptation enhances the ability to detect variations and novel features in the stimulus. The predominance of one perceptual strategy over another is not fixed but depends on a combination of interacting factors. For instance, under conditions of uncertainty (particularly when the current stimulus is unreliable or noisy), the visual system tends to rely more heavily on information from the recent past, implicitly biasing perception toward previous experience (Ceylan et al., 2021; Cicchini et al., 2018; Manassi et al., 2018; Pascucci et al., 2019).

A central role is played by perceptual experience and learning history: both long-term exposure and adaptation to specific tasks influence the weight assigned to particular sensory cues (Jasmin et al., 2021). Task demands and environmental characteristics also modulate strategic selection, sometimes favoring stability grounded in past experience and, at other times, sensitivity to novelty (Cicchini et al., 2021; P. R. Jones & Dekker, 2018). Confidence in one's decisions and the type of feedback received further contribute to the updating of perceptual strategies, especially under conditions of uncertainty (Balsdon et al., 2020;

Domenici & Mamassian, 2025; Lak et al., 2020). Finally, individual differences, attentional resources, and cognitive predispositions shape how each person selects and maintains a particular strategy (Quinton & Fellows, 1975). The interplay of these factors makes perception a flexible and adaptive process, able to respond to diverse demands and dynamically changing contexts.

More recent studies have shown that the influence of preceding stimuli extends beyond merely facilitating or accelerating the perceptual processing of subsequent ones. In some cases, recent experience can systematically bias current perceptual responses, leading to deviations from the objective properties of the present stimulus. This phenomenon, known as serial dependence, represents a pivotal development in the study of the temporal integration mechanisms underlying perception and will be examined in greater detail in the following paragraphs.

1.1.2 The concept of serial dependence

Serial dependence is a term introduced to study quantitatively the effects of temporal contextual information on perception: it is a systematic behavioral bias in which current perceptual judgments are influenced by stimuli encountered in the recent past.

First formally described by Fischer and Whitney (J. Fischer & Whitney, 2014), serial dependence manifests as an *attractive bias*, whereby the perception of a stimulus is pulled toward previously seen stimuli (see Figure 1.2). This mechanism is thought to enhance perceptual stability by smoothing noisy input across time (Pascucci et al., 2023). Serial dependence is often discussed in relation to sensory adaptation and perceptual hysteresis, and the distinction between these phenomena remains a matter of debate. It's been argued that, unlike adaptation, serial dependence usually manifests as an attractive bias toward recently encountered stimuli, and unlike hysteresis, it does not primarily reflect a persistence of discrete perceptual states but rather a continuous integration of past and present sensory information. As such, serial dependence is thought to have a stabilizing role in perception, promoting continuity in perceptual experience by smoothing moment-to-moment variability in noisy sensory signals, rather than recalibrating sensitivity or maintaining categorical perceptual states.

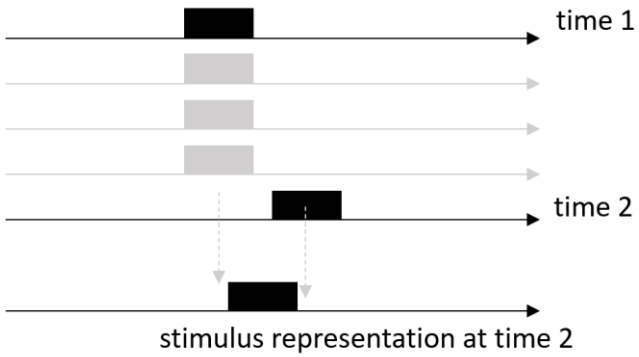

Figure 1.2 – Visual representation of serial dependence effect propagation across time. Visual object representations can carry over across time, biasing perception toward the recent past and producing systematic errors in perceptual decisions.

Serial dependence was initially observed in an orientation reproduction task (J. Fischer & Whitney, 2014) in which participants were asked to view a Gabor stimulus – a pattern of light and dark lines blurred at the center and fading at the edges, commonly used to study orientation perception (Figure 1.3 panel A) – and then reproduce its orientation by adjusting a response bar. It was found that, although participants' responses were on average correctly centered on the presented orientations across the experiment, trial-by-trial responses were systematically biased toward the orientation of the preceding trial. In other words, when the Gabor in the previous trial was oriented more clockwise than the current Gabor, participants perceived the current Gabor as tilted more clockwise than its actual orientation.

A simple way to represent this effect is to plot the relative orientation of the previous trial against the error on the current trial (Figure 1.3 panel B). The effect is well captured by a first derivative-of-Gaussian (DoG) function, given by:

$$y = xawce^{-(xw)^2} \tag{1.1}$$

where x is the relative orientation of the previous trial, a is the amplitude of the curve peaks (which quantify the magnitude of the serial dependence effect), w is the curve width and c is the normalized constant $c = \sqrt{2}/e^{-0.5}$.

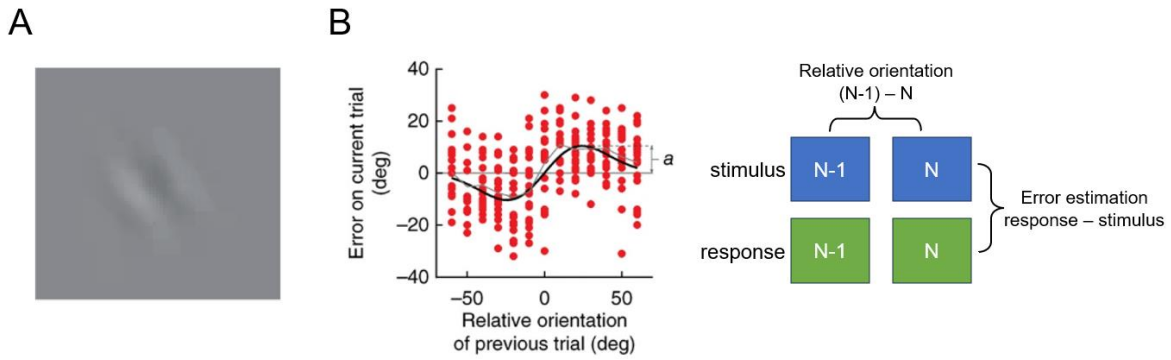

Figure 1.3 – Serial dependence effect disclosed in Fischer & Whitney's (J. Fischer & Whitney, 2014) work. (A) The stimulus used in the experiment was a Gabor patch with an orientation varying between -60° and +60°, which participants were then asked to reproduce using a response bar. In orientation reproduction experiments, the Gabor patch is the most commonly used stimulus. (B) The error plot shows representative data from a single participant and clearly exhibits a derivative-of-Gaussian pattern, where the amplitude (*a*) reflects the magnitude of the serial dependence effect. On the x-axis, the relative orientation is plotted, defined as the difference in orientation between the previous stimulus (N–1) and the current stimulus (N). On the y-axis, the response error is shown, defined as the difference between the orientation reported by the participant and the actual orientation of the presented stimulus.

In the same study, the authors also employed another widely used method to assess serial dependence: the two-alternative forced choice (2AFC) discrimination task (J. Fischer & Whitney, 2014). In this specific experiment, the 2AFC task was used to determine whether serial dependence directly alters stimulus appearance, rather than merely influencing decision processes. First, a Gabor "inducer" was presented at one of two positions, with its orientation tilted 20° clockwise or counterclockwise relative to the Gabor that would subsequently appear in the same position. Then, two Gabor stimuli were presented simultaneously, and participants were asked to judge which of the two was more tilted clockwise (Figure 1.4 panel A).

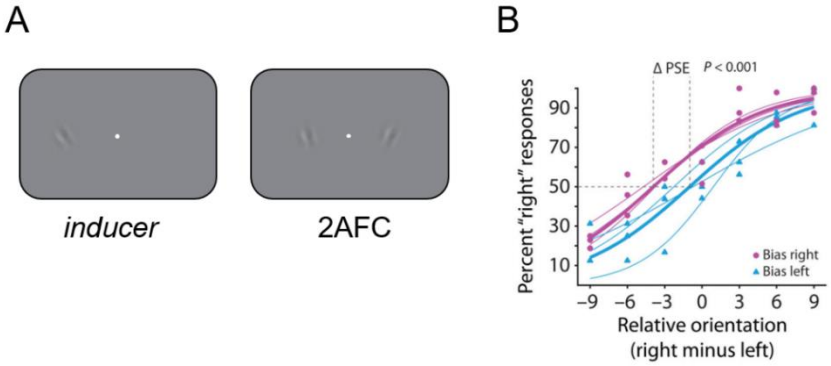

Figure 1.4 – Sequence of stimuli and results of the 2AFC experiment from Fischer & Whitney's (J. Fischer & Whitney, 2014) work. (A) The first stimulus presented to participants was the *inducer* stimulus, followed shortly by the simultaneous presentation of two Gabor

stimuli for the 2AFC task, which participants had to judge. (B) The two psychometric curves represent group-level responses, depending on whether the inducer influenced the stimulus in the right visual hemifield (purple) or the left hemifield (blue). The shift between the two curves, calculated as the difference in PSE, provides a quantitative measure of the serial dependence effect.

To assess the magnitude of the serial dependence effect, the relationship between the inducer stimulus and the subsequent response in the 2AFC task was analyzed. Trials were grouped according to the direction of the inducer's tilt relative to the reference (for example, whether the inducer was tilted clockwise or counterclockwise relative to the right Gabor) and how this tilt influenced participants' choices. For each group of trials, the data were analyzed by fitting psychometric functions, relating the relative orientation of the stimuli to the percentage of "right" responses (Figure 1.4 panel B). From each psychometric curve, the point of subjective equality (PSE) was calculated, representing the point at which participants responded "right" and "left" equally often. The serial dependence effect was then quantified as a shift in the PSE between the psychometric functions (ΔPSE). This shift is informative because it indicates whether the perception of the current stimulus was influenced by the preceding inducer stimulus.

These two experimental paradigms – orientation reproduction and 2AFC tasks – are to date the primary methods used to investigate serial dependence in behavioral experiments. The nature of the effect and the factors influencing it have been identified and characterized through analyses (including various complementary approaches) performed on the data collected from these experiments.

1.1.3 The serial dependence effect can be both attractive and repulsive

Across all the serial dependence experiments, it has been observed that the effect can take two different directions: one attractive and one repulsive. Importantly, however, whether both attractive and repulsive biases should be considered expressions of the same phenomenon remains a matter of debate.

Attractive serial dependence, also known as positive, primarily occurs in perceptual judgments where the perception of current stimuli is pulled toward recently experienced

stimuli (Manassi et al., 2023; Pascucci et al., 2023). This effect is especially pronounced when successive stimuli are only moderately similar, resulting in a characteristic S-shaped curve or a pattern resembling a derivative-of-Gaussian function (Fritsche et al., 2017; Manassi et al., 2023; Pascucci et al., 2023), as described previously. It is also commonly observed when the previous stimulus requires an explicit perceptual response (Feigin et al., 2021). In such cases, the effect is often attributed to forms of decision inertia (Akaishi et al., 2014) or post-perceptual biases that influence both perception and decision-making, particularly under conditions of uncertain sensory input (Pascucci et al., 2019). Although it can also emerge in the absence of explicit attention, attractive serial dependence tends to strengthen when attentional demands and task requirements are higher, and it has often been associated with consciously perceived stimuli (Cicchini et al., 2021; Fritsche & de Lange, 2019; Rafiei et al., 2021). For example, Fischer and Whitney (J. Fischer & Whitney, 2014) demonstrated that stimuli receiving focused attention produce stronger attractive effects: in their study, perceived orientation was systematically pulled toward that of the previous stimulus, with the effect being more pronounced when attention was directed to the stimulus's relevant location.

The effect of attractive serial dependence seems to be supported by mnemonic processes operating on different time scales. In particular, in experiments on visual serial dependence, it has been shown that visual working memory contributes to modulating attractive biases, which are minimal or absent at the time of perceptual encoding but progressively increase with longer retention intervals – that is, the delay periods during which the current stimulus must be actively maintained in memory before a response is made: this pattern suggests that serial dependence reflects an active integration process between current and recently stored representations during memory maintenance rather than a purely perceptual or attentional effect (Bliss et al., 2017; Fritsche et al., 2017). However, this integration is highly dependent on the temporal proximity between stimuli, as biases are more pronounced for events in the immediate past (in the order of a few seconds), suggesting that perceptual stability in vision derives from the interaction between residual sensory traces and short-term working memory processes (Fritsche et al., 2020; Gekas et al., 2019; Pascucci et al., 2019). The extent to which such interplay generalizes to other perceptual dimensions is yet to be determined.

Repulsive, or negative, effects in serial dependence, by contrast, tend to emerge under different conditions: they typically occur as a bias away from the previously encountered

stimulus. Importantly, several authors have argued that these repulsive biases may not reflect serial dependence in the strict sense, but rather forms of sensory adaptation or negative aftereffects arising from recent sensory stimulation. In classical adaptation paradigms, prolonged exposure to a stimulus induces perceptual distortions away from the adapting stimulus, a mechanism thought to improve sensitivity to novel information and reduce redundancy in sensory coding (Clifford et al., 2000; Kohn, 2007). Repulsive effects in serial dependence share several characteristics with adaptation-like phenomena, particularly when stimuli are strong, prolonged, unattended, or task-irrelevant. These effects are especially pronounced when prior stimuli are irrelevant to the task (Pascucci et al., 2019; Pascucci & Plomp, 2021; J. Fischer & Whitney, 2014). For example, inducer stimuli that do not require a response can exert a strong repulsive bias on subsequent judgments, especially when the magnitude difference between the inducer and the current target is large. Likewise, when participants are instructed to retain a perceptual decision – that is, to maintain in working memory their previously selected response rather than the sensory features of the stimulus itself – past stimuli frequently elicit repulsive biases (Ceylan & Pascucci, 2023). This phenomenon is particularly evident when the feature distance between the previous and current stimulus is substantial: in orientation tasks, for example, attractive biases dominate for small orientation differences, whereas repulsive effects emerge when the discrepancy exceeds approximately 45-50 degrees (Ceylan et al., 2021; Ceylan & Pascucci, 2023). The properties of the stimulus itself play a crucial role: strong and persistent stimuli tend to cause neural adaptation, giving rise to repulsive effects, while weak or uncertain stimuli promote positive serial dependence (Gibson, 1937). When the duration and intensity of stimuli increase, negative adaptation mechanisms become predominant and repulsive biases end up prevailing (Cicchini et al., 2017). Repulsive biases have also been observed within the same trial, for instance between representations simultaneously maintained in working memory. This occurs when an observer must remember multiple objects or orientations presented within the same temporal window. In such cases, the representations of different items tend to repel each other to minimize interference or confusion between the stored contents, thus generating a repulsive effect among elements of the same working memory representation (Czoschke et al., 2019). In contrast, serial dependence across different trials typically remains attractive, reflecting a process of temporal integration between consecutive events rather than one of separation (C. Fischer et al., 2020). Finally, in the absence of a response or a perceptual decision, repulsive

effects, similar to those of low-level adaptation, tend to predominate (Pascucci et al., 2019): if adaptation is weak, as after very brief stimuli, decision-making processes may prevail, but when adaptation is strong, it becomes dominant and leads to the emergence of negative biases (Fritsche et al., 2017).

The duality of novelty and consistency

Serial dependence, as previously described, can manifest in both attractive and repulsive forms. Importantly, these opposing biases are not mutually exclusive but can coexist within the same experimental trial, giving rise to a characteristic duality: attraction toward the previous response and repulsion away from the previous stimulus (Pascucci et al., 2019; Sadil et al., 2024). This phenomenon highlights a crucial dissociation in serial dependence, showing how perception appears shaped by the interaction of two opposing forces operating at different stages of processing (Pascucci et al., 2019).

Consistent with earlier observations of negative serial dependence, the influence of the preceding stimulus often takes the form of a repulsive bias, attributable to sensory adaptation mechanisms that bias perception away from recently processed physical inputs (Pascucci et al., 2019; Sadil et al., 2024). This repulsive bias is typically linked to low-level sensory adaptation, analogous to classic visual aftereffects such as the tilt-aftereffect (Morimoto & Makioka, 2024). Such mechanisms are thought to enhance sensitivity to environmental changes and promote differentiation of new incoming stimuli (Pascucci et al., 2019). These repulsive effects are consistent with findings from Fritsche, Mostert, and de Lange (Fritsche et al., 2017), who showed that recent visual history can bias low-level sensory encoding, producing effects on perception that are independent of decision-making processes, indicating that repulsive serial dependence can originate at the sensory-perceptual level. This stimulus-driven effect is particularly evident when a stimulus is presented without requiring a behavioral response (Jin et al., 2005; Pascucci et al., 2019) – as in catch trials or unreported stimuli – and also when the stimulus is irrelevant to the task (Ceylan & Pascucci, 2023).

In contrast, and in line with previously discussed attractive serial dependence, the influence of the previous response manifests as an attractive bias. This attraction is thought to be linked to forms of decision-making inertia: once a perceptual decision has been formed, the corresponding internal representation or response criterion may persist over time and bias

subsequent judgments toward the same choice. In line with this, Feigin and colleagues (Feigin et al., 2021) demonstrated that perceptual decisions are systematically biased toward relevant prior choices, indicating that post-perceptual memory and decision-history mechanisms play a central role in pulling perception toward previous responses. Unlike stimulus-driven repulsion, this attractive effect acts at the post-perceptual level (Fritsche et al., 2020; Pascucci et al., 2019), depends primarily on task relevance and prior decisions rather than on the physical properties of the stimulus (Feigin et al., 2021; Pascucci et al., 2019), and can partially counterbalance the repulsive effects of low-level adaptation (Pascucci et al., 2019).

These two mechanisms operate concurrently, with their relative strengths determining the overall observed serial dependence (Pascucci et al., 2019; Zhang & Alais, 2020): this indicates that the visual system simultaneously integrates information from the physical environment, which gives rise to adaptation and repulsion, and internal decision-making states, which generate attraction.

1.1.4 From simple to complex features

Serial dependence has been investigated across a wide range of visual perceptual features and objects, from basic visual properties to more abstract concepts.

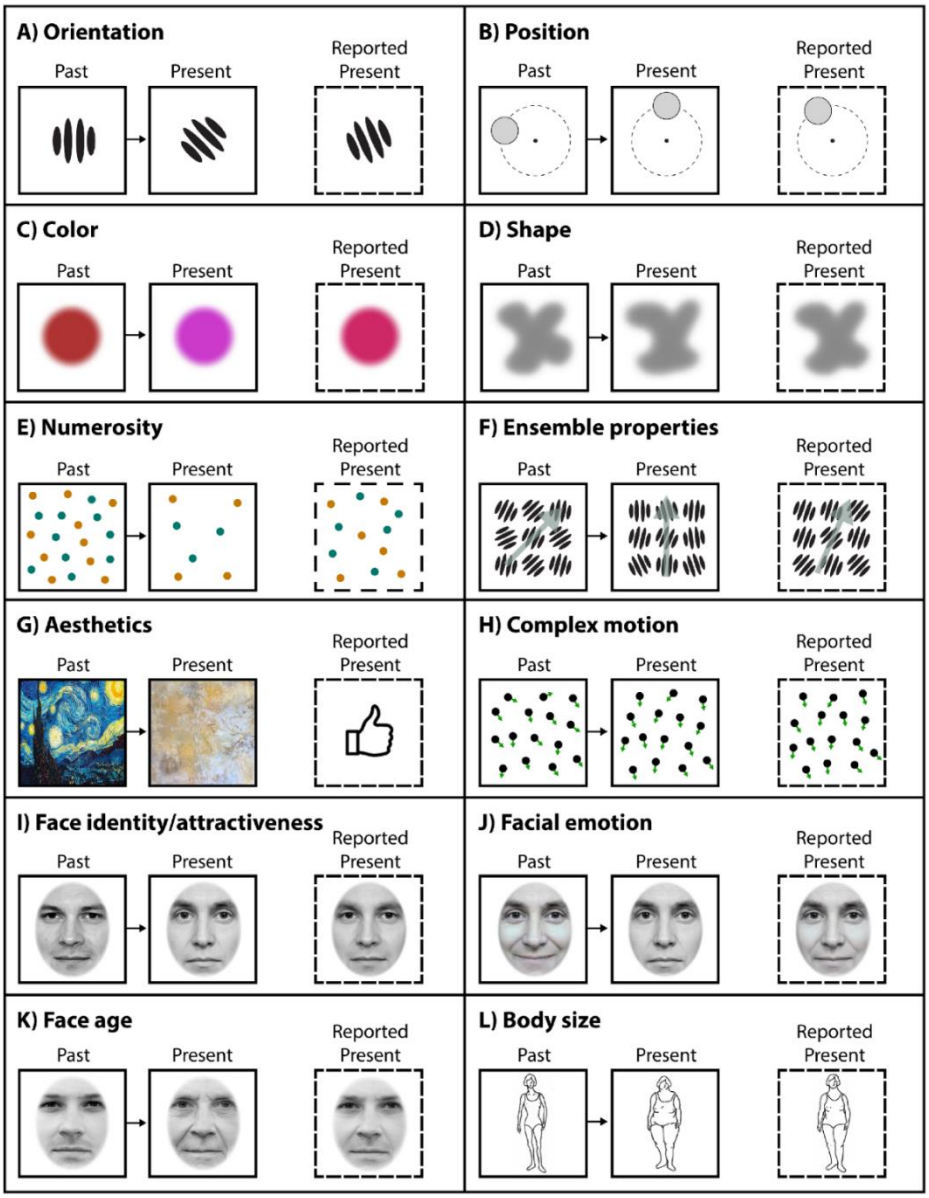

Figure 1.5 – Visual stimuli adopted in serial dependence studies, to evaluate the effect across different visual features. Figure extracted from Manassi, Murai and Whitney's review (Manassi et al., 2023).

The first visual feature in which the phenomenon of serial dependence was systematically investigated is orientation. Numerous studies have shown that the orientation of a Gabor stimulus can influence the perceived orientation of a subsequently presented stimulus, and this effect emerges consistently across the various experimental paradigms introduced in the literature.

Concurrently, the phenomenon of serial dependence has been investigated by Cicchini and colleagues in the context of visual numerosity (Cicchini et al., 2014), which refers to the

perceived number of elements (e.g., dots) in a visual array. In this domain, the perceived numerosity of a current array is systematically influenced by the numerosity of previously presented arrays. The serial dependence effect in numerosity has been demonstrated at both behavioral and neural levels, with evidence showing that both perceptual judgments and neural representations of numerosity are attracted toward recently encountered stimuli (Corbett et al., 2011; Fornaciai & Park, 2018b, 2018a, 2020), supporting perceptual continuity and stability in a noisy environment. Most studies employ numerosity discrimination or estimation tasks, where participants judge the number of dots in a series, often following exposure to an "inducer" stimulus with a different numerosity (Corbett et al., 2011; Fornaciai & Park, 2018b, 2018a). Moreover, serial dependence in numerosity has been shown to differ between subitizing (small numbers) and estimation (larger numbers), and can be modulated by whether participants provide explicit responses or merely observe the stimuli (Fornaciai & Park, 2018a; Morimoto & Makioka, 2024).

Another aspect that has been investigated is serial dependence in spatial position, primarily studied using localization tasks (Liberman et al., 2014; Manassi et al., 2018). In these tasks, participants are presented with targets at random locations within the visual field and are asked to report the perceived position. Consistently, an attractive effect is observed: the perceived position of the current target tends to be biased toward the location of the previous stimulus, reflecting temporal continuity in spatial estimates.

Among the various visual features investigated, color has received particular attention, as it is strongly linked to the structure of natural scenes. This feature has been studied using delayed-estimation tasks (Barbosa & Compte, 2020; Guan & Goettker, 2024), in which participants report the color of a stimulus after a brief delay. In the case of color, it has been observed that the serial dependence effect develops gradually over the course of the entire experimental session, suggesting that it does not rely on immediate adaptation but instead involves a slower, cumulative mechanism, indicating that memory processes may play an important role.

Another element that characterizes natural environments is the shape of surrounding objects. Serial dependence in shape has been investigated using both adjustment (Manassi et al., 2022) and classification (Collins, 2022b, 2022a) tasks, and this effect also manifests as an attractive bias, whereby the current shape judgment is pulled toward the shape presented on the previous

trial. Notably, studies have shown that this effect decays over time, is stronger for similar shapes, and is spatially localized, meaning that the bias is enhanced when the shapes appear in the same spatial position (Manassi et al., 2019, 2023).

The final basic feature considered is motion perception. Whether using stimuli that are simple (e.g., dot motion) (Alais et al., 2017; You et al., 2023) or complex (e.g., biological motion, smooth pursuit eye movements) (Chaney et al., 2016; Hong et al., 2024; Y. Li et al., 2021), studies consistently report an attractive serial dependence effect. For this feature, magnetoencephalography (MEG) and electroencephalography (EEG) evidence shows that neural representations of current motion are biased toward the motion direction of the previous trial. Notably, this shift emerges at late, post-encoding stages, suggesting a substantial contribution of working memory and decision-related processes (C. Fischer et al., 2022, 2025).

After examining basic visual features, research on serial dependence has expanded to encompass more complex and abstract dimensions. These do not relate solely to the sensory encoding of physical properties but instead involve higher-level representations, often related to face processing and to social or affective evaluations.

Serial dependence robustly influences facial identity judgments, biasing the perception of a current face toward recently seen identities, even when viewpoint or low-level visual features differ (Lidström, 2023; Turbett et al., 2019, 2021). Similarly, judgments of facial emotion are systematically shaped by the expressions observed on preceding trials, producing a perceptual tendency toward emotional continuity (Lidström, 2023; Manassi et al., 2023). Evaluations of attractiveness are likewise affected, with current ratings being pulled toward the attractiveness of recently viewed faces (Ho & Newell, 2020; Van der Burg et al., 2019; Xia et al., 2016; Yu et al., 2023).

Finally, serial dependence has also been documented for a wide range of other social and perceptual facial attributes, including gender, age, gaze direction, trustworthiness, dominance, and additional high-level traits, supporting the idea of a general mechanism operating in higher-order facial processing (Alais et al., 2018; Manassi et al., 2023; Xia et al., 2016).

1.1.5 Other modalities beyond vision: auditory and tactile

To date, serial dependence has been studied primarily within the context of visual perception. However, several studies have demonstrated that this effect also occurs in the auditory domain across various features, and preliminary research is beginning to explore its presence in the tactile modality as well.

Serial dependence in the auditory domain manifests in different ways, depending on the perceived attribute and the level of participant engagement required.

In the perception of emotion conveyed through prosody – that is, the rhythmic, melodic, and intonational features of speech that communicate emotional information – a positive serial dependence effect has been observed: the perceived emotion in a given sound tends to be biased toward that of the preceding trial (Van der Burg et al., 2024). However, the effect can become repulsive when participants are required to withhold their response before reporting it, suggesting that the attractive component is driven by automatic perceptual mechanisms, whereas the retention period introduces post-perceptual or decisional influences (Van der Burg et al., 2024).

In the context of rate perception, a positive serial dependence is typically observed when participants are required to provide a response, with current judgments being attracted toward the previously experienced rate. In contrast, in the absence of a response, a repulsive effect emerges, which appears to reflect a perceptual mechanism aimed at optimizing the detection of changes. These findings suggest that serial dependence in rate perception arises from the interaction between a stronger post-perceptual, attractive component and a weaker perceptual, repulsive component. Furthermore, working memory can amplify the magnitude of the attractive effect (Motala et al., 2020).

Serial dependence is also observed in the perception of time within auditory rhythms (B. Li et al., 2024). In unimodal conditions (e.g., auditory-to-auditory), participants' choices tend to be attracted toward previous responses (an attractive decision-level effect), whereas the perception of the rhythm itself can be slightly repelled away from preceding stimuli (a perceptual repulsive effect). In cross-modal conditions (e.g., auditory followed by visual), a

repulsive decision-level effect predominates, with current responses turning away from the previous stimuli.

Attractive effects of serial dependence have also been observed in pitch judgments and in the perception of auditory stimulus duration (Arzounian et al., 2017; Motala et al., 2020; Wearden & Jones, 2021). For example, Arzounian and colleagues (Arzounian et al., 2017) showed that people's judgments of pitch are systematically influenced by the preceding stimulus: when participants compared successive pure tones and judged their relative pitch, responses were biased toward the pitch of the previous tone; this attractive sequential dependence was observed even when the task required fine pitch discrimination. Similarly, in duration-discrimination tasks, the perceived length of a sound interval was attracted toward the duration of preceding auditory stimuli, indicating an integration of temporal information over successive trials (Burr et al., 2013).

However, evidence for serial dependence across different sensory modalities appears to depend critically on stimulus format. For example, Fornaciai and Park (Fornaciai & Park, 2019) reported no influence of preceding auditory tones on visual numerosity judgments, suggesting limited cross-modal generalization. Importantly, this null effect may reflect differences in representational format rather than modality per se, as their comparison involved spatial visual arrays and temporally sequential auditory stimuli. In contrast, Hashimoto and Makioka (Hashimoto & Makioka, 2025b) demonstrated cross-modal serial dependence in numerosity perception when auditory and visual stimuli shared an equivalent spatial structure, both consisting of sequential events. These findings indicate that serial dependence can generalize across sensory modalities when stimuli are matched in their spatial format, highlighting that cross-modal integration is constrained not simply by sensory modality but by the underlying perceptual representation.

Another line of research has investigated serial dependence in multimodal audiovisual contexts, with findings suggesting that the phenomenon is more pronounced in the visual domain than in the auditory domain. In a study by Lau and Maus (Lau & Maus, 2019), participants were presented with compound stimuli consisting of a visual Gabor and a vocal sound and were asked to report either the orientation of the Gabor or the auditory stimulus on each trial. The results revealed serial dependence only for the visual modality, whereas auditory judgments were not influenced by preceding stimuli. Moreover, the visual effect

persisted even when previous trials contained only auditory stimuli or did not require any response, indicating that serial dependence is primarily linked to visual perception of the preceding trial rather than to auditory decision-making or task execution.

In the domain of tactile perception, recent work by Wang and Alais demonstrates that a similar serial dependence phenomenon occurs during haptic exploration (G. Wang & Alais, 2025b, 2025a). Specifically, when participants judge the orientation of tactile surfaces, their perception of the current trial is attracted toward the orientation perceived in the preceding trial, indicating that recent tactile experiences actively influence current perceptual estimates. This tactile serial dependence effect is robust and persists even under passive exploration. Additionally, the bias does not appear to arise solely from physical contact with the previous stimulus: it is also shaped by the participant's prior responses. These findings suggest that tactile orientation perception is influenced by recent experience, integrating information both from the previously encountered stimulus and the participant's interaction with it.

1.2 Objective and scope of the thesis

Based on the evidence presented thus far, serial dependence has been investigated primarily within the visual domain. Nevertheless, several aspects remain poorly understood, particularly its relationship with time perception (both visual and auditory) and the possibility that the phenomenon also emerges in other domains and features, such as tactile motion direction perception, or under conditions of cross-sensory integration.

The aim of this dissertation is therefore to extend the study of serial dependence to temporal perception and additional sensory modalities, in order to clarify its generality, the conditions under which it emerges, and the underlying mechanisms. The work is organized into four experimental chapters, each guided by specific research questions.

In Chapter 2, focused on visuo-temporal perception, we investigate whether serial dependence emerges across different tasks – temporal discrimination and temporal reproduction – and whether the underlying mechanisms are shared or distinct. We also explore the extent to which working memory modulates the integration of past and current stimuli.

In Chapter 3, the focus shifts to audio-temporal perception, addressing three main questions: (i) whether serial dependence is present in this sensory domain, (ii) how the serial dependence effect emerges based on how the temporal information is conveyed (via continuous sounds versus discrete intervals), and (iii) whether the temporal interval between the inducer and the target influences the strength or presence of the phenomenon.

Chapter 4 extends the investigation to the tactile domain, examining whether serial dependence also occurs in the perception of motion direction explored through touch. Furthermore, we assessed how visual input influences the generation of serial dependence by comparing sighted and visually impaired participants designing a tactile reproduction task supported by custom-designed haptic devices for response collection.

In Chapter 5, we explore visuo-haptic integration in the perception of object size. The central question is whether and how serial dependence emerges independently in the visual and haptic modalities and in a cross-sensory context. To address this, we developed an experimental paradigm using a mixed-reality device (Microsoft HoloLens 2), first validating its rendering accuracy and tracking reliability, and then applying it to dimensional discrimination tasks to analyze the specific and joint contributions of vision and touch.

Finally, Chapter 6 provides an overview of the results obtained in this dissertation in relation to the experimental questions addressed in the preceding chapters.

Chapter 2

Serial Dependence in Visual Time Perception

This chapter is partially extracted from:

"Bertolasi, J., Esposito, D., Vitale, A., Gori, M. (2025). Exploring the role of serial dependence in visual time perception. Journal of Vision, 25(8):7. https://doi.org/10.1167/jov.25.8.7".

2.1 Introduction

In the previous chapter, we introduced the concept of serial dependence as a perceptual phenomenon in which the perception of the current stimulus is influenced by the preceding stimulus or response. In this chapter, we focus specifically on investigating serial dependence in visuo-temporal perception.

As previously started, serial dependence has been extensively investigated across several perceptual visual domains, including numerosity (Fornaciai & Park, 2018b), shape (Collins, 2022a), face identity (Turbett et al., 2021) and aesthetic judgment (Kim et al., 2019), color discrimination (Barbosa & Compte, 2020), and motion direction (Y. Li et al., 2021). However, much of the evidence concerning serial dependence in the temporal domain remains inconclusive, and additional research is needed to clarify how serial dependence operates in

relation to time, independently of other contributing factors (Manassi et al., 2023; Van der Burg et al., 2015).

Although serial dependence in time perception remains a relatively underexplored topic, several studies have begun to elucidate its underlying mechanisms. Roseboom (Roseboom, 2019) demonstrated that duration estimates can be influenced by the duration of the preceding trial, revealing both attractive and repulsive effects depending on the task. Togoli and colleagues (Togoli et al., 2021) further showed that serial dependence in the temporal domain does not generalize to other dimensions, such as numerosity, suggesting domain-specificity. More recently, Li, Wang, and Zaidel (B. Li et al., 2024) reported that, in unimodal tasks, the perception of temporal dynamics tends to exhibit repulsive sensory effects, which are modulated by stimulus uncertainty.

These findings, in addition to confirming the sensitivity of temporal perception to the recent history of stimuli, highlight the critical role of the experimental paradigm in revealing or failing to reveal the presence of serial dependence.

As discussed previously, serial dependence can be investigated using different experimental paradigms, namely temporal discrimination tasks and temporal reproduction tasks. While these paradigms are well established in other visual features, a gap remains in the literature regarding their application to the perception of temporal durations. Specifically, it is still unclear how the effects observed across these two types of tasks relate to one another. The open question concerns whether the mechanisms underlying the emergence of serial dependence in temporal discrimination and temporal reproduction tasks are shared or reflect two distinct processes.

In this chapter, we present an experiment specifically designed to address these questions, building on previous work by Togoli and colleagues (Togoli et al., 2021). In their study, a discrimination task was employed to investigate both numerosity and the perception of temporal durations, using an *inducer* stimulus intended to elicit serial dependence by biasing the perception of the subsequent target stimulus. In addition, we conducted a second experiment involving a reproduction task (Jazayeri & Shadlen, 2010) to assess serial dependence by examining the extent to which previous stimuli and responses influence the perception of the current stimulus.

Finally, an open question in the literature concerns the processing stage at which serial dependence operates: whether it primarily emerges at a perceptual level or at a higher cognitive-decisional stage. This ambiguity arises from the fact that the effect can be influenced by multiple stages of perceptual and decision-making processes. Some studies suggest that serial dependence may arise during early sensory processing (J. Fischer & Whitney, 2014; John-Saaltink et al., 2016), whereas others highlight the involvement of cognitive and decisional components, implicating higher-order circuits responsible for integration and final response selection (Barbosa & Compte, 2020; Neto & Bartels, 2021; Sheehan & Serences, 2022).

In this context, working memory has been proposed as a key mechanism for integrating past and current information, as demonstrated in several studies (Bilacchi et al., 2022; Bliss et al., 2017; Fritsche et al., 2017). Accordingly, a second focus of this chapter is to investigate the relationship between serial dependence effects observed across two different types of tasks and working memory, with the aim of clarifying the processing stage at which serial dependence emerges.

We therefore present the serial dependence effects that emerged from the two experiments – temporal discrimination and temporal reproduction – and examine the relationship between these effects. Finally, we investigate how both effects relate to working memory, using a memory-span index derived from a task specifically designed to assess visual working memory.

2.2 Materials and methods

2.2.1 Participants

A total of 33 individuals participated in this study (age 27.0 ± 7.5 years). All participants had normal or corrected-to-normal vision and no known history of neurological conditions. Prior to participation, each individual was given both written and verbal explanations of the study's objectives and procedures and provided informed consent. The study protocol was reviewed and approved by the local ethics committee (Comitato Etico, ASL3 Genovese, Italy) and carried out in accordance with the principles outlined in the Declaration of Helsinki.

2.2.2 Apparatus, stimuli, and procedure

Visual stimuli were displayed on a 24-inch high-resolution monitor (ASUS VG248QE) with a 144 Hz refresh rate and a resolution of 1920×1080 pixels. Participants were seated in a quiet, darkened room at a viewing distance of 57 cm from the screen and with their heads positioned on a chinrest.

The study followed a within-subjects design, with all participants completing a duration discrimination task, a temporal interval reproduction task, and the working memory Corsi block test. The tasks are described in the following subsections. To control for order effects, the sequence of tasks was counterbalanced across participants. The three tasks were distributed randomly throughout a single testing session lasting approximately one hour. Participants were allowed to take breaks after each experimental block during the session.

2.2.2.1 Duration Discrimination task

The stimuli were adapted from the duration task condition used by Togoli and colleagues (Togoli et al., 2021). Each stimulus consisted of a white, blurred disc displayed on a grey background, with a field area of 220 pixels (corresponding to 6.2° of visual angle), a radius of 90 pixels, and a sigma smoothing parameter of 40 pixels. Stimuli were presented 12° to the right or left of a central fixation point (a black dot, 10 pixels in diameter, or 0.28°). All stimuli were generated using the Psychophysics Toolbox for MATLAB (Brainard, 1997).

The experimental task featured a sequence of three discs per trial: the first stimulus, or *inducer*, was not task-relevant; the second served as the reference; and the third was the test stimulus. The inducer had a duration of either 199 ms or 481 ms, the reference duration was fixed at 310 ms, and the test stimulus varied across seven durations ranging from 199 ms to 600 ms. The inducer and reference were always presented on the same side of the screen, while the test appeared on the opposite side, in line with findings that serial dependence effects are spatially specific (Fornaciai & Park, 2018b; Togoli et al., 2021). A 750 ms inter-stimulus interval (ISI) separated the inducer offset and reference onset, followed by a 300 ms ISI between the reference offset and test onset. After viewing the test stimulus, participants indicated whether the reference or test appeared longer by pressing the left or right arrow key on a standard keyboard. Each trial was followed by a 750 ms pause before the next trial began

automatically (see Figure 2.1 panel A for an illustration of the procedure). The design incorporated a 2×7 matrix, combining the two inducer durations with the seven test durations, resulting in 14 unique conditions. Each condition was repeated 20 times, totaling 280 trials, which were evenly divided into five blocks of 56 trials. The entire task took approximately 20 minutes to complete.

2.2.2.2 Temporal Interval Reproduction task

The stimuli were adapted from studies by Cicchini and Jazayeri (Cicchini et al., 2012; Jazayeri & Shadlen, 2010), featuring white disc stimuli measuring 140 pixels (corresponding to 4° of visual angle) displayed on a grey background, positioned 5° of visual angle to the left and right of the screen center. A black central fixation point (0.28° in diameter) was used to maintain visual focus, with stimuli appearing 12° to the left or right of this fixation. Stimuli were generated using the Psychophysics Toolbox for MATLAB (Brainard, 1997).

In each trial, two white discs were presented sequentially for 20 ms each, separated by a randomly selected sample interval ranging between 494 and 847 ms. The first disc always appeared in the left visual field and the second in the right. Following the second disc's disappearance, participants were instructed to reproduce the duration of the sample interval by pressing and holding the space bar on a standard keyboard for what they perceived to be the same amount of time. Unlike the original protocol used by Jazayeri and colleagues (Jazayeri & Shadlen, 2010), no feedback was provided to participants regarding their performance. The experiment consisted of 5 blocks of 30 trials each, totaling 150 trials, with an approximate overall duration of 10 minutes. The experimental timeline is illustrated in Figure 2.1 panel B.

2.2.2.3 Corsi Block test

The Corsi Block Tapping Test was administered using the PEBL platform (Mueller & Piper, 2014). The visual display consisted of nine blue squares arranged randomly against a black background. During each trial, a sequence was presented by highlighting the squares in yellow one at a time. After the sequence ended, participants were required to reproduce the order by clicking on the squares in the same sequence in which they were highlighted (see Figure 2.1 panel D). The difficulty increased every three trials by adding one more item to the sequence, up to a maximum of nine blocks, or until the participant made two consecutive errors.

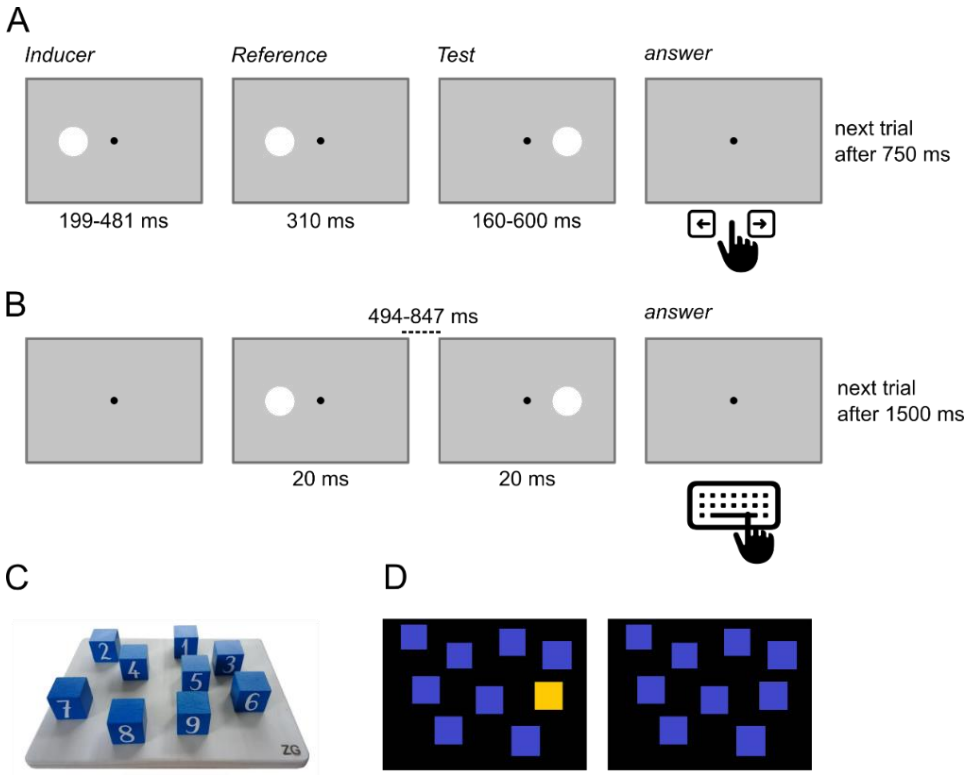

Figure 2.1 – Illustration of the experimental paradigms used across tasks. (A) Experimental procedure for the duration discrimination task. The first stimulus presented is the *inducer* one (duration 199 or 481 ms, randomized within trials), followed by the reference one in the same position (duration 310 ms) and in the end, the test stimulus, positioned in the opposite hemifield (with variable duration from 199-600 ms). Participants had to determine which lasted longer between reference and test. (B) Temporal reproduction task procedure. Two white discs were presented on the screen for 20 ms (the first one on the left hemifield and the second on the right one), with a delay between the presentations that varied in a range of 494-847 ms. Participants were asked to reproduce the perceived duration that passed between the two discs. (C) Example of Corsi block test in physical setup. The experiment is conducted with wooden blocks: the experimenter touches the blocks sequentially with one hand, and the participant is then asked to repeat the sequence. (D) Digital PEBL version of Corsi block test. In this experiment, some of the squares would change color from blue to yellow sequentially, and participants were asked to click on the sequence of the squares that lit up.

2.2.3 Data analysis

2.2.3.1 Duration Discrimination task

Participants who made 20% or more errors (i.e., at least 4 out of 20 trials) in the conditions involving the shortest and longest test stimulus durations were excluded from the analysis. Based on this criterion, six participants were removed. Additionally, participants whose just

noticeable difference (JND) deviated more than 2.5 standard deviations from the sample mean were to be excluded; however, no participants met this exclusion threshold.

To quantify the serial dependence effect, we fitted a cumulative Gaussian function to the proportion of "test longer" responses as a function of test duration. The point of subjective equality (PSE) – indicating the perceptual bias – was computed as the median of the fitted function, separately for each participant and inducer condition, while the JND was computed as the average value between the 75% and 25% thresholds for each psychometric function. The serial dependence effect was defined as the difference in PSE between the two inducer conditions for each participant.

To ensure the robustness of the observed effects and support the reliability of subsequent correlation analyses, we conducted an intra-experiment consistency check. The dataset was split in half, and the serial dependence effects derived from each subset were compared using a Bayesian paired-samples t-test.

A paired-sample t-test was also performed to assess whether the PSE distributions significantly differed between the two inducer conditions, and Cohen's d was calculated to determine the standardized effect size.

Finally, to examine the influence of the previous response on the perception of the current stimulus, we did a paired-sample t-test to compare the PSEs based on whether the prior response was "reference" or "test", to evaluate the presence of a response-history effect.

All analyses were conducted using MATLAB R2022b (The MathWorks Inc., 2022), except for the Bayesian test performed in JASP version 0.17.1.0 (JASP Team, 2023).

2.2.3.2 Temporal Interval Reproduction task

Participants whose correlation between stimulus duration and response was not statistically significant were excluded from further analysis, resulting in the removal of three participants.

In interval reproduction tasks, behavioral responses typically show a central tendency bias, such that reproductions are systematically biased toward the mean of the stimulus distribution (Cicchini et al., 2012; Hollingworth, 1910; Jazayeri & Shadlen, 2010). Since this effect can artificially contribute to manifest serial dependence, we first implemented a data-cleaning procedure. Specifically, we fit a linear model to each participant's response error, defined as

the difference between the reported and actual stimulus duration, as a function of stimulus duration. The residuals from this model, representing error variance independent of central tendency bias, were then used as response errors. This resulted in a corrected measure of duration estimation, free from central tendency influences.

To quantify the magnitude of serial dependence from both the preceding stimulus and the preceding response, we used a linear mixed-effects model (LMEM). In the model, the dependent variable was the distribution of participants' response errors across trials. Predictor variables included the durations of both current and previous stimuli, as well as the previous response, and all were treated as random effects. The inclusion of current stimulus duration as a predictor was justified by the prior cleaning step, ensuring the model captured only serial dependence and not residual central tendency. Participant identifier was used as a grouping variable to account for individual variability in the LMEM. The model figured as $\mathrm{error_N} \sim 1 + \mathrm{stimulus_N} + \mathrm{stimulus_{N-1}} + \mathrm{response_{N-1}} + (1 + \mathrm{stimulus_N} + \mathrm{stimulus_{N-1}} + \mathrm{response_{N-1}}|\mathrm{name})$ in Wilkinson notation. The model was implemented using the *lme4* package in R.

To further confirm the reliability of the observed effects, we conducted an internal consistency check by dividing the dataset in half and comparing the effects of stimulus and response serial dependence across the two subsets using a Bayesian paired-samples t-test in JASP.

Finally, to assess the strength of the evidence, we performed a Bayesian analysis using the *BayesFactor* package in R. Bayes Factors (BFs) were computed using the ttest.tstat function, which calculates BFs based on the t-statistic and sample size, with an intermediate prior scale (r = 0.707) applied.

The cleaning procedure was performed on MATLAB R2022b (The MathWorks Inc., 2022), the consistency test performed in JASP version 0.17.1.0 (JASP Team, 2023), while the model and BF were performed using R version 4.4.2 (R Core Team, 2021).

2.2.3.3 Corsi Block test

The study assessed participants' working memory performance using two key measures: memory span and block span. Memory span refers to the number of items a participant can recall in the correct sequence, reflecting the capacity to retain and reproduce ordered

information. Block span, on the other hand, specifically measures the ability to recall sequences of spatial locations. On average, memory span typically ranges from 5 to 9 items, while block span scores are usually slightly lower, falling between 4 and 7 locations. Higher scores on both measures indicate stronger working memory function, suggesting efficient encoding, storage, and retrieval processes. Lower scores may point to difficulties in attention or memory, potentially reflecting cognitive limitations (Kessels et al., 2008). Memory span is a particularly important metric, as it serves as a robust tool for studying cognitive processing, predicting broader cognitive abilities, and exploring individual differences in working memory capacity.

2.2.3.4 Interindividual variability and working memory

To examine potential associations among participants' performances across the three tasks, we calculated Pearson correlation coefficients for each relevant pair of variables. The variables included the individual differences in PSE from the duration discrimination task (normalized by the duration of the reference stimulus), the slope coefficients derived from the temporal interval reproduction task, and the memory span scores obtained from the Corsi Block test.

To further evaluate the strength of the observed relationships, we also conducted Bayesian correlation analyses, providing a measure of relative evidence in support of or against the presence of an association.

The Pearson correlation was performed on MATLAB R2022b (The MathWorks Inc., 2022), while the Bayesian one on JASP version 0.17.1.0 (JASP Team, 2023).

2.3 Results

2.3.1 Temporal Discrimination task

We assessed serial dependence by examining how the inducer influenced the perceived duration of a subsequent reference stimulus presented in the same spatial location. Specifically, we measured shifts in the PSE as a function of inducer duration.

As shown in the representative psychometric curve in Figure 2.2 panel A, the PSE following a 481 ms inducer was 301.7 ± 13.9 ms, while that following a 199 ms inducer was

282.7 ± 13.24 ms – a 19.1 ms difference, indicating attraction toward the inducer. Across participants (Figure 2.2 panel B), PSEs were generally higher for the shorter inducer, with most data points falling above the equality line. While a few subjects showed stronger effects, they were not outliers, as their JNDs fell within 2.5 standard deviations of the group mean (Figure 2.3).

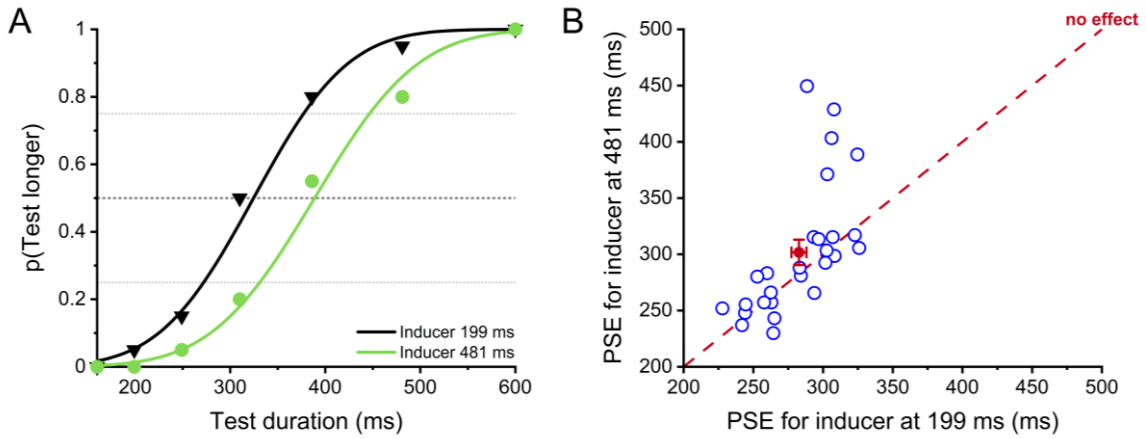

Figure 2.2 – Effect of inducer duration on temporal perception. (A) Representative single-subject psychometric curve for the temporal discrimination task condition for the two levels of inducer duration. When the inducer was smaller than the reference, the curve shifted leftward compared with when it was larger than the reference, indicating an under- or overestimation of the reference magnitude in the direction of the inducer. (B) Proportion between the PSE at 199 ms and PSE at 481 ms. The red dot and error bars refer to the average value for both distributions.

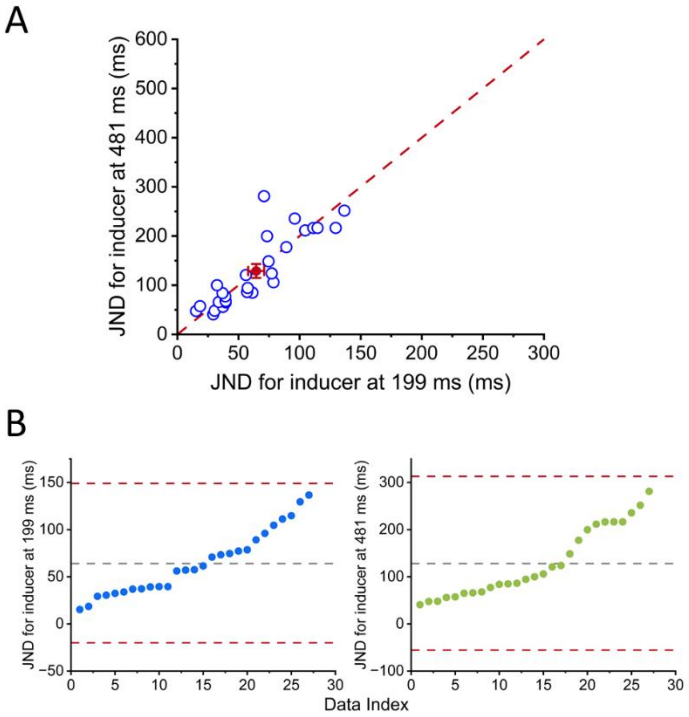

Figure 2.3 – Stability of JND across inducer conditions. (A) Scatter plot comparing JND values across participants for the two inducer time conditions: 199 ms (x-axis) and 481 ms (y-axis). Each dot represents a participant; the red dot indicates the group mean with standard error. Data are symmetrically distributed around the bisector, suggesting consistency between conditions. (B) JND values for 199 ms (left) and 481 ms (right), with means shown as solid black lines and ± 2.5 standard deviation limits as dashed red lines. All data points fall within these limits, indicating no outliers.

The consistency of the observed effects was confirmed by the Bayesian paired-samples t-test comparing the serial dependence magnitudes obtained from the two halves of the dataset which yielded a BF of 0.284 (error % = 0.025); the median of the posterior distribution was 0.101, with a 95% credibility interval ranging from -0.27 to 0.48, which includes zero and thus suggests evidence for the absence of a difference between subsets, suggesting consistent effects across the sample.

The paired-sample t-test revealed that the effect on the PSE was statistically significant, $t(26) = -2.15$, $p = 0.040$. This result indicates that there was a reliable difference between the compared inducer conditions. The effect size, as measured by Cohen's *d*, was 0.402, with a 95% confidence interval (CI) for the effect size that ranged from 0.01 to 0.84.

To investigate whether the previous response influenced the perception of the current stimulus, we compared the PSE following a "reference" response to the PSE following a "test" response using a paired-sample t-test. The analysis revealed no significant effect of the previous response on current perception, $t(26) = 0.63$, $p = 0.532$, with a 95% CI of [-0.01, 0.02].

2.3.2 Temporal Interval Reproduction task

To investigate serial dependence in the temporal reproduction task, participants estimated the interval between two visual stimuli and reproduced it by holding the spacebar. We examined how the previous trial influenced current duration perception, referring to "stimulus duration" as the interval between the two stimuli. To isolate serial dependence effects, reproduction errors were first residualized to remove confounds like the central tendency effect. The residualized data were then analyzed using a linear mixed-effects model (LMEM) to assess the influence of previous stimuli and responses (Figure 2.4 panel A).

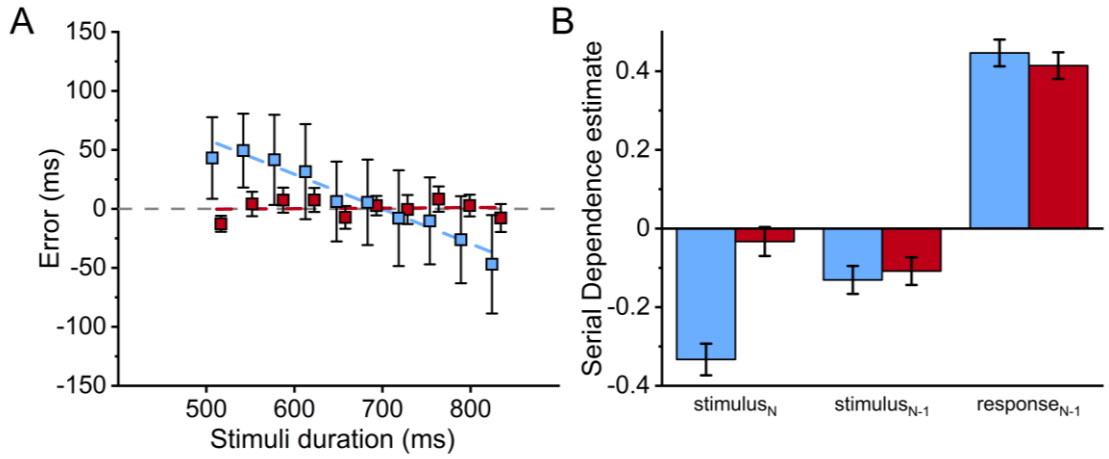

Figure 2.4 – Impact of central tendency correction on serial dependence components. (A) Pre- (blue) and post- (red) residualization of subjects' error in response was performed to account for the central tendency effect. In the biased data, a clear central tendency trend is observed, as indicated by a regression curve with a negative coefficient. (B) Results of the LMEM used to estimate serial dependence both before (blue) and after (red) the residualization process. After residualization, the effect of the N-stimuli was strongly reduced and approached zero, while the effects of previous stimuli (negative) and previous responses (positive) remained significant, indicating robust associations with serial dependence.

Results (Table 2.1) showed a significant negative association between current reproduction error and the previous stimulus, and a positive association with the previous response. No effect was observed from the current stimulus as expected after the residualization.

Table 2.1 – Coefficients of the LMEM with corresponding BF for each term.

	Estimate	**SE**	**tStat**	**DF**	**BF**
Stimulus $_N$	-0.033 [-0.11 0.04]	0.04	-0.896	26	0.298
Stimulus $_{N-1}$	-0.108 [-0.18 -0.04]	0.04	-3.076	26	8.464
Response $_{N-1}$	0.414 [0.35 0.48]	0.03	12.279	26	1.89×10^{9}

Again, the consistency of the observed effects was confirmed by the Bayesian paired-samples t-test between the two halves of the dataset (as reported in section 2.2.3.2), suggesting consistent effects across the sample: for the effect of the previous response, the BF was 0.218 (error % = 0.024), with a median of 0.035 and a 95% credibility interval of [-0.340, 0.412]; for the previous stimulus, the BF was 0.265 (error % = 0.025), with a median of -0.122 and a 95% credibility interval of [-0.504, 0.253].

Figure 2.4 panel B illustrates the LMEM results both before and after residualization, highlighting how central tendency biases hide the interpretation: the current stimulus shows a

significant effect only in the non-residualized model ($p < 0.001$). Post-residualization, opposing trends emerge for trial N-1: previous stimulus duration negatively affects error, while previous response has a positive influence.

2.3.3 Interindividual variability and working memory

We explored the relationship between serial dependence effects in both tasks and individual working memory span.

Bayesian analysis performed between the serial dependence effect of the temporal discrimination task and the temporal reproduction task provided evidence for the null hypothesis, for both the previous stimulus ($r = 0.07$, $BF = 0.265$) and previous response ($r = -0.13$, $BF = 0.303$) from the temporal reproduction task, suggesting no cross-task consistency in the effect.

Finally, we analyzed the association between working memory span and the serial dependence effect for both tasks. For the temporal discrimination task, results were inconclusive ($r = -0.17$, $BF = 0.338$). In the temporal reproduction task, Bayes Factors supported the null hypothesis for both the previous stimulus ($r = -0.14$, $BF = 0.305$) and previous response ($r = -0.06$, $BF = 0.264$), indicating no reliable link between memory span and serial dependence in either case.

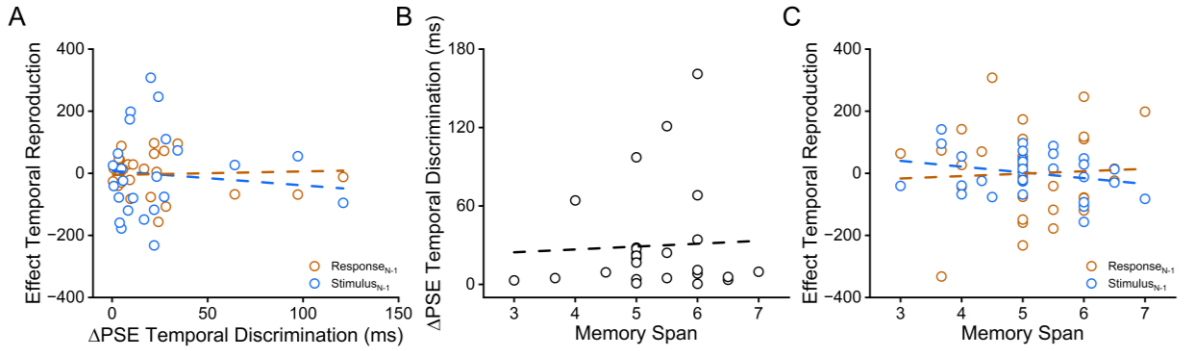

Figure 2.5 – Relations between serial dependence effects related to temporal reproduction task, temporal discrimination task, and working memory capacity. (A) Scatter plot showing the correlation between the change in PSE in the temporal discrimination task and the serial dependence effect in the temporal reproduction task. Data are grouped by type of predictor: previous stimulus or previous response (N-1). (B) Correlation between individual memory capacity scores and PSE variation in the temporal discrimination task. (C) Correlation between memory capacity and serial dependence effects in the temporal reproduction task, separately for stimulus-based and response-based effects, as in panel (A).

2.4 Discussion

This study was conducted to investigate how serial dependence emerges in temporal perception within the visual system. To this end, 33 participants were tested using two tasks designed to assess serial dependence through different approaches: a temporal discrimination task, which included an *inducer* stimulus to elicit the serial dependence effect, and a reproduction task, in which the influence of the previous stimulus and previous response on reproduction error were evaluated. The use of these two distinct tasks allowed us to examine whether different experimental approaches reveal comparable or distinct serial dependence effects. Additionally, we aimed to explore the relationship between serial dependence and working memory, given its proposed central role in the effect, while the nature of this relationship remains under debate.

Temporal Discrimination task

The results demonstrated that serial dependence emerges in a temporal discrimination task in which an inducer stimulus is designed to bias the perceived duration of the subsequent target stimulus. This finding aligns with previous literature (Togoli et al., 2021), where the inducer elicits an attractive effect on the target. Importantly, our study also showed that the effect can arise with a relatively small number of trials, indicating that serial dependence manifests almost immediately and does not necessarily require extensive repetition. This is particularly relevant, as longer trial sequences may sometimes lead to decreased participant attention, potentially compromising the clarity of the results.

Moreover, the serial dependence effect observed in our temporal discrimination task appears to be larger than that reported in the original study by Togoli and colleagues (Togoli et al., 2021). This difference may be attributed to the nature of the stimuli we employed: unlike their study, which used stimuli incorporating the numerosity feature, our experiment utilized solid circular discs. Although no direct correlation was found between the serial dependence effect in temporal perception and the numerosity feature in their work, it is possible that the presence of the numerosity *feature* in their stimuli influenced temporal perception to some extent. This could explain why the effect we observed was more pronounced.

Within this task, our results indicated that a small subset of participants exhibited a particularly strong serial dependence effect compared to the rest of the group. This suggests that the overall

effect we observed may be driven, at least in part, by this cluster of individuals. So, inter-individual differences in sensitivity to the effect could reflect variations in temporal perception abilities or the use of different cognitive strategies during task performance. It is worth noting, however, that similar variability has been reported in visuospatial abilities. Thus, it is plausible that comparable individual differences exist in visuo-temporal perception as well. This notion is supported by evidence indicating that visuo-spatial and visuo-temporal attention share overlapping neural substrates (Coull & Nobre, 1998), reinforcing the idea that individual differences observed in the spatial domain may also manifest in the temporal domain.

Regarding the potential influence of the previous response on the PSE, no statistically significant relationships were observed. This may be explained by the fact that the PSE, computed based on the effect of the inducer stimulus, is not affected by prior responses. The task structure itself directs participants' attention toward the effect of the inducer, thereby reducing the probability that other recent information impacts their judgments. Nevertheless, despite the absence of a detectable effect, it cannot be conclusively ruled out, as the influence of previous responses may be weak or covered by other factors.

Temporal Reproduction task

Regarding the temporal interval reproduction task, it is important to note that this experiment was based on the works of Cicchini and Jazayeri (Cicchini et al., 2012; Jazayeri & Shadlen, 2010), who primarily investigated the effect of central tendency. Consequently, in our analyses, we first removed this effect in order to isolate and examine only the serial dependence effect, which was the focus of our study.

The effect we observed is consistent with previous findings in the literature. By applying an LMEM, we aimed to disentangle the influence of both the previous stimulus and the previous response on the reproduction error of the current temporal interval. Our results revealed an attractive serial dependence effect relative to the previous response, alongside a repulsive effect relative to the previous stimulus. This pattern of opposing effects suggests that such a dual nature of serial dependence may be generalizable across different features and domains, indicating that it represents an intrinsic property of the phenomenon itself (Blondé et al., 2023; Sadil et al., 2024).

This dual effect of attraction and repulsion may reflect how the brain integrates prior information at two distinct stages of processing. At the sensory level, the brain adapts to the previous stimulus so that the current stimulus is perceived as different, thereby preventing redundancy and enhancing sensitivity to change. In contrast, when a reproduction of the stimulus is required, processes emerge that bias perception toward the previous response; this attractive effect serves to stabilize perception over time. Thus, the brain employs both mechanisms simultaneously, relying on prior experience to maintain perceptual stability while also adapting to ensure greater accuracy in representing the surrounding environment.

Different serial dependence effects emerge from different tasks

Although our results indicate the presence of serial dependence in both tasks, we did not observe any correlation between the two effects. This may suggest that the different task types elicit distinct mechanisms underlying serial dependence. In contrast, studies in the literature, such as Guan and Goettker (Guan & Goettker, 2024), have shown that when the same task type is employed but different features are analyzed, serial dependence effects tend to correlate with one another; however, this correlation does not extend to oculomotor tasks. These findings indicate that the nature of the task itself can modulate which components of serial dependence become apparent. In fact, the two tasks have different structures: in the discrimination task, an inducer stimulus is specifically designed to elicit the serial dependence effect, whereas in the reproduction task, both the previous stimulus and the prior response contribute to inducing serial dependence. Consequently, the effects that emerge from each task may differ and, therefore, may not correlate.

Additionally, a recent study suggests that in temporal reproduction experiments, the serial dependence effect may primarily arise from motor components – namely, the way the response is physically executed – rather than from the perception of the stimulus itself. Specifically, Wang and colleagues (T. Wang et al., 2023) demonstrated that the serial dependence observed in temporal estimates largely reflects the influence of motor actions from previous trials. This finding may account for the lack of correlation between tasks, indicating that it may not solely stem from perceptual differences across paradigms, but also from how responses are actually implemented in different tasks.

These factors likely account for the absence of a significant correlation between the serial dependence effects observed across these two distinct paradigms.

Absence of correlation with working memory

Although working memory is considered the most likely candidate underlying the memory processes involved in serial dependence, in this study no significant correlation was found, neither between working memory and the serial dependence effect observed in the temporal discrimination task, nor between working memory and the attractive or repulsive effects emerging from the reproduction task.

Some studies suggest that working memory can modulate serial dependence by integrating past and present stimuli to stabilize perception and memory, additionally engaging brain regions involved in memory and prediction, such as the right dorsomedial prefrontal cortex (Schwiedrzik et al., 2014). However, serial dependence can also occur without active involvement of working memory, for instance, in the absence of an explicit task requiring the maintenance of information (Fornaciai & Park, 2018a). When working memory is engaged, it can guide attention or modulate perceptual integration, thereby enhancing the effect of serial dependence; however, serial dependence can also occur without the conscious maintenance of information and thus without active involvement of working memory (Bliss et al., 2017; Mei et al., 2019).

Overall, our findings suggest that the structure of the task – including both the nature of the stimuli and the format of the required response – can substantially modulate the contribution of working memory to serial dependence. From this perspective, the absence of a correspondence between the effects observed in our two tasks may reflect the fact that they engage working memory to different extents, thereby eliciting distinct forms of serial dependence depending on the specific cognitive demands imposed by each task.

2.5 Conclusion

This chapter presented a study examining the presence of serial dependence in visual time perception. To this end, we employed two complementary paradigms – temporal discrimination and temporal reproduction – to assess whether the effects arising from each would be comparable. Our results indicate that the two tasks yield qualitatively different patterns of serial dependence, likely for several reasons. Mainly, structural differences between the tasks may further explain the absence of correlation: in the discrimination task,

serial dependence seems to be driven primarily by the previous stimulus (specifically, the inducer), whereas in the reproduction task, both the previous stimulus and the previous response may shape the observed effect.

We also sought to examine the relationship between working memory and serial dependence, a topic that remains a subject of ongoing debate. In the present study, no correlation emerged between working memory and serial dependence in either the temporal discrimination task or the reproduction task. This finding aligns with prior literature showing that, although working memory can amplify serial dependence by guiding attention or facilitating perceptual integration, it is not a necessary condition for the effect to arise. Consequently, the relationship between the two appears to depend strongly on task characteristics, stimulus properties, and response requirements.

The dissociation observed between the two tasks – both with respect to each other and to working memory – opens avenues for future research aimed at examining how serial dependence operates across different experimental and sensory modalities. Measuring serial dependence in temporal judgments and reproductions offers a valuable framework for investigating the contribution of distinct sensory inputs to time perception and for determining whether similar patterns arise in non-visual contexts. Such investigations could help clarify whether serial dependence reflects a modality-general principle of perceptual processing or whether it is shaped by domain-specific mechanisms.

Chapter 3

Serial Dependence in Auditory Timing: Stimulus and Interval Effects

This chapter is partially extracted from:

"Bertolasi, J., Esposito, D., Domenici, N., Gori, M. Serial dependence in auditory temporal perception is influenced by temporal proximity but not stimulus type. Acta Psychologica, 266, 106997. https://doi.org/10.1016/j.actpsy.2026.106997".

3.1 Introduction

In the previous chapter, we demonstrated the presence of serial dependence in visuo-temporal perception using two complementary tasks: temporal discrimination and temporal reproduction. These findings confirm that the effect is not confined to spatial or shape-related features but extends to the temporal domain as well, suggesting a more general mechanism that operates across multiple dimensions of visual perception.

From this perspective, a crucial next step is to extend the investigation of serial dependence beyond the visual domain, focusing in particular on audio-temporal perception. This direction

is motivated by well-established evidence that sensory modalities do not contribute equally to information processing: vision is the dominant channel for encoding spatial properties, whereas audition plays a primary role in representing temporal information. This functional dichotomy has been extensively documented in the literature (Gori et al., 2014; Gori, Sandini, et al., 2012), demonstrating that each sensory system provides a distinct and specialized contribution to perceptual processing.

A substantial body of research has consistently shown that the auditory system exhibits superior temporal sensitivity and precision compared to the visual system across a range of tasks, including rhythm perception (Hildebrandt et al., 2022), duration discrimination (Amadeo et al., 2020; Hildebrandt et al., 2022), and sensorimotor synchronization (Comstock et al., 2018). When auditory and visual stimuli are presented simultaneously, auditory information typically dominates temporal judgments, often overriding visual input, especially in tasks that demand high temporal accuracy (Recanzone, 2003).

Despite the central role of audition in time perception, the mechanisms underlying temporal processing remain only partially understood. Several theoretical frameworks have been proposed to explain how the nervous system represents duration. A first class of models posits the existence of dedicated timing mechanisms. One prominent example is the Scalar Expectancy Theory (Gibbon, 1977; Gibbon et al., 1984), which assumes that temporal judgments rely on an internal pacemaker that generates pulses that are accumulated and compared with memory traces, yielding duration estimates characterized by scalar variability. Other approaches, in contrast, argue that time is not encoded by an internal clock but instead emerges from distributed neural dynamics. Temporal entrainment models, such as those discussed by McAuley and Jones (McAuley & Jones, 2003) propose that the auditory system synchronizes to external rhythmic structures and that perceived duration arises from oscillatory states shaped by the surrounding temporal context.

Despite their conceptual differences, these models converge on the idea that duration judgments are not independent from recent perceptual history. A substantial body of evidence demonstrates that temporal estimates are systematically biased by immediately preceding stimuli, consistent with the phenomenon of serial dependence (Ivry & Hazeltine, 1995; Large & Jones, 1999; Pashler, 2001). This suggests that temporal processing integrates past and current information to promote perceptual stability.

Although studies have investigated serial dependence in auditory perception, all of this research has focused on specific *features* of auditory stimuli – e.g., tone frequency (Motala et al., 2020; Zhang & Luo, 2023), rate (Motala et al., 2020), vowel elements (Van der Burg et al., 2024) – or has examined auditory stimuli presented in conjunction with visual information (Murai & Whitney, 2021). In contrast, serial dependence in perception of temporal durations has received far less direct attention. Among these, Li, Wang, and Zaidel (B. Li et al., 2023) examined both sensory and decisional carryover effects in duration perception, demonstrating that past stimuli and previous responses can bias current temporal judgments in a modality-specific manner.

Some studies have also investigated temporal features, such as duration, and their relationship to serial dependence. For example, Burr and colleagues found evidence of an effect adaptable with the concept of serial dependence in an auditory discrimination task using empty stimuli (singletons, i.e., intervals delimited by two separate sounds) (Burr et al., 2013), while Li and colleagues provided analogous evidence with full stimuli (i.e., continuous sounds) (B. Li et al., 2023). Taken together, these studies suggest that the previous temporal context does indeed influence current perception; however, the question remains unresolved as to whether the effect is shared among all possible structures of stimuli that convey temporal information or whether it is independent of specific stimulus characteristics.

Additionally, it has been shown that performance in discriminating temporal auditory stimuli depends on the time interval between them and becomes progressively worse as the two stimuli occur closer together in time (Karmarkar & Buonomano, 2007). However, whether comparable dynamics can also affect serial dependence is still to be explored. Given the crucial interaction between two subsequent stimuli, we thus expanded our original scientific question, focusing on the role of the interval between the two as well.

In this chapter, we explored auditory temporal serial dependence starting from these questions. This led us to design a series of two-alternative forced-choice tasks where participants were presented with a reference stimulus, an inducer, and a test stimulus. In all tasks, participants were required to indicate which stimulus appeared to be longer between the reference and test. We implemented different experimental conditions, crossing the type of temporal intervals (full vs. empty) with the interstimulus interval (ISI) between inducer and test (short vs. long).

More specifically, we formulated two main hypotheses. First, based on evidence that full and empty intervals rely on partially distinct timing mechanisms, we expected the magnitude of serial dependence to differ between these two types of stimuli. Second, given that temporal discrimination performance varies with the delay between successive events, we hypothesized that increasing the ISI would reduce the effect of serial dependence.

3.2 Materials and methods

3.2.1 Participants

A total of 17 participants (age 28.9 ± 2.5 years) were recruited for this study. Participants were selected based on the inclusion criterion of having no history of neurological disorders and no hearing impairments. All individuals received both written and verbal explanations of the study's procedures and objectives and provided informed consent before participation. The experimental protocol was approved by the ethics committee of the local health authority (Comitato Etico, ASL3 Genovese, Italy) and conducted in accordance with the Declaration of Helsinki.

3.2.2 Apparatus, stimuli, and procedure

The stimuli design followed the auditory setup described by Burr and colleagues (Burr et al., 2013). We used auditory tones at a frequency of 400 Hz, sampled at 21.4 kHz, generated in MATLAB R2022b (The MathWorks Inc., 2022). Sounds were delivered through a Sony WH-CH720N headset, which has a frequency response of 50 Hz to 20 kHz. Instructions marking the start and end of each experimental block were displayed on a monitor using the MATLAB Psychophysics Toolbox (Brainard, 1997). Participants were seated in a quiet room, wearing the headset, with a keyboard for responses and a monitor directly in front of them.

In this experiment, participants were presented with a sequence of three stimuli: a first reference stimulus, followed by an inducer stimulus, and finally the test stimulus. The inducer stimulus was used to induce the serial dependence effect on the test interval. The reference stimulus had a fixed duration of 50 ms in all cases; the inducer stimulus could have three durations (25, 50, or 75 ms), while the test stimulus could take one of 11 values between 10

ms and 90 ms. After the presentation of the test, participants were asked to respond which interval, reference or test, they perceived as *longer*, by pressing on the keyboard the left key to respond "reference" or the right key to respond "test". After responding, the next trial started automatically after 1000 ms.

Since the aim of this study was to investigate whether the effect of serial dependence depended on the characteristics of the stimulus (i.e., whether prolonged sounds were used as stimuli or empty intervals delimited by two short sounds) or on the temporal distance between the inducer and its target (long or short), we adopted a 2×2 design so that we could evaluate all combinations.

In the case of experimental conditions with empty intervals (hereinafter referred to as *empty* stimuli), sinusoidal pulses of 4 ms were used to determine the intervals, while in the case of full intervals (*full* stimuli), the stimuli were continuous sinusoidal tones. As regards the distance between the inducer and test stimuli (understood as inter-stimuli interval, ISI), in the case of a short ISI, 4 ms was considered, while in the case of a long ISI, 300 ms was considered. For clarification purposes, experimental conditions will be labeled as empty-short ISI, empty-long ISI, full-short ISI, and full-long ISI.

In the empty-short ISI experimental condition, we employed five sinusoidal pulses of 4 ms: the first two pulses delimited the reference stimulus (with a fixed duration of 50 ms), subsequently, there was a pause of 2 seconds, and then, the third and fourth pulses for the *inducer* stimulus (with a duration of 25 ms, 50 ms or 75 ms), and, finally, the fifth pulse to define the end of the test stimulus (with a duration varying from 10 ms to 90 ms) (see Figure 3.1 panel A for the design of the experimental procedure).

For the full-short ISI experimental condition, unlike the previous one, the stimuli consisted of prolonged sounds. In this case, an ISI of 4 ms – corresponding to the duration of one pulse in the previous condition – was inserted between the inducer and the test stimuli. Specifically, the first sound covered the duration of the reference interval. After a 2-second pause, the second sound covered the duration of the inducer interval, followed by a brief 4-ms silence, which was then followed by a sound corresponding to the duration of the test interval (Figure 3.1 panel B).

In the empty-long ISI and full-long ISI experimental conditions, the structure of the stimuli was analogous to that of the previous conditions. Also in this case, there was a pause of 2 seconds between the first and second stimulus, while a pause of 300 ms between the second and third stimulus to evaluate the temporal relationship between the inducer and its target (the test stimulus). In the empty-long ISI, the nature of the stimuli was sinusoidal pulses like in the empty-short ISI condition, but in this case, a sixth pulse was added to create three distinguishable stimuli intervals (see Figure 3.1 panel C); in the last experimental setup (full-long ISI), the same format was followed, but with three continuous stimuli as in the full-short ISI condition (see Figure 3.1 panel D).

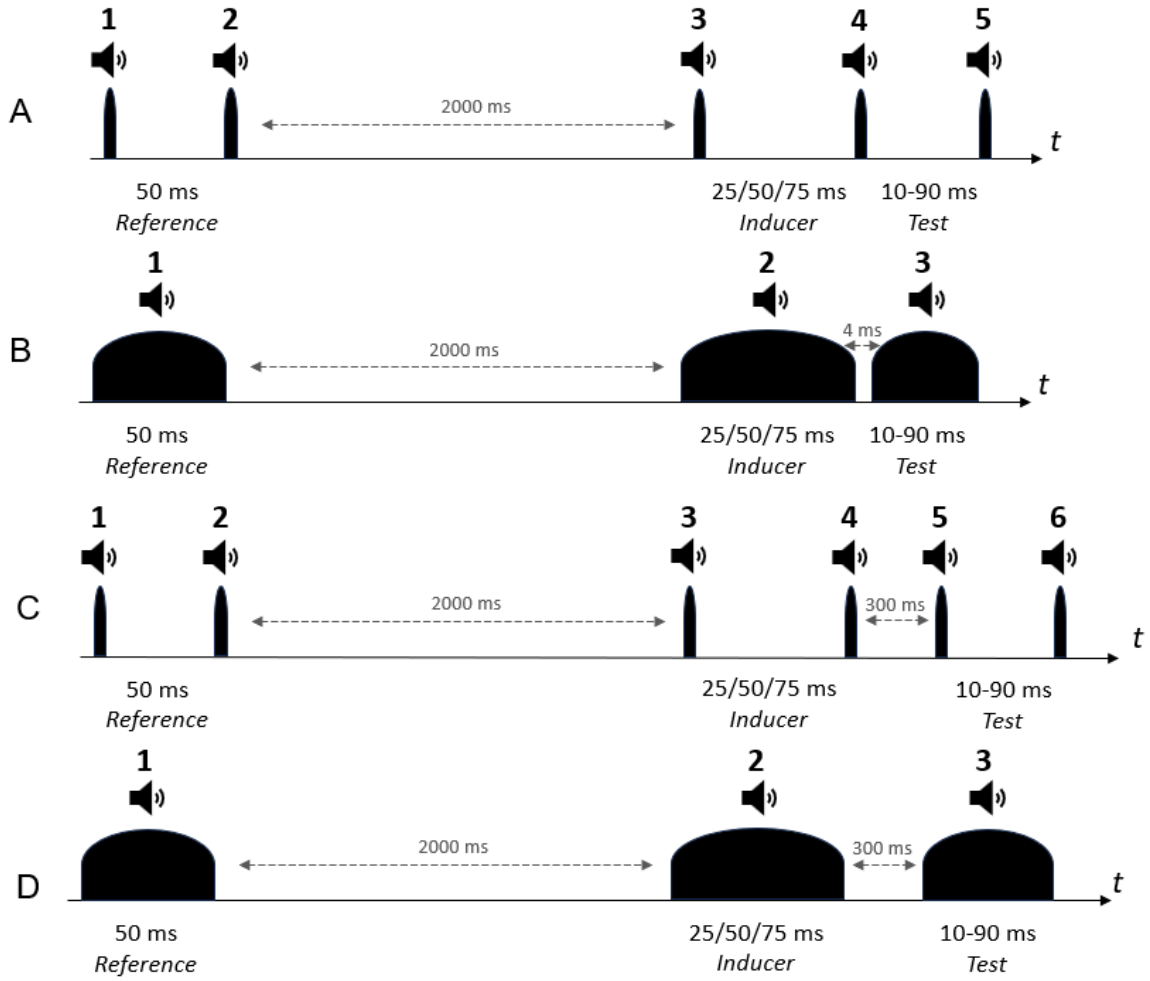

Figure 3.1 – Overview of the experimental conditions. In each experimental condition, the general structure consisted of a reference stimulus, followed by a short pause of a few seconds, an inducer stimulus, and finally a test stimulus. (A) 4 ms pure tone sounds delimit the sequence of stimuli presented. (B) The three stimuli proposed are full sounds, with a time pause of 4 ms between the inducer and the test one, like the opposite copy of the first experiment. (C) Empty intervals with pure tones of 4 ms as a delimiter, but with an additional pure tone sound and a pause of 300 ms to make clear the difference between the inducer and test stimuli. (D) Full-

stimuli version of the previous experimental condition, with prolonged sounds as stimuli and a pause of 300 ms between the last two stimuli.

For each experimental condition, inducer and test were combined in a 3×11 matrix design, thus defining 33 couples. Each combination of inducer and test was presented 1 time per block (for a total of 5 blocks, so 165 trials total). A single experimental condition duration was approximately 15 minutes. Participants were allowed to take short breaks at the end of each experimental block.

Before starting the main experiment, a pre-test control task was conducted to assess participants' individual ability to correctly discriminate between auditory stimuli without the inducer stimulus. This discrimination pre-test involved only the reference and test stimuli (with a 2-second ISI between them) and included both *empty* and *full* stimuli conditions. The durations of the two stimuli were identical to those used in the main experimental conditions. Each reference-test combination (1×11) was presented five times, for a total of 55 trials within a single experimental block. The total duration of this control task was approximately 5 minutes.

3.2.3 Data analysis

To estimate the required sample size for our study, we conducted a power analysis on a pilot dataset of five participants. Using an α of 5% and a power of 80%, we found that a sample of 10 individuals was sufficient to measure the effect of interest. From our initial sample of 17 participants, two participants were excluded from the final analysis due to poor performance in the control task (as their error rate exceeded 20% on trials with the shortest and longest test stimuli durations). This resulted in a total final sample of 15 participants, which is in line with the result of our power analysis.

To assess the magnitude of the serial dependence effect, we employed a cumulative Gaussian function to model the relationship between the magnitude of the test stimulus and the proportion of "test longer" responses. This enabled us to calculate the point of subjective equality (PSE), which is determined as the median of the cumulative Gaussian curve, thereby indicating the participant's bias. This analysis was conducted individually for each participant and each inducer stimulus value. The serial dependence effect was computed as the difference in PSE (delta, Δ) when the inducer was 75 ms and 25 ms. In addition, we estimated the just

noticeable difference (JND) as half the difference between the stimulus magnitudes corresponding to 75% and 25% "test longer" responses on the fitted psychometric function.

To evaluate the effects of ISI (long vs. short) and type (empty vs. full) on ΔPSE, we performed a two-way repeated measures ANOVA using the *aov* function with ΔPSE as the dependent variable, ISI and type of stimuli as within-subject factors, and participants (ID) as a repeated measures factor. Prior to the analysis, the assumptions of normality and homogeneity of variance were assessed. Then we evaluate whether ΔPSE differed significantly from zero in each experimental condition: to this end, ΔPSE values were first averaged within participant for each combination of ISI and stimulus type. Then, one-sample t-tests against zero were conducted separately for each condition. To control for multiple comparisons, p-values were adjusted using the Bonferroni correction.

As previously said, generally, the serial dependence effect is defined as the difference between the PSE obtained with the longest and shortest inducer durations; the baseline condition, corresponding to the case in which the inducer and the reference stimulus had the same duration (50 ms), was not included in the computation of ΔPSE. To evaluate the effect of the inducer stimulus in generating serial dependence, as well as the influence of stimulus type (i.e., prolonged sound or empty interval) and the ISI between the inducer and the test, we employed a Linear Mixed-Effect Model (LMEM). In this model, the PSE was used as the dependent variable, while the inducer, stimulus type, and ISI served as predictors. Participants' ID was included as a grouping variable to account for inter-individual variability. The model was specified as $\mathrm{PSE} \sim 1 + \mathrm{inducer} * \mathrm{stimulus}_{\mathrm{type}} * \mathrm{ISI} + (1|\mathrm{ID})$ in Wilkinson notation. The overall effects of the factors and their interactions were assessed through ANOVA using the *lmerTest* package. Subsequently, to examine how the relationship between PSE and the inducer varied as a function of stimulus type and the ISI between the inducer and test stimuli, we conducted post-hoc analyses using the *emtrends* function from the emmeans package. This function was used to estimate the slope of the inducer variable within each level of the factors. Differences between slopes across levels were then compared, with corrections for multiple comparisons applied. To assess whether the observed PSE shifts could be explained by other temporal effects (e.g., temporal summation or recency bias), we performed an additional analysis comparing the PSE in the control condition (so, without inducer) with the PSE in the

short-ISI condition when inducer and reference durations were matched (50 ms). Bayesian paired-samples t-tests were conducted separately for each stimulus type.

As it is known that auditory empty and full intervals show significant differences at the perceptual level (Grondin, 1993; Wearden et al., 2007), we also assessed this element. To judge perceptual sensitivity, indexed by the JND, we fitted an LMEM with JND as the dependent variable: the model included the inducer, ISI (short vs. long), and stimulus type (empty vs. full) as fixed effects, as well as all their interactions. Participants (ID) were included as a random intercept to account for repeated measures. The model was defined as $\mathrm{JND} \sim 1 + \mathrm{inducer} * \mathrm{stimulus}_{\mathrm{type}} * \mathrm{ISI} + (1|\mathrm{ID})$ in Wilkinson notation. Statistical significance of overall effects was assessed using an ANOVA (*lmerTest* package).

The power analysis was performed using G*Power 3.1 (Faul et al., 2009), psychometric curve plotting, PSE, and JND extraction were carried out in MATLAB R2022b (The MathWorks Inc., 2022), Bayesian tests were conducted in JASP 0.17.1.0 (JASP Team, 2023), and the LMEM, ANOVA, and post-hoc analyses were conducted in R version 4.4.2 (R Core Team, 2021).

3.3 Results

To assess the presence of the serial dependence effect, we examined how the inducer stimulus influenced participants' perception of the subsequent target stimulus – that is, the test stimulus. To this end, we computed the PSE for each inducer condition using a psychometric function and quantified the magnitude of the serial dependence effect as the difference between the PSE corresponding to the 25-ms inducer and that corresponding to the 75-ms inducer (ΔPSE).

Figure 3.2 displays representative psychometric curves for each experimental condition, with each panel corresponding to one experimental condition.

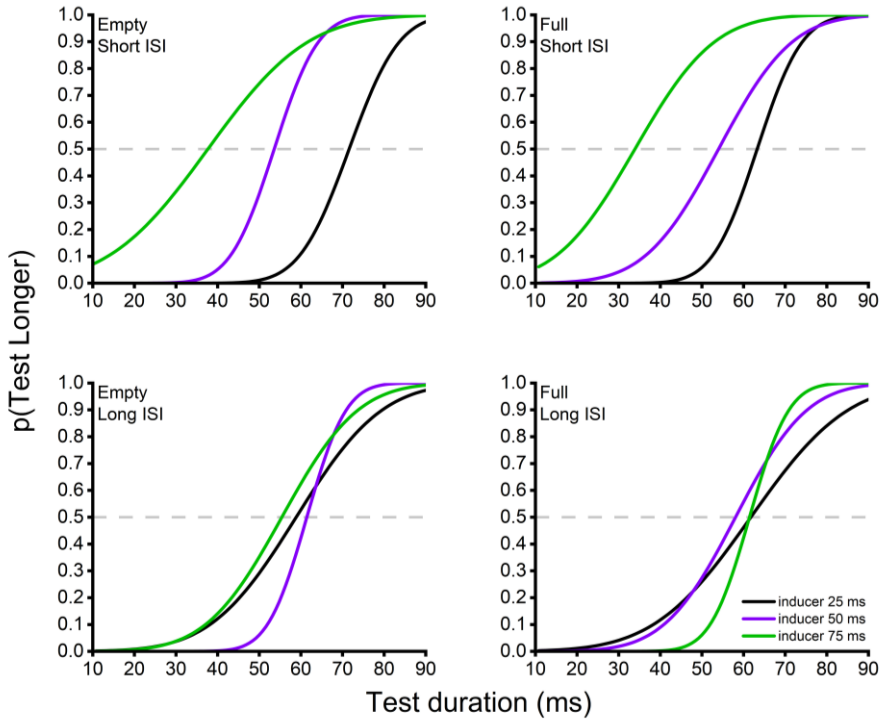

Figure 3.2 – Representative single-subject psychometric curves for each experimental condition. Each psychometric represents the proportion of "test longer" responses as a function of test duration, across different inducer durations (25 ms, 50 ms, and 75 ms). The psychometric corresponding to the 50 ms inducer represents the baseline for the other two inducer conditions.

Table 3.1 reports the PSE values for each inducer across all four experimental conditions. The table also presents the corresponding serial dependence values (ΔPSE) for each experimental condition. While for the control tasks, the PSE in the empty condition was 52.1 ± 2.4 ms, whereas in the full condition was 53.0 ± 0.9 ms.

Table 3.1 – PSE values for each experimental condition and serial dependence magnitude. For each inducer value, the corresponding PSE is reported as the mean ± SD across all participants. The serial dependence effect (ΔPSE) is then presented as the difference between the PSE obtained when the inducer was 75 ms and the PSE obtained when the inducer was 25 ms.

Condition	Inducer 25 ms	Inducer 50 ms	Inducer 75 ms	ΔPSE
Empty stimuli ISI short	76.0 ± 3.4 ms	49.6 ± 2.4 ms	39.9 ± 2.3 ms	36.1 ± 2.8 ms
Full stimuli ISI short	65.5 ± 5.7 ms	54.6 ± 3.1 ms	32.5 ± 3.4 ms	33.0 ± 7.3 ms
Empty stimuli ISI long	53.2 ± 1.9 ms	51.6 ± 2.2 ms	50.7 ± 1.5 ms	2.5 ± 2.0 ms
Full stimuli ISI long	56.3 ± 1.6 ms	49.6 ± 1.2 ms	51.6 ± 1.7 ms	4.7 ± 2.2 ms

To evaluate the effect of the stimulus type (empty vs. full) and ISI (short vs. long), as well as their interaction, on ΔPSE, we run a two-way repeated-measure ANOVA. Our analysis highlighted a main effect of the *ISI* ($F(1,14) = 45.49$, $p < 0.001$). In contrast, no significant main effect of the *stimulus type* ($F(1,14) = 0.01$, $p = 0.91$) and interaction ($F(1,14) = 0.88$, $p = 0.36$) were found. Overall, these results confirmed the occurrence of significant changes in performance due to the inducer's presence at lower ISI, but not for longer ones, regardless of the stimulus type (Figure 3.3).

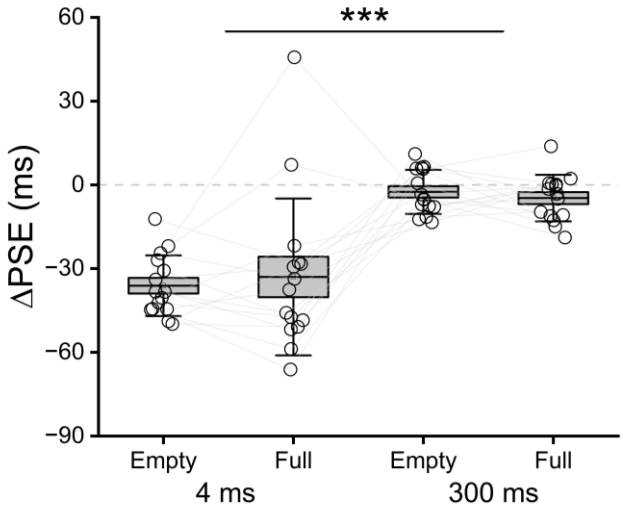

Figure 3.3 – Effect of serial dependence (ΔPSE) based on stimulus type and ISI. ΔPSE was calculated as the difference between PSE with 75 ms and 25 ms inducers. As from the ANOVA, this plot shows that serial dependence affects serial dependence at short ISI, regardless of stimulus type.

To further confirm the presence of serial dependence at shorter ISIs, we performed one-sample t-tests comparing ΔPSE in each condition against zero. ΔPSE differed significantly from zero in both *short ISI* conditions (empty: $t(14) = -12.90$, $p < 0.001$; full: $t(14) = -4.55$, $p = 0.002$), while it did not significantly differ from zero with *long ISI* (empty: $t(14) = -1.24$, $p = 0.94$; full: $t(14) = -2.20$, $p = 0.18$).

While these analyses highlighted the impact of short ISI on the insurgence of serial dependence, they inevitably precluded the inclusion of the PSE when the inducer lasted 50 ms. To provide a more exhaustive overview of the inducer's influence, the type of stimulus (empty or full), and the ISI (short or long) on the PSE, we thus applied an LMEM. The overall effects were verified with ANOVA followed by post-hoc analysis using slope estimation to explore differences between factor levels.

The results of the ANOVA applied to the LMEM showed significant main effects for *inducer* ($F(1,158) = 94.57$, $p < 0.0001$) and *ISI* ($F(1,158) = 56.07$, $p < 0.001$), while the *type* of stimulus was not significant ($F(1,158) = 0.30$, $p = 0.59$). Among the interactions, only *inducer* × *ISI* was significant ($F(1,158) = 62.00$, $p < 0.001$), while the others were not significant ($p > 0.22$) (Figure 3.4). Post-hoc analysis of the slopes of the inducer stimulus revealed a significant difference between the two *ISI* levels (contrast ISI 4 ms – ISI 300 ms: estimate = -0.62 ± 0.08, $p < 0.001$), while no significant difference was observed between the empty or full *type* of stimulus (contrast empty stimuli – full stimuli: estimate = -0.01 ± 0.08, $p = 0.91$).

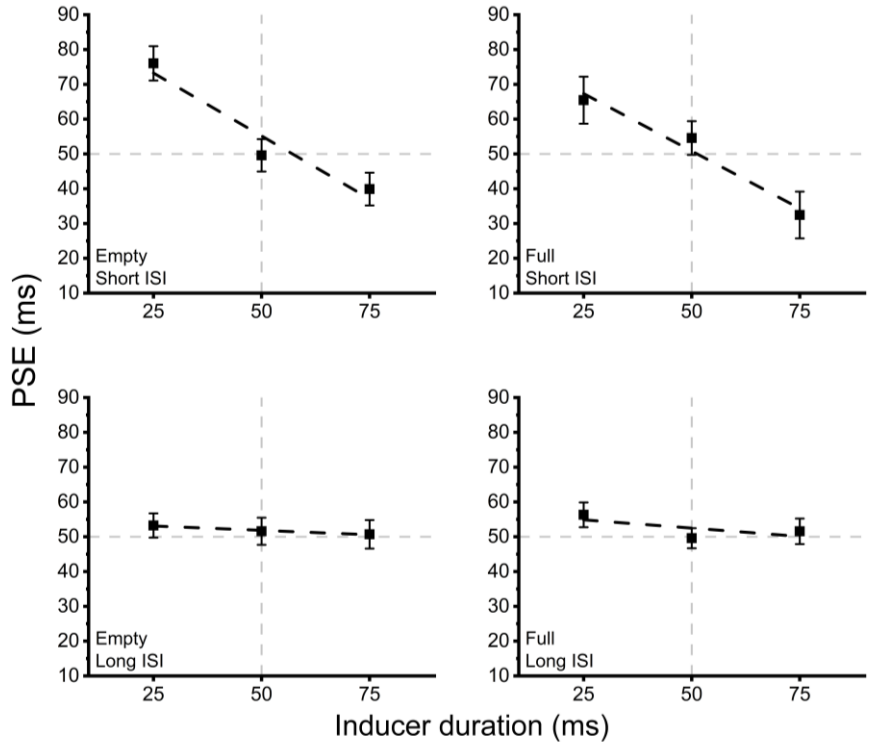

Figure 3.4 – PSE as a function of inducer duration (25, 50, and 75 ms). Each subplot corresponds to a different experimental condition defined by the combination of inter-stimulus interval (short vs. long) and stimulus type (empty vs. full). The pattern of results shows a systematic modulation of PSE by inducer duration, with this effect being significantly influenced by ISI.

Furthermore, Bayesian paired-samples t-tests provided moderate evidence in favor of the null hypothesis for both stimulus types, indicating no reliable difference between the PSE in the control condition and the PSE obtained with a 50 ms inducer in the short-ISI condition (empty stimuli: $BF_{01} = 3.112$, error = 0.013; full stimuli: $BF_{01} = 3.445$, error = 0.012). These findings suggest that the mere presence of an inducer stimulus does not systematically shift the PSE,

making other temporal effects like temporal summation account for the observed effects unlikely.

Finally, the perceptual sensitivity (JND) was analyzed by applying an ANOVA to the overall effects of an LMEM including inducer, ISI (long vs. short), stimulus type (empty vs. full), and their interactions as fixed effects, and a random intercept for participants.

The ANOVA revealed a significant main effect of stimulus *type* ($F(1,158) = 4.25$, $p = 0.041$), with the JND with empty stimuli (12.8 ± 1.02 ms) being larger than that with full stimuli (12.2 ± 1.02 ms), and no significant effects for the *inducer* ($F(1,158) = 3.24$, $p = 0.074$) or *ISI* ($F(1,158) = 1.90$, $p = 0.170$). None of the two-way or three-way interactions reached statistical significance (all $p > 0.05$).

3.4 Discussion

This study was conducted to advance our understanding of serial dependence in the perception of auditory temporal durations, a topic that is comparatively underexplored relative to serial dependence effects observed across other auditory stimulus features. What we did was to fill this gap by focusing on auditory time perception, examining the role of the type of stimuli involved and the ISI between the inducer and the subsequent stimulus to be judged. To address this, we built upon a well-established study in the literature that reported findings consistent with serial dependence (Burr et al., 2013).

First, we confirmed that serial dependence occurs in auditory temporal perception, as inducers of different durations elicited coherent shifts in performance (i.e., longer ones determined temporal overestimation, and vice versa). Second, we highlighted serial dependence when employing either empty or full intervals, i.e., irrespective of stimulus type, showing how auditory serial dependence is not specific to a given temporal format. However, such an effect was significantly modulated by the ISI between the inducer and the subsequent stimulus, with longer ISI determining no serial dependence effects at all.

The nature of the stimuli doesn't influence the serial dependence effect

Given the critical role of timing in auditory perception (M. R. Jones & Mcauley, 2005; McAuley & Jones, 2003), and since previous studies have predominantly employed pure

tones, varying the intensity or pitch of the stimuli (B. Li et al., 2023; Motala et al., 2020; Wiener et al., 2014), making it challenging to identify whether serial dependence magnitude depends on the structural characteristics of the stimuli presented, we investigated potential differences in auditory serial dependence by comparing temporal performance when using "empty" (i.e., delimited by two brief tones at the onset and offset) and "full" (i.e., continuous sounds) stimuli (Grondin et al., 1998).

Our results demonstrated no significant difference in the perception of temporal stimuli between empty and full intervals: both were equally effective in eliciting serial dependence effects, with the inducer stimulus coherently influencing the perception of the test stimulus. This suggests that the serial dependence effect in auditory time perception is not specific to the type of temporal information conveyed but can be elicited irrespective of it. Crucially, significant differences at the perceptual level have been observed when discriminating between auditory empty and full intervals (Grondin, 1993), with full intervals often being overestimated (Wearden et al., 2007). Consistent with this literature, our analysis of perceptual sensitivity revealed a significant main effect of stimulus type on JND, indicating different levels of temporal discrimination for empty and full intervals. However, despite this, serial dependence emerged for both types of stimuli, suggesting that perceptual shifts induced by serial dependence might not be a sole consequence of differences in sensory precision but may reflect more complex interactions within the brain.

One possibility is that serial dependence reflects a general stabilization mechanism in auditory time perception, independent of the specific carrier of temporal information. Alternatively, the effect may extend beyond stimulus features – or even beyond a single sensory modality – given the proposed supramodal nature of temporal processing (Buhusi & Meck, 2009; Heron et al., 2012; Merchant et al., 2013).

Effect of temporal relationship between the inducer and the target stimulus

A central question also concerns how the temporal interval separating two stimuli influences their perception. Specifically, it is relevant to ask whether the magnitude of the serial dependence effect depends on the time elapsed between the inducer and the test stimulus. To investigate this, we introduced two different inter-stimulus intervals (ISIs): a very short interval (4 ms) (Burr et al., 2013) and a longer interval (300 ms) (Togoli et al., 2021), allowing us to assess how this variable modulates performance. Notably, as shown in Chapter 2 of this

thesis, a 300 ms gap in the visual modality is sufficient to allow the inducer to influence the perception of the test stimulus duration (Togoli et al., 2021). However, the same temporal gap might be too large to elicit comparable effects in audition. In fact, Goldstone and Lhamon (Goldstone & Lhamon, 1974) demonstrated early on that there is a difference between sensory modalities in the perception of temporal durations, a finding that has been reconfirmed in subsequent studies (Burr et al., 2009; Fitzgibbons, 1984; Fornaciai & Park, 2019; Lau & Maus, 2019), including both cross-modality and single-sense specific research. This refined auditory temporal sensitivity suggests that long intervals, such as the 300 ms used in our studies, may not be optimal for observing serial dependence in auditory perception with a temporal discrimination task.

These results are in conflict with Li and Wang's experiment (B. Li et al., 2023), where they used continuous audio or visual stimuli with a 300 to 900 ms duration of the stimuli in a temporal bisection task, which provides a precise characterization of how the serial dependence effect emerges. Nonetheless, we argue that this difference may stem from the fact that temporal bisection differs from a simple duration comparison: in temporal bisection, participants are presented with various durations and must classify each stimulus as either "more similar to the short duration" or "more similar to the long duration", based on their current percept. In contrast, our experiment employs a temporal discrimination task, in which participants directly compare a reference stimulus with a test stimulus and determine which one lasted longer and, to elicit the serial dependence effect, an *inducer* stimulus is employed. As a result, the serial dependence effects observed in those tasks could be elicited differently due to the different nature of the task and analysis involved.

Within this framework, the diminished serial dependence observed at longer temporal intervals underscores the importance of temporal precision for perceptual carryover effects. This pattern suggests that, in the auditory domain, serial dependence may preferentially operate over time scales where fine-grained temporal discrimination is required, rather than over longer intervals that encourage categorical or decision-based processing.

3.5 Conclusion

In this chapter, we investigated the effect of serial dependence in the temporal domain within the auditory modality. Our results demonstrate that serial dependence is present in the auditory perception of stimuli within discrimination tasks, where an inducer stimulus is used to alter the perception of the subsequent target stimulus, thereby eliciting serial dependence. We further showed consistent serial dependence effects regardless of the type of stimuli (whether full or empty) but only with short ISI, suggesting that the serial dependence effect is contingent upon the temporal relationships between the inducer and test stimuli. Our results challenge the hypothesis that auditory temporal serial dependence depends on the type of stimulus conveying temporal information, and instead show that it varies as a function of the temporal interval between the inducer and the subsequent stimulus. Further studies might be needed to deepen the role of the type of stimulus on serial dependence, e.g., comparing the effect of cross-stimulus effects between empty and full intervals, and also to determine the minimal ISI required between the inducer and its target for a robust emergence of serial dependence in auditory temporal perception.

Chapter 4

Serial Dependence in Tactile Motion Direction Perception with and without Vision

This chapter is partially extracted from:

"Vitale, A.†, Bertolasi, J.†, Orciari, L., Lorini, C., Parmiggiani, A., Murray, M. M., Wallace, M., Gori, M. TaK: a Tactile Knob to Investigate Orientation Perception, 2025 IEEE Medical Measurements & Applications (MeMeA), Chania, Greece, 2025, pp. 1-6, doi: 10.1109/MeMeA65319.2025.11068010".

"Vitale, A., Bertolasi, J., Esposito, D., Parmiggiani, A., Gori, M. Just noticeable difference in motion direction perception: assessing the effect of blindness onset and orientation, 15th International Conference on Human Haptic Sensing and Touch Enabled Computer Applications (EuroHaptics). Accepted."

4.1 Introduction

In the preceding chapters, serial dependence was examined within the visual and auditory domains, with a specific focus on temporal perception in each system. Having demonstrated

that the effect reliably emerges across these two sensory modalities, we turned our attention to a third system, aiming to investigate whether serial dependence similarly extends to the tactile domain.

Touch constitutes a fundamental sensory modality, playing a crucial role in human perception, communication, and interaction with the environment (Saluja et al., 2024). It encompasses a wide range of sensations – including pressure, vibration, temperature, and pain – mediated by specialized receptors located in the skin and deeper tissues (Owens & Lumpkin, 2014). These tactile signals are conveyed to the brain through a complex network of neural pathways, where they are integrated to form a coherent representation of the tactile world. In particular, tactile motion perception relies on the integration of spatiotemporal cues delivered to the skin, requiring the nervous system to combine information about the timing, intensity, and spatial progression of mechanoreceptor activation to infer how an object is moving across the surface of the body (Coelho et al., 2025; Ryan et al., 2021). This process engages direction-selective mechanisms in the somatosensory system, which operate in ways that share important analogies with visual motion processing (Ryan et al., 2021). Prior research has shown that these mechanisms do not develop in isolation: the presence of vision, particularly during early developmental stages, can shape how spatial and directional tactile cues are encoded and interpreted (Coelho et al., 2025). Conversely, when vision is absent from birth or lost later in life, the brain may reorganize differently, sometimes enhancing low-level tactile acuity while altering or even impairing more complex spatial computations.

Visually impaired individuals provide a particularly informative contrast when discussing human touch, because their tactile perception is shaped not only by the same mechanoreceptive principles as sighted people but also by the absence of visual input. Numerous studies show that blind adults tend to detect finer textures and spatial details than sighted controls, with reliably lower grating-orientation thresholds even after accounting for factors such as age, gender, and Braille experience (Goldreich & Kanics, 2003). Importantly, this enhanced acuity is not limited to those who were blind from birth or who read Braille regularly, but it also appears in people who lost their vision later in life and never engaged in systematic tactile training, suggesting that the improvement reflects a broad, experience-independent reorganization rather than the result of specialized practice (Goldreich & Kanics, 2003). What most clearly differentiates blind individuals is the way their brains support this

heightened performance: during tactile tasks, especially those involving spatial judgments, regions of the occipital cortex normally devoted to vision become engaged, demonstrating a form of cross-modal plasticity that effectively repurposes visual circuitry to enhance touch (Cohen et al., 1997; Sadato et al., 1996, 1998, 2002).

In light of this, the present chapter turns to an unexplored question: does serial dependence operate in the perception of tactile motion direction, and does visual experience have a role in this process? Research on tactile serial dependence remains scarce overall, with the only available study indicating that judgments of tactile orientation perception exhibit systematic attraction toward previously experienced stimuli (G. Wang & Alais, 2025b, 2025a); this scarcity contrasts sharply with the extensive body of work describing serial dependence in vision (Cicchini et al., 2018; J. Fischer & Whitney, 2014; Manassi et al., 2023). Despite these initial insights, the field still lacks any systematic investigation of tactile serial dependence both in sighted and visually impaired individuals. This gap is particularly striking, as the reorganization of tactile processing that accompanies visual impairment may directly affect the mechanisms through which serial dependence integrates previous stimuli into current perceptual judgments.

To achieve this, we adapted the orientation reproduction paradigms commonly employed in visual serial dependence research and translated them into the tactile domain: participants haptically explored a moving grating and were subsequently asked to reproduce its direction of motion.

Before proceeding, it was first necessary to ensure that visually impaired and sighted participants could respond in the same way, as most knobs used to indicate directions lack tactile references and do not provide any physical indication of the set orientation, or they require visual support from a screen for correct use. To this end, we developed a custom device specifically designed to deliver clear haptic feedback corresponding to the selected direction.

Secondly, it was necessary to quantify the baseline performance in perceiving tactile motion direction across both (sighted and visually impaired) participant groups. This step allowed us to ascertain the ability of all the populations involved to correctly discriminate the stimuli presented.

The chapter is consequently organized into three main sections. The first section presents the tactile knob developed in our laboratories. The second section describes the preliminary experiment aimed at investigating tactile perception of motion direction. Finally, the third section provides a detailed description of the serial dependence experiment conducted with both sighted and visually impaired participants and the preliminary results we achieved.

4.2 Addressing the gap: a tactile tool for orientation study with visually impaired people

As previously said, the ability to perceive and interact with the environment is crucial for human adaptation. For individuals with visual impairments, touch and auditory cues become primary sources of information, often compensating for the absence of vision. Previous research has shown that tactile processing can partially substitute for vision, even leading to cortical reorganization (Sadato et al., 2002; Wanet-Defalque et al., 1988), and this highlights the importance of touch as a modality for perceiving spatial information and guiding behavior, enabling visually impaired individuals to construct mental representations of their surroundings for navigation, obstacle avoidance, and orientation (Bertonati et al., 2020; Tivadar et al., 2019, 2020).

Recognizing the crucial role of touch, many assistive technologies have been developed to provide spatial cues through tactile feedback, including raised-line maps (Brock & Jouffrais, 2015), braille-based interfaces (Mascetti et al., 2011), and vibrotactile navigation systems (Mattheiss et al., 2015). While these tools improve the users' spatial understanding, they often focus on large-scale navigation and do not provide information concerning the local properties of spatial information, such as tactile orientation. Few devices allow for a precise, quantitative assessment of how visually impaired individuals perceive tactile orientation (Gori et al., 2021; Postma et al., 2008), and existing solutions typically depend on keyboard inputs or static tactile patterns, limiting their applicability to continuous, real-time haptic exploration.

To address this gap, we developed a tactile goniometer called TaK (Tactile Knob), designed to deliver clear, tactile-only feedback for orientation reproduction. Unlike conventional knobs, TaK enables participants to reproduce perceived orientations accurately and quantitatively,

ensuring that responses are grounded in conscious tactile perception. This new device combines accessibility, reproducibility, and precise measurement to offer an easy tool for studying visually impaired individuals' perception of orientation and direction, to contribute to a deeper understanding of tactile spatial processing in this population.

4.2.1 Mechanical and electronic design

The knob design was developed based on previous experience within our team (Cuturi & Gori, 2017, 2019), in which a 3D-printed arrow was mounted on a circular base to measure orientation (Figure 4.1 panel A). In that earlier device, however, measurements were recorded manually by the operator, with precision limited to whole degrees and no capacity for detecting decimal values. The primary innovation introduced with TaK is the integration of an electronic system for automatic angle reading, which eliminates human error and substantially improves measurement accuracy.

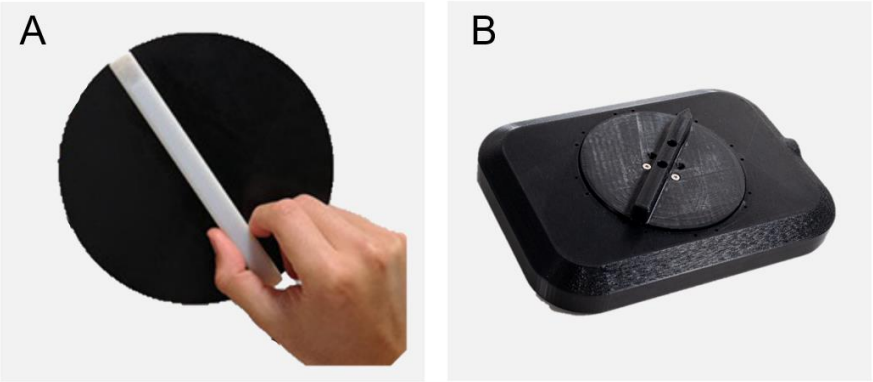

Figure 4.1 – Previous orientation knob prototype (A) compared to the new TaK device (B). The first picture is extracted and readapted from a work by Cuturi and Gori (Cuturi & Gori, 2017).

From a mechanical perspective, all components were fabricated in ABS M30 using a Fortus 400 FDM printer (Figure 4.2 panel A). The overall dimensions of the device correspond to an A4 sheet (30×21×6 cm) with rounded edges. The base houses the electronic components, while the upper section features a rotating platform with a radius of 15 cm and an arrow-shaped bar (15×1.5×1.5 cm), measuring 13 cm at the base and tapering to 2 cm at the tip. To allow mechanical locking at specific positions, holes were added every 45°, enabling stops in both clockwise and counterclockwise directions.

The electronic system (Figure 4.2 panel B) is based on an MA710 angle sensor paired with a diametrically magnetized cylindrical magnet mounted on the rotating shaft, connected to an Arduino Nano programmed to read data using the SimpleFOC library (version 2.3.4). Communication between the sensor and the board occurs via an SPI interface, while connection to a computer is achieved through USB, compatible with both Windows and Linux systems. The device continuously acquires the rotation angle and transmits the data in ASCII format with two decimal places of precision via a UART serial interface. Additionally, the knob can be operated in either a horizontal or vertical plane by simply redefining the zero position in the code.

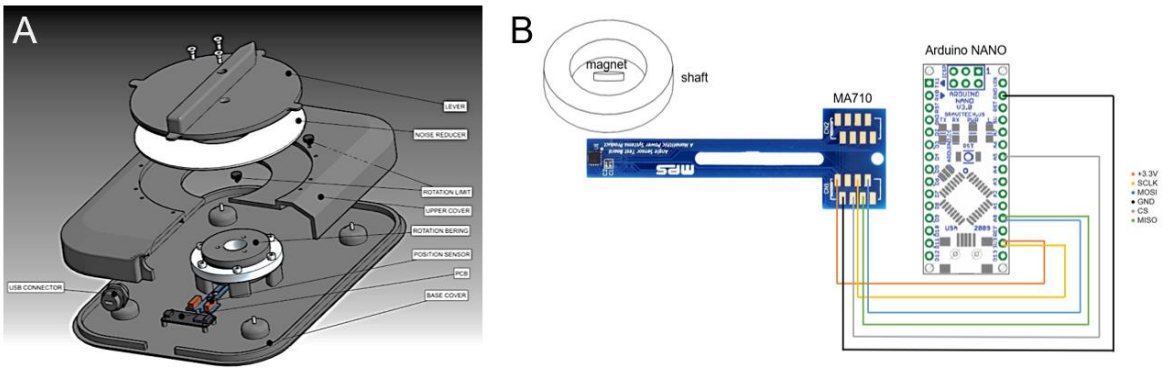

Figure 4.2 – Mechanical structure and electronic circuitry of TaK. (A) Exploded view of the TaK device from an isometric perspective, highlighting each component and its placement. (B) Electronic circuitry of the knob, showing the 3.3 V power supply to the encoder, SPI connection to the Arduino, and UART-over-USB communication to the PC.

4.2.2 Experimental design and procedure

Our objective was to address two main experimental questions to evaluate the effectiveness of TaK: first, whether sighted participants could achieve performance comparable to that obtained using a visual knob versus TaK; and second, whether visually impaired participants could reach performance levels similar to those of sighted individuals when using TaK.

The task employed in this experiment was a reproduction task in which participants were asked to perceive the direction of motion of a grating and reproduce it using a knob.

To present the tactile stimuli, we used a device developed in our laboratories, called RoMAT (Robot for Multisensory Analysis and Testing) (Gori et al., 2021), a robotic platform designed for multisensory integration studies (see Figure 4.3). The device consists of two vertically

aligned rotating platforms, spaced 20 cm apart: an upper wheel for visual stimulation and a lower wheel for tactile stimulation. Each wheel is equipped with a belt composed of 3D-printed ridges, 1 mm in height and spaced 2 mm apart, simulating the texture of a grating. The wheels move at a constant speed of 3 cm/s and rotate within an angular range of ±40° (for a total of 80°).

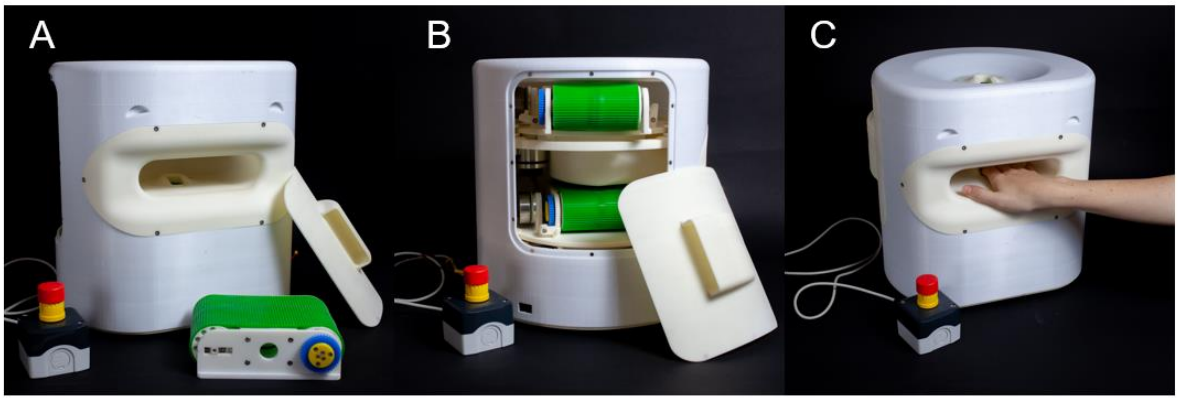

Figure 4.3 – View of the RoMAT device. (A) External view of the device with the access compartment and modular components removed. (B) Internal view showing the two rotating platforms mounted on motorized axes for tactile stimulation. (C) Example of use with the hand inserted into the front opening for tactile interaction.

To address the first question, sighted participants completed the task twice: once using a commercial visual knob (Griffin PowerMate USB Programmable Controller), where the selected direction was displayed on-screen as a vector, and once using TaK. To address the second question, we compared the performance of sighted and visually impaired participants using TaK exclusively.

Participants sat in a quiet room, in front of RoMAT and the knob; they were asked to feel the tactile wheel movement for 3 seconds with their right-hand index finger, then use the same hand to reproduce the perceived direction with the knob.

Five orientations were tested (-40°, -20°, 0°, 20°, 40°), with 0° as horizontal, negatives indicating top-left, and positives top-right movement. The grating pattern was always perpendicular to the movement direction (see Figure 4.4 panel A). Each participant completed 15 trials per orientation (75 trials total per condition). A familiarization phase preceded testing, during which participants practiced setting the knob to horizontal or vertical positions. The experiment lasted a total of 15 minutes.

4.2.2.1 Participants

5 sighted participants (age 28.4 ± 1.8 years) were recruited from our laboratory to participate in the experimental protocol. Additionally, 5 visually impaired participants (age 41.2 ± 5.3 years) were recruited from the general population. The visually impaired group comprised two individuals with late-onset blindness and three with early-onset blindness, where early-onset refers to congenital blindness and late-onset refers to blindness acquired after two years of age (Lewis & Maurer, 2005), which is a vulnerable age for damage from visual deprivation (see Table 4.1 for visually impaired participants clinical details).

Table 4.1 – Demographic and clinical information of visually impaired participants.

Participant ID	Sex	Age	Blindness onset	Pathology
01	M	47	22 years	Retinitis pigmentosa
02	F	38	Before birth	Retinopathy of prematurity
03	M	37	Before birth	Retinal detachment
04	F	37	Before birth	Retinitis pigmentosa
05	M	50	34 years	Retinitis pigmentosa

All participants were given detailed written and verbal information about the study's objectives and procedures and provided their informed consent before taking part. The experimental protocol was approved by the local health authority's ethics committee (Comitato Etico, ASL3 Genovese, Italy) and was carried out in full compliance with the Declaration of Helsinki.

4.2.3 Data Analysis

First, an outlier removal procedure was applied to identify trials in which responses exceeded 2.5 standard deviations from each participant's mean. This procedure was conducted separately for each group (sighted and visually impaired) and for both conditions experienced by sighted participants (visual knob and TaK).

A total of 33 trials were removed from the dataset (15 from the visually impaired group, 10 from sighted participants in the TaK condition, and 8 from sighted participants using the visual knob) out of 1,125 observations.

Normality test on our data was assessed using the Shapiro-Wilk test for each group (sighted and visually impaired) and condition for sighted participants (Tak and visual knob) on the reproduction error (defined as the difference between the participant's response and the real stimulus orientation), and we found that our data didn't follow a normal distribution.

To compare performance between sighted participants using the visual knob and TaK, a Bayesian repeated-measures ANOVA was conducted, with reproduction error as the dependent variable, condition (visual knob vs. TaK) and stimulus orientation as fixed factors, and participant ID included as a random factor to account for inter-individual variability. Similarly, to evaluate whether visually impaired participants differed from sighted participants when using TaK, a Bayesian repeated-measures ANOVA was performed with reproduction error as the dependent variable, group (visually impaired vs. sighted) and stimulus orientation as fixed factors, and participant ID modeled as a random factor. Model selection in Bayesian repeated-measures ANOVA was performed by comparing candidate models generated by including main effects and interactions between fixed factors, considering participant ID as a random factor, and using prior standards ($r = 0.5$), where r indicates the scale of the prior distribution of fixed effects. Models were then evaluated using Bayes Factor and posterior probabilities of the model.

In our results, the Bayes Factor (BF_{01}) expresses the evidence in favor of the null model compared to the alternative model, the posterior probability of the model ($P(M|data)$) represents the probability that a given model is the best among those tested, and the Bayes Factor of inclusion (BF_m) was used to evaluate the evidence in favor of including specific factors or interactions in the models.

Outlier removal and normality test were conducted using R version 4.3.1 (R Core Team, 2021), while Bayesian ANOVA were conducted on JASP version 0.17.1.0 (JASP Team, 2023).

4.2.4 Results and discussion

Descriptive statistics summarized by the mean and standard error of responses across groups and conditions are presented in Figure 4.4 panel B.

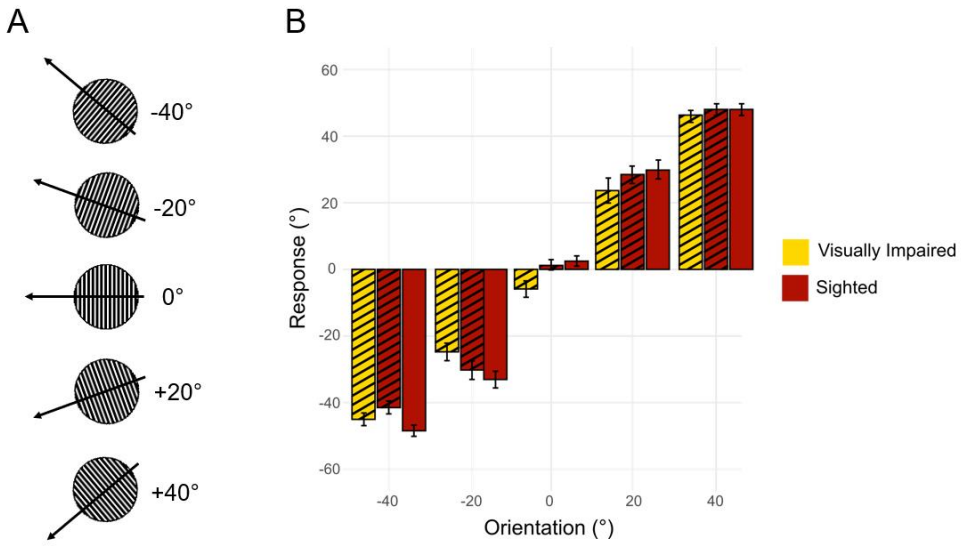

Figure 4.4 – Accuracy in reproducing the proposed orientations by comparing the two groups and the two conditions. (A) Diagram of the target orientations presented (from -40° to +40°). (B) Average responses (± standard error) as a function of target orientation, comparing sighted (red) and visually impaired (yellow) participants, both using TaK (stripes) or, for sighted subjects, using the visual knob (full).

To evaluate whether performance differed between the commercial visual knob and TaK in sighted participants, a Bayesian repeated-measures ANOVA was conducted. Model comparison revealed that the model including only *orientation* as a predictor was the most likely ($P(M|data) = 0.74$; $BF_m = 11.57$). Adding the *condition* factor (visual knob vs. TaK) did not improve model fit ($P(M|data) = 0.22$; $BF_{01} = 3.38$), indicating moderate evidence in favor of the reduced model without condition. Furthermore, including the *orientation* × *condition* interaction was strongly disfavored ($P(M|data) = 0.04$; $BF_{01} = 19.92$), and the model containing only the *condition* factor was drastically unsupported ($P(M|data) \approx 4.9\times10^{-36}$). These results indicate that orientation exerts an influence on reproduction bias, whereas the *condition* does not, showing no difference in mean reproduction error between the two knobs. Overall, these findings highlight a high degree of consistency between the two modalities, supporting the validity of TaK as a reliable tool for reproducing perceived spatial orientations.

A subsequent Bayesian repeated-measures ANOVA was conducted to assess whether performance differed between sighted and visually impaired participants using TaK. Again, *orientation* emerged as the strongest predictor ($P(M|data) = 0.63$; $BF_m = 6.93$). Inclusion of the *group* factor did not improve model fit ($P(M|data) = 0.21$; $BF_{01} = 3.03$), and the *group* × *orientation* interaction was further disfavored ($P(M|data) = 0.16$; $BF_{01} = 4.04$). The model

containing only the *group* factor was strongly unsupported ($P(M|data) \approx 4.9\times10^{-15}$), providing very strong evidence against a main effect of *group*. To summarize, we found a systematic variation of reproduction error depending on stimulus orientation, but no difference between sighted and visually impaired participants, suggesting that tactile processing of motion direction is largely comparable across groups when using the same device.

Together, these findings underscore the value of TaK as a reliable and inclusive tool for assessing spatial perception, such as orientation in motion direction. By relying exclusively on tactile input, TaK is particularly well-suited for individuals with visual impairments, ensuring consistency between perception and response within the same sensory modality and avoiding the challenges associated with cross-modal translation.

4.3 Just noticeable difference in motion direction perception in sighted and visually impaired people

Before conducting our serial dependence experiment, in which participants were asked to perform a reproduction task, it was necessary to ascertain the ability of all the populations involved to correctly discriminate the stimuli presented. This preliminary step was essential not only to ensure that participants could reliably perceive the motion of the stimuli, but also to better understand how basic tactile processing might differ depending on an individual's visual experience.

As discussed in the introduction of this chapter, tactile motion perception depends on the integration of spatiotemporal cues and can be shaped by visual experience: as a result, individuals with different visual histories may rely on distinct strategies or neural resources when processing dynamic tactile information (Boven et al., 2000; Goldreich & Kanics, 2003).

Thus, before examining higher-order biases such as serial dependence, we first needed to establish whether sighted, early-onset blind, and late-onset blind individuals shared comparable levels of sensitivity to motion direction. To this end, we measured the differential threshold of tactile motion direction discrimination across multiple orientations, allowing us to determine not only if they varied across groups overall, but also whether certain directions were easier or harder to discriminate than others and whether these differences emerged

differently depending on visual history. This initial assessment provided a necessary foundation for interpreting the following task performance and for understanding how visual experience shapes the mechanisms underlying tactile motion processing.

4.3.1 Experimental design and procedure

To assess participants' ability to tactually discriminate the direction of motion of the stimuli delivered via RoMAT, we implemented a two-alternative forced-choice (2AFC) task.

Participants were seated in a quiet room in front of the robot and were instructed to perceive the stimuli using the index finger of their right hand. Each trial consisted of a first stimulus (*reference*) presented for 3 seconds, followed by a 5-second pause, and then a second stimulus (*test*). After the presentation of both stimuli, participants were asked to indicate which of the two felt more upwardly oriented (see Figure 4.5 for the definition of "upward" relative to the grating orientation and for an overview of the experimental procedure). The experimenter manually recorded all responses.

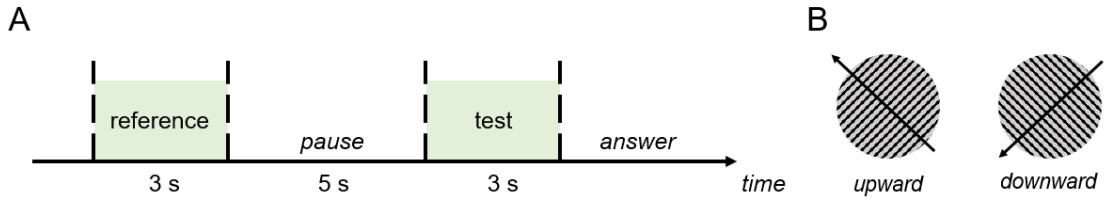

Figure 4.5 – Experimental design procedure. (A) Experimental procedure. Participants were asked to perceive the first stimulus (reference) for 3 seconds, followed by a 5-second pause, and then a second stimulus (test) for an additional 3 seconds. Afterward, they were required to indicate which of the two stimuli had a motion direction that felt more upwardly oriented. (B) In this context, upward refers to a direction pointing toward the northwest. Given that RoMAT can reach a maximum inclination of 40° relative to the horizontal axis, participants were instructed to make their judgments with respect to the two diagonal orientations, both upper and lower.

Three reference orientations were used as stimuli: -20° (upper diagonal), 0° (horizontal), and +20° (lower diagonal). Each reference stimulus was paired with nine test orientations, spanning a range of -20° to +20° relative to the corresponding reference in steps of ±5°. As a result, the test stimulus ranges were -20° to +20° for the 0° reference, 0° to +40° for the +20° reference, and -40° to 0° for the -20° reference.

To determine the number of repetitions for each test stimulus relative to its reference, we employed a variable repetition scheme. Test stimuli at ±20° from the reference were presented 5 times per experimental block; those at ±15° were presented 4 times; those at ±10° were presented 3 times; those at ±5° were presented 2 times; and the test stimulus identical to the reference (0° difference) was presented only once. This scheme allowed us to increase repetitions for the most extreme test values while balancing task difficulty.

In each experimental block, 29 trials were presented for each reference stimulus, yielding a total of 87 trials per block with randomized reference-test pairings. Participants completed two blocks, resulting in a total of 174 trials per participant. They were allowed to take a break at the end of the block. The full experiment lasted approximately 1 hour and 30 minutes.

4.3.1.1 Participants

A total of 42 participants took part in this study, comprising 23 visually impaired individuals and 19 sighted controls (age of 47.8 ± 14.4 years). Among the visually impaired group, 8 participants had early-onset blindness (age 43.6 ± 13.0 years), and 15 had late-onset blindness (age 55.9 ± 12.9 years), with early-onset and late-onset defined as for section 4.2. Clinical details for the visually impaired participants are provided in Table 4.2. All participants met the inclusion criterion of having no history of neurological disorders. Before taking part in the study, all participants were given detailed written and verbal information about the procedures and objectives and provided written informed consent. The study protocol received approval from the local health authority's ethics committee (Comitato Etico, ASL3 Genovese, Italy) and was carried out in compliance with the principles of the Declaration of Helsinki.

Table 4.2 – Demographic and clinical information of visually impaired participants.

Participant ID	Sex	Age	Blindness onset	Pathology
20	M	33	Before birth	Leber's amaurosis
21	M	30	19 years	Brain surgery
22	F	35	Before birth	Premature retinopathy
23	F	48	18 years	Accident, retinal loss
24	F	60	40 years	Nystagmus and retinitis pigmentosa
25	F	61	7 years	Retinitis pigmentosa and nystagmus
26	F	60	46 years	Leber's congenital amaurosis
27	M	54	6 years	Congenital glaucoma

29	F	75	49 years	Degenerative maculopathy
30	F	73	67 years	Retinitis pigmentosa
31	F	26	Before birth	Premature retinopathy
32	F	66	Since birth	Microstalmic
33	M	59	Before birth	Premature retinopathy
34	M	58	45 years	Retinitis pigmentosa
35	M	41	10 years	Accident
36	F	59	35 years	Degenerative maculopathy and retinitis pigmentosa
38	M	74	35 years	Progressive ipovision
39	F	36	Since birth	Retinitis pigmentosa
41	M	47	22 years	Retinitis pigmentosa
42	M	62	14 years	Optic chiasm tumor
43	M	53	Before birth	Congenital optic nerve atrophy
44	M	37	10 years	Retinal detachment and glaucoma
45	F	39	Since birth	Premature retinopathy

4.3.2 Data analysis

To compare performance across the three participant groups (sighted, early-onset blind, and late-onset blind), just noticeable differences (JNDs) were computed by fitting a cumulative Gaussian to the proportion of "perceived difference" as a function of angular differences. The JND was defined as the distance between the 25% and 75% thresholds of the fitted curve. This procedure was applied individually for each participant and for each reference orientation (-20°, 0°, +20°).

Outliers were removed to prevent extreme values from biasing the results. Two participants (1 from the sighted group and 1 from the early-blind group) whose mean JND exceeded the Q3+3×IQR cutoff were therefore excluded from further analyses.

Normality of JND distributions was evaluated using the Shapiro-Wilk test for every group-by-reference combination, and all distributions met the normality assumption.

To assess the effects of the reference stimulus (-20° vs. 0° vs. +20°) and group (sighted vs. early-onset blind vs. late-onset blind) on JND, we fitted a linear mixed-effects model with group, reference stimulus, and their interaction as fixed factors, and participant-specific random intercepts (ID) to account for individual variability. The model was implemented

using the *lmer* function in the lme4 package, with group, reference stimulus, and ID treated as categorical factors. Significance of fixed effects was evaluated via ANOVA, and post-hoc pairwise comparisons were conducted using estimated marginal means (*emmeans*, emmeans package) to examine differences between factor levels.

All statistical analyses were conducted in R version 4.4.2 (R Core Team, 2021), except for the psychometric curve fitting and JND extraction, which were performed in MATLAB R2022b (The MathWorks Inc., 2022).

4.3.3 Results and discussion

We assessed participants' ability to discriminate the motion direction of the two stimuli by asking which one was oriented more upward and calculated their perceptual threshold using the JND.

Sighted participants showed perceptual thresholds of 11.90 ± 2.64° at -20°, 11.30 ± 4.91° at 0°, and 11.10 ± 3.63° at 20°. Visually impaired participants varied by the onset of blindness. Early-onset blind individuals showed thresholds of 11.80 ± 4.23°, 8.60 ± 3.95°, and 12.40 ± 3.19° at -20°, 0°, and 20°, respectively. Late-onset blind individuals exhibited slightly lower thresholds overall, with values of 9.97 ± 3.46°, 9.80 ± 3.13°, and 10.60 ± 5.41° for the same reference orientations (see Figure 4.6).

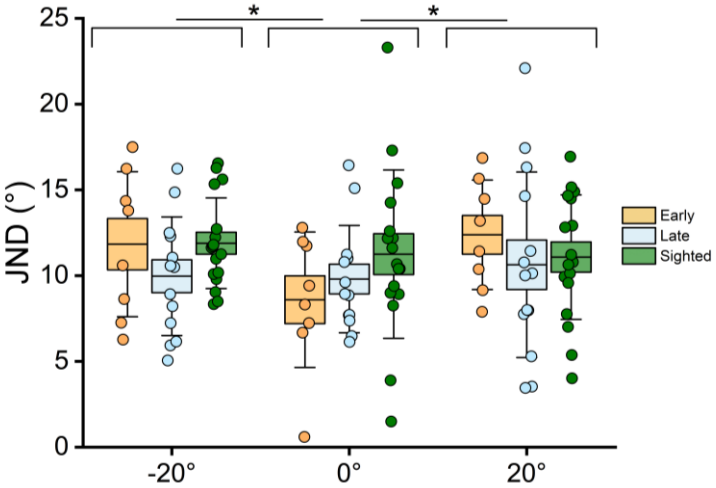

Figure 4.6 – JND values for each group within each orientation. Boxplots represent the standard error, while the error bar represents the standard deviation. The mean line inside the boxplot is the average of the distribution of data.

The linear mixed-effects model revealed a significant main effect of *reference stimulus* on JND ($F(2, 68.84) = 3.60$, $p = 0.033$), while the main effect of *group* was not significant. The *reference stimulus* × *group* interaction showed a trend toward significance ($F(4, 68.92) = 2.13$, $p = 0.086$). Post-hoc comparisons of estimated marginal means indicated that JNDs were significantly lower at 0° than at -20° ($t(69.5) = 2.32$, $p = 0.023$) and +20° ($t(69.5) = -2.33$, $p = 0.023$), with no difference between -20° and +20° ($t(70) = 0.007$, $p = 0.99$).

Those results could not confirm that, in the tested conditions, visual experience and the timing of visual deprivation affect basic motion discrimination. This finding stands in partial contrast with previous evidence showing enhanced tactile spatial abilities in blind individuals (Boven et al., 2000; Goldreich & Kanics, 2003; Stevens et al., 1996), but is also consistent with studies reporting no superior performance in complex haptic tasks (Coelho et al., 2025; Gori et al., 2010), suggesting that visual deprivation does not uniformly affect tactile processing. Reference stimulus orientation, instead, had a clear impact on performance, revealing a tactile oblique effect consistent with prior reports in both vision (Heeley et al., 1997) and touch (Gentaz et al., 2008): similar thresholds for the two oblique angles suggest this reflects directional anisotropies rather than response biases, and its presence across all groups points to somatosensory or biomechanical origins rather than to mechanisms related to visual experience (Gentaz et al., 2008).

These results provide a well-defined baseline of tactile motion sensitivity, setting the stage to investigate serial dependence and allowing us to examine how past tactile experiences influence current motion perception independently of visual experience.

4.4 Serial Dependence in tactile motion direction perception and the role of visual experience

In this final section, we present the chapter's main experiment, namely the investigation of the serial dependence effect in the tactile perception of motion direction.

Having established in the previous sections both the methodological tools needed for accessible orientation reproduction and the baseline differences with which different participant groups discriminate tactile motion direction, we now turn to the central question

motivating this work: does the tactile system integrate past perceptual experiences into current judgments in a manner analogous to vision and audition? And if so, how is this process shaped by visual experience? This question is crucial since, to date, no study has explored whether serial dependence in the tactile domain is modulated by visual experience, given also the extensive cross-modal plasticity documented in visually impaired individuals (Sadato et al., 2002; Wanet-Defalque et al., 1988). Since vision can shape the development and refinement of tactile motion mechanisms, if the computations underlying serial dependence depend on cortical areas typically engaged in visual prediction or spatial processing, their expression may differ in early- or late-onset blindness. Conversely, if serial dependence reflects a more general predictive strategy implemented across sensory systems, the effect may emerge robustly and comparably across all groups.

By comparing sighted, early-onset blind, and late-onset blind individuals, we aimed to reveal whether visual input (and its absence) modulates the integration of past tactile information within this preliminary study.

4.4.1 Materials and methods

4.4.1.1 Participants

A total of 39 participants were recruited for this study, comprising 20 visually impaired individuals, 11 with late-onset blindness (age 51.3 ± 11.3 years), and 9 with early-onset blindness (age 45.7 ± 13.6 years), and 19 sighted participants (age 43.6 ± 13.7 years). Early-onset and late-onset are defined as in the previous sections of this chapter. Two participants (one from the sighted group and one from the early-onset blind group) were excluded from the analysis because they didn’t complete the experiment.

Clinical data for the visually impaired participants are provided in Table 4.3. All participants were fully informed about the study and gave written consent. The protocol was approved by the local ethics committee (Comitato Etico, ASL3 Genovese, Italy) and complied with the Declaration of Helsinki.

Table 4.3 – Demographic and clinical information of visually impaired participants.

Participant ID	Sex	Age	Blindness onset	Pathology
01	M	65	7 years	Uveitis
02	M	61	54 years	Corroyderemia
03	M	37	15 years	Stargardt syndrome and retinitis pigmentosa
04	M	41	10 years	Accident
05	F	67	Since birth	Microstalmic
06	M	33	Before birth	Leber's amaurosis
07	M	60	Before birth	Premature retinopathy
08	M	37	Before birth	Retinal detachment and glaucoma
09	M	29	19 years	Brain surgery
10	F	47	30 years	Stargardt syndrome and retinitis pigmentosa
11	M	54	6 years	Congenital glaucoma
12	M	63	14 years	Optical chiasm tumor
13	F	38	Since birth	Premature retinopathy
14	F	60	Since birth	Nystagmus and retinitis pigmentosa
15	F	59	35 years	Stargardt syndrome and retinitis pigmentosa
16	F	27	Before birth	Premature retinopathy
17	F	60	46 years	Leber's congenital amaurosis
18	F	48	18 years	Accident, retinal loss
19	M	53	Before birth	Congenital optic nerve atrophy
20	F	36	Before birth	Premature retinopathy

4.4.1.2 Apparatus, stimuli, and procedure

To provide the tactile motion direction stimuli, we used RoMAT as in the previous studies, while for the response, we adopted TaK for both visually impaired and sighted populations.

Participants were presented with nine orientations ranging from -40° to +40° in 10° increments. The orientations were presented in a randomized order, and each one was repeated 5 times per block, resulting in 45 trials per block. The experiment comprised 4 blocks, totaling 180 trials per participant.

Before beginning the experiment, all participants were given the opportunity to familiarize themselves with both the RoMAT robot and TaK to ensure a clear understanding of the task before starting the main trials.

Participants from both groups (sighted and visually impaired) were instructed to perceive the tactile stimulus for 3 seconds with the index finger of their right hand; after that, the robot halted, and participants were asked to reproduce the perceived direction of motion using TaK with the same hand. Once the participant confirmed their response, the next trial started.

Sighted participants completed the task under two different response conditions:

- In the first condition, they reproduced the perceived orientation with their eyes closed (condition T);
- In the second condition, they were allowed to visually observe the knob while responding (condition V).

The order of the conditions was randomized for each participant.

Participants were allowed to take short breaks after each block. For sighted participants, the experimental session lasted 1 hour and 30 minutes, while for visually impaired participants 30 minutes.

4.4.1.3 Data analysis

Outlier detection and bias residualization

Initial data screening was conducted through visual inspection of participants' response patterns. This step revealed several cases of qualitatively abnormal behavior, which suggested non-compliance or misunderstanding of the task. As a result, 6 sighted participants and 1 late-onset blind participant were removed before quantitative analysis. After this preliminary cleaning, outlier detection was performed on the remaining dataset using a Root Mean Squared Error (RMSE) criterion. For each condition in the sighted population (V and T) and for the visually impaired population, we computed the RMSE between each participant's responses and the stimulus positions, and identified outliers based on the threshold median(RMSE) + 1.5 × MAD(RMSE), MAD being the median absolute deviation. This procedure resulted in the exclusion of 2 sighted participants, 4 early-onset blind participants, and 1 late-onset blind participant.

Subsequent data cleaning was performed through a multi-step procedure to prepare the dataset for statistical analysis. For each participant (and experimental condition for the sighted group), the error variable was calculated as the difference between the participant's response and the stimulus angle. Trials with absolute errors greater than 45° or responses associated with reaction times exceeding 10 seconds were removed. To reduce systematic nonlinear stimulus orientation biases such as the oblique effect identified in sections 4.2 and 4.3, errors were residualized using robust local fitting (*malowess*), subtracting the estimated systematic component from each individual error. Outliers were identified within each test angle using quartile-based methods (which removes values that deviate from the central 50% of the data for each test angle) and were removed. Also, initial trials of each experimental block were removed to avoid transition effects between blocks. Cleaned data were then centered by subtracting the mean of each participant's observations to remove any residual directional biases.

Serial dependence modeling

In line with the approach adopted in Chapter 2, the analysis of the serial dependence effect was designed to distinguish and jointly evaluate the contributions of the previous stimulus and the previous response to the error in a given trial. So, to evaluate the angular difference between consecutive trials (ΔS) and the difference between previous responses and present stimuli (ΔR) on response error, we fitted one model based exclusively on ΔS, one based exclusively on ΔR, and a combined model (ΔS+ΔR). For each predictors set, we fitted two models: a linear mixed model (LMEM) and a non-linear version based on the Derivative of Gaussian (DoG) function implemented using non-linear mixed models (NLME DoG). The LMEMs were estimated using the *fitlme* function, including a random effect per subject (ID) and appropriate fixed predictors, and the serial dependence effect size was obtained from the fixed coefficient estimates (β) and statistics (t, p). At the same time, the DoG models were estimated using the *nlmefit* function, adapting the DoG components to the predictors of interest and calculating parameter estimates (amplitude of the DoG, α, and width, *w*) and statistical tests (z, p) using Wald tests. To identify the model that best described our data, we compared the models in terms of goodness of fit using the Akaike Information Criterion (AIC).

The formula for describing DoG applied to the non-linear model, including both stimulus history and response history, can be defined as:

$$y = \beta_0 + \Delta_S a_S w_S c e^{-(w_S \Delta_S)^2} + \Delta_R a_R w_R c e^{-(w_R \Delta_R)^2} \quad (4.1)$$

Where β_0 is the intercept representing a constant response bias, while a and w are the terms associated with the amplitude and the width of the DoG function, associated with the terms Δ_S or Δ_R, scaled by a normalization constant $c = \sqrt{2}/e^{-0.5}$.

In addition, the Variance Inflation Factor (VIF) was calculated to assess the presence of multicollinearity between the variables ΔS and ΔR in the model that included both (James et al., 2023). Specifically, for each subject, the correlation matrix between ΔS and ΔR was calculated, and then the VIF was obtained as the diagonal element of the inverse of this correlation matrix. The VIFs obtained for each subject were averaged, yielding an overall estimate of the degree of collinearity between ΔS and ΔR in the sample.

Data were analyzed by group (sighted, early-onset blindness, and late-onset blindness) and, within the sighted group, by condition (V and T).

All the analyses were conducted on MATLAB R2022b (The MathWorks Inc., 2022).

4.4.2 Results

Serial dependence was assessed by fitting linear mixed-effects models and non-linear DoG mixed-effects models, relating response error to the angular difference between consecutive trials (ΔS) or the difference between previous responses and the present stimuli (ΔR). Within each group (sighted, early-onset, late-onset, and, due to the reduced number of participants in the early-onset group, also all visually impaired participants together), three models were compared: ΔS, ΔR, and ΔS+ΔR, with random intercepts for participants. Statistical significance and model fit were evaluated using Wald tests for model parameters and AIC comparisons. Results for each model for each group are reported in Table 4.4.

Table 4.4 – Results of the linear mixed-effects models and non-linear DoG mixed-effects models assessing serial dependence across groups and conditions. For each group and condition, three models were compared: ΔS, ΔR, and ΔS+ΔR. The table reports fixed-effect estimates (β, t, p) for LMEM, parameter estimates (α, z, p) for DoG models, and AIC values. In bold character, the winning models.

		LMEM				**NLMEM DoG**			
Group	**Model**	**β ± SE**	**t**	**p-value**	**AIC**	**α ± SE**	**z**	**p-value**	**AIC**
Early-onset blindness	ΔS	-0.02 ± 0.01	t(555) = -1.19	0.235	4358.08	0.34 ± 1.31	z(554) = 0.26	0.797	4363.09
	ΔR	-0.00 ± 0.01	t(555) = -0.35	0.725	4359.37	1.31 ± 0.79	z(554) = 1.65	0.099	4360.58
	ΔS+ΔR	**ΔS: -0.07 ± 0.03 ΔR: 0.05 ± 0.03**	**ΔS: t(554) = -2.02 ΔR: t(554) = 1.67**	**ΔS: 0.044 ΔR: 0.096**	**4357.31**	ΔS: -6.03 ± 6.83 ΔR: 3.99 ± 1.51	ΔS: z(552) = -0.88 ΔR: z(552) = 2.64	ΔS: 0.377 ΔR: 0.008	4357.39
Late-onset blindness	ΔS	-0.00 ± 0.01	t(1312) = -0.13	0.895	10374.32	0.56 ± 0.66	z(1311) = 0.85	0.398	10375.36
	ΔR	0.02 ± 0.01	t(1312) = 1.37	0.172	10372.46	1.51 ± 0.91	z(1311) = 1.66	0.098	10356.76
	ΔS+ΔR	ΔS: -0.07 ± 0.02 ΔR: 0.06 ± 0.02	ΔS: t(1311) = -3.11 ΔR: t(1311) = 3.40	ΔS: 0.001 ΔR: 0.001	10364.83	**ΔS: -3.51 ± 1.80 ΔR: 3.58 ± 1.16**	**ΔS: z(1309) = -1.95 ΔR: z(1309) = 3.09**	**ΔS: 0.051 ΔR: 0.002**	**10351.77**
All visually impaired	ΔS	-0.01 ± 0.01	t(1869) = -0.75	0.455	14726.56	1.05 ± 0.74	z(1868) = 1.43	0.153	14727.01
	ΔR	0.01 ± 0.01	t(1869) = 1.00	0.320	14726.12	1.38 ± 0.65	z(1868) = 2.12	0.034	14710.30
	ΔS+ΔR	ΔS: -0.07 ± 0.02 ΔR: 0.06 ± 0.02	ΔS: t(1868) = -3.76 ΔR: t(1868) = 3.82	ΔS: 0.0002 ΔR: 0.0001	14714.04	**ΔS: -4.64 ± 2.64 ΔR: 3.77 ± 0.93**	**ΔS: z(1866) = -1.76 ΔR: z(1866) = 4.05**	**ΔS: 0.078 ΔR: 0.0001**	**14695.65**
Sighted eyes-closed (T)	ΔS	0.0241 ± 0.0083	t(1607) = 2.92	0.0036	12631.84	1.4276 ± 1.0127	z(1606) = 1.41	0.1586	12601.36
	ΔR	0.0333 ± 0.0077	t(1607) = 4.35	<0.0001	12621.56	2.1757 ± 1.1564	z(1606) = 1.88	0.0599	12568.38
	ΔS+ΔR	ΔS: -0.05 ± 0.02 ΔR: 0.08 ± 0.02	ΔS: t(1606) = -2.59 ΔR: t(1606) = 4.13	ΔS: 0.0010 ΔR: <0.0001	12616.86	**ΔS: -0.53 ± 0.99 ΔR: 2.60 ± 1.18**	**ΔS: z(1604) = -0.53 ΔR: z(1604) = 2.21**	**ΔS: 0.594 ΔR: 0.027**	**12567.86**
Sighted eyes-open (V)	ΔS	0.01 ± 0.01	t(1641) = 1.06	0.288	12666.70	0.46 ± 0.39	z(1640) = 1.20	0.230	12670.40
	ΔR	0.02 ± 0.01	t(1641) = 3.14	0.002	12657.97	1.40 ± 0.55	z(1640) = 2.54	0.011	12655.75
	ΔS+ΔR	ΔS: -0.11 ± 0.02 ΔR: 0.11 ± 0.02	ΔS: t(1640) = -5.11 ΔR: t(1640) = 5.91	ΔS: <0.0001 ΔR: <0.0001	12634.10	**ΔS: -6.71 ± 2.05 ΔR: 7.15 ± 1.54**	**ΔS: z(1638) = -3.28 ΔR: z(1638) = 4.65**	**ΔS: 0.001 ΔR: <0.0001**	**12633.61**

Model comparison based on AIC consistently indicated that the ΔS+ΔR model provided the best fit for all participants (Figure 4.7 panel A). In the early-onset blindness group, the combined model showed a marginal win for the LME model (AIC = 4357.31) against the NLME DoG model (AIC = 4357.39), suggesting that, in this subgroup, the data do not allow us to reliably distinguish which of the two models best describes the observed effect. Coherently, the variance inflation factor (VIF) computed for the combined model was relatively high (VIF = 7.79), indicating substantial collinearity between ΔS and ΔR and therefore making the coefficient estimates unreliable for further interpretation. For the late-onset blindness group, the NLME DoG model, including both ΔS and ΔR, showed the lowest AIC (AIC = 10351.77) even with elevated collinearity between predictors (VIF = 8.08). These results were also confirmed when considering all visually impaired participants together, with the NLME DoG combined model yielding the lowest AIC (AIC = 14695.65) and a comparable VIF (VIF = 7.99).

In sighted participants (Figure 4.7 panel B), the NLME DoG ΔS+ΔR model provided the best fit for both the eyes-open (V) (AIC = 12633.61) and the eyes-closed (T) condition (AIC = 12567.86). Collinearity between ΔS and ΔR was anyway substantial in both conditions (V: VIF = 10.50; T: VIF = 8.59), suggesting that, across groups, the combined models capture shared variance between stimulus- and response-related effects.

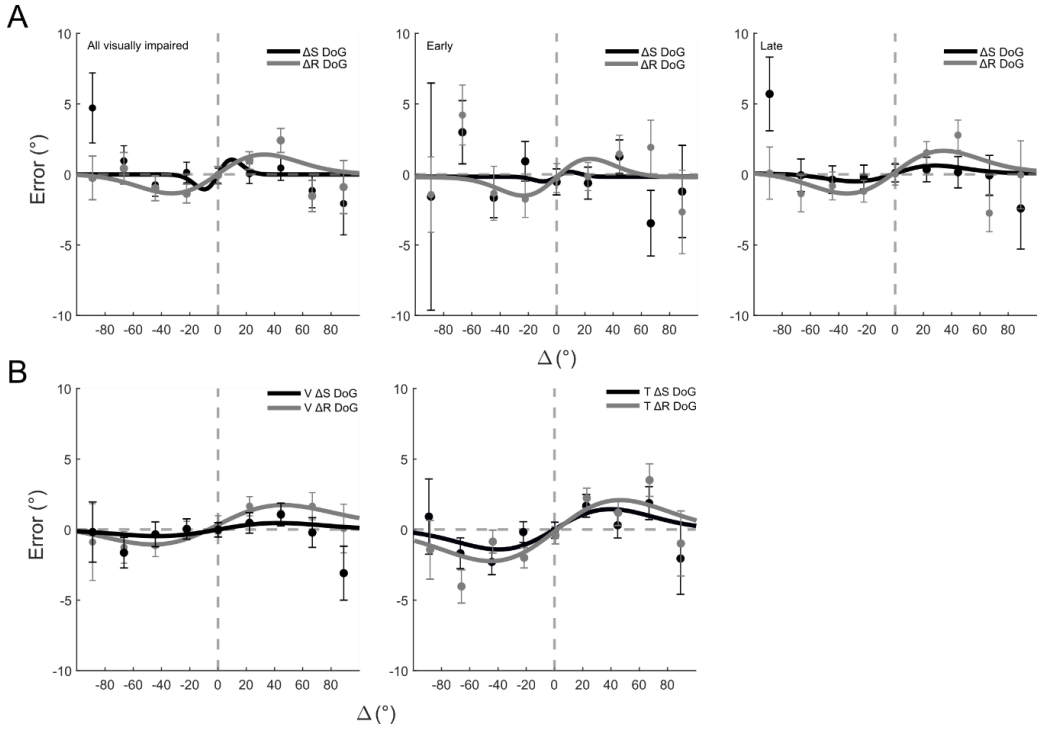

Figure 4.7 – Serial dependence effect approximation for NLME DoG model for each group and condition. Mean response error (°) is plotted as a function of the angular difference between consecutive trials (ΔS) or the difference between previous responses and the present stimuli (ΔR). Data points represent the mean error for each Δ value, with error bars indicating standard deviation. Solid lines show the fitted model predictions. (A) Visually impaired participants, early-onset and late-onset groups shown separately (right panel) and collapsed across onset (left panel). (B) Sighted participants in the eyes-open (V) and eyes-closed (T) conditions.

Notably, across all ΔS+ΔR models, parameter estimates showed a consistent sign pattern, with positive coefficients for ΔR (β and $\alpha > 0$) and negative coefficients for ΔS (β and $\alpha < 0$).

4.4.3 Discussion

This latest study wanted to investigate the presence of the serial dependence effect in the perception of tactile motion direction, using a reproduction task. A further objective of the work was to understand whether this effect was modulated by visual experience, comparing sighted and visually impaired subjects. To do so, we analyzed models based on stimulus history (ΔS), response history (ΔR), and a combination of the two: the results consistently showed that serial dependence is not attributable to a single source but can emerge from the interaction between perceptual processes and response-related processes, with distinct and opposite contributions.

Serial dependence exists in tactile motion direction estimation

Our results provide evidence for the presence of a serial dependence effect in sighted participants. This result is in line with that reported by Wang and Alais (G. Wang & Alais, 2025a), who observed a serial dependence effect in the perception of tactile orientation: their results show that the current perceptual estimate is attracted towards the orientation of the previous stimulus. However, their work does not explicitly dissociate the specific contribution of the previous response, although they suggest that this bias may also reflect post-perceptual processes related to memory and decision-making.

Particularly, the ΔS+ΔR mixed-effects model based on a non-linear DoG function provided the best fit to the data. Crucially, the two predictors elicited opposite influences on the response error, with ΔS exerting a negative effect, indicating a repulsion of the current response with respect to the previous stimulus, and ΔR exerting a positive effect, indicating

an attraction towards the response produced in the previous trial. The coexistence of a repulsive effect linked to the stimulus and an attractive effect linked to the response suggests a push-pull dynamic, in which perceptual and response-related history simultaneously shape behavior through competing biases. This dynamic has been previously observed in the visual domain (Ceylan & Pascucci, 2023; Gallagher & Benton, 2024; Sadil et al., 2024), where repulsive effects are typically linked to sensory adaptation and attractive effects are interpreted as temporal integration or continuity priors acting at the cognitive level (Cicchini et al., 2017; J. Fischer & Whitney, 2014; Fritsche et al., 2017).

This effect is observed both when participants could see while giving their answer (V) and when they were completely blindfolded (T), suggesting that the push-pull dynamic is a fundamental feature of the tactile reproduction task and does not depend solely on visual input. Overall, these results indicate that serial dependence in tactile reproduction reflects a balance between differentiating current stimuli from previous ones and repeating previous responses.

The existence of serial dependence in the perception of tactile motion direction suggests that this mechanism is a characteristic shared by different perceptual systems. However, the results observed in sighted participants do not allow us to establish to what extent the presence of this ability depends on the influence exerted by visual experience on the organization and functioning of other sensory systems. For this reason, it was important to investigate how serial dependence manifests itself in individuals with visual impairment, in order to understand whether this phenomenon reflects a perceptual mechanism independent of vision or whether it is modulated by visual experience.

Serial dependence in visually impaired people

In both groups with early-onset and late-onset blindness, and also when analyzing the entire sample of visually impaired participants, the ΔS+ΔR model provided the best fit to the data, with a repulsive effect for ΔS and an attractive effect for ΔR. This pattern closely mirrors the dynamics observed in sighted participants and aligns with previous findings in visual tasks, where stable and redundant sensory input promotes the coexistence of adaptation-like perceptual repulsion and continuity-promoting response attraction (J. Fischer & Whitney, 2014; Fritsche et al., 2017). In visually impaired participants, the presence of the ΔR factor may be especially pronounced due to the absence of visual feedback during action execution, leading to a greater reliance on internal motor representations and proprioceptive memory:

maintaining continuity with previous responses could thus reduce uncertainty during the reproduction of tactile motion direction (Feigin et al., 2021; Fritsche et al., 2017). It is known that tactile perception in visually impaired individuals is supported by a profound cortical reorganization, which also involves traditional visual areas (Pascual-Leone et al., 2005; Sadato et al., 1996); such reorganization may enhance the precision of tactile representations while simultaneously strengthening memory-related and sensorimotor processes, thereby favoring the coexistence of repulsive and attractive biases.

The presence of serial dependence in participants with late-onset blindness is an interesting finding, as it suggests that this phenomenon does not depend exclusively on visual experience, but probably reflects a more general perceptual mechanism shared between different sensory modalities. So far, we have observed this effect not only in vision but also in hearing and now in touch, despite the fact that these systems are based on different neuroanatomical pathways and information processing. This evidence supports the hypothesis that serial dependence represents a generalizable computational strategy of perceptual systems, aimed at stabilizing perception in the presence of sensory noise, rather than a mechanism specific to the visual system. However, the results obtained in the group with early-onset blindness are less robust and should be interpreted with caution, since the small sample size does not allow definitive conclusions to be drawn about the possible role of vision in the development and calibration of the temporal integration mechanisms underlying serial dependence.

General considerations and limitations of the study

Our findings highlighted a systematic pattern: in the models that best explain the data, ΔS is associated with a repulsive effect, while ΔR is associated with an attractive effect. The robustness of this mechanism in visually impaired participants suggests that the tactile system is able to support a stable form of integration even in the absence of vision. In both visually impaired and sighted participants, serial dependence is generally governed by this push-pull mechanism that has been previously observed in the visual domain, suggesting that it could be a generalizable process that underlies the mechanism of serial dependence in all sensory modalities.

However, given the exploratory nature of the study and the relatively small sample sizes following data cleaning, these interpretations should be considered preliminary: the present results highlight the importance of sensory context and perceptual history in shaping tactile

judgments, and motivate further investigations with larger samples and refined paradigms to clarify the mechanisms underlying serial dependence across sensory modalities. Additionally, our analyses show very high collinearity between the variables ΔS and ΔR, suggesting that although the model that includes both variables best explains the data, the resulting estimates of α and β are unreliable. Therefore, further investigations should aim to quantify the contribution of the previous stimulus and of the previous response on the current percept to fully unveil the push-pull nature of the serial dependence effect.

In general, this work suggests that the serial dependence effect could be extended to the tactile motion direction perception, suggesting that similar computational principles could manage serial dependence across sensory modalities, even in the absence of visual input.

Chapter 5

Separating Haptic from Visual Feedback in Serial Dependence of Size Perception

This chapter is partially extracted from:

"Bertolasi, J.†, Garcia-Hernandez, N.V.†, Memeo, M., Guarischi, M., Gori, M. (2025). Evaluation of HoloLens 2 for Hand Tracking and Kinematic Features Assessment. Virtual Worlds, 4(3), 31. https://doi.org/10.3390/virtualworlds4030031".

"Bertolasi, J., Garcia-Hernandez, N.V., Gori, M. Assessing Human Size Perception in Real and Mixed-Reality Environments, 2025 IEEE Medical Measurements & Applications (MeMeA), Chania, Greece, 2025, pp. 1-5, doi: 10.1109/MeMeA65319.2025.11066289".

"Bertolasi, J., Garcia-Hernandez, N.V., Caroglio, E., Petri, S., Gori, M. Isolating haptic feedback from visual feedback using mixed reality technology: a case study on serial dependence experiment, 2025 IEEE International Symposium on Mixed and Augmented Reality (ISMAR), Daejeon, Korea (South), 2025, pp. 779-780, doi: 10.1109/ISMAR-Adjunct68609.2025.00186".

5.1 Introduction

In the preceding chapters, we investigated serial dependence across multiple sensory modalities: visual, auditory, and tactile. Together, these findings suggest that serial dependence is not confined to a single sensory system or stimulus dimension, but rather reflects a more general mechanism that shapes perceptual judgments over time.

A natural extension of this work is to examine whether serial dependence also operates in cross-sensory contexts: research on serial dependence has extended beyond investigations within single sensory modalities (e.g., visual or auditory) to encompass cross-modal interactions (Burg et al., 2021; Lau & Maus, 2019; Roseboom, 2019), examining how information from one sensory system can influence (and potentially induce) serial dependence effects in another modality.

An important study in this context is that carried out by Fornaciai and Park (Fornaciai & Park, 2019), who investigated cross-modal serial dependence in numerosity perception by asking participants to judge visual dot arrays following task-irrelevant sequences of visual flashes or auditory tones. While visual sequences biased subsequent visual judgments, auditory sequences did not, leading the authors to conclude that serial dependence does not operate across sensory modalities. However, Hashimoto and Makioka (Hashimoto & Makioka, 2025a) proposed the same task but, instead of having arrays of numerosity stimuli, they maintained the same stimulus consistency, proposing sequences of visual flashes or auditory tones both as task-irrelevant stimuli and as stimuli to be actively compared. By manipulating the modality of successive stimuli, they found bidirectional cross-modal serial dependence, with auditory and visual judgments influencing each other. This discrepancy likely reflects differences in task structure and modality relevance: unlike the alternation of sequential numerosity (used as *inducer* stimulus) and simultaneous numerosity (so, the array of dots stimuli) used by Fornaciai and Park, the all-sequential numerosity design of Hashimoto and Makioka allowed cross-modal interaction, providing stronger evidence that serial dependence can emerge across sensory modalities when task demands support it.

Another relevant study by Van der Burg and colleagues (Burg et al., 2021) examined whether serial dependence in emotional perception generalizes across sensory modalities. Across two experiments, participants rated the valence and arousal of emotional sounds and images that

were randomly alternated within the same stimulus sequences. A second experiment further tested whether passive exposure alone could induce serial dependence by interleaving active and passive trials. The results revealed positive serial dependence for both valence and arousal, which was independent of the sensory modality of consecutive stimuli, indicating robust cross-modal generalization of serial dependence in emotional perception.

These findings prompted us to ask whether this phenomenon extends to other cross-sensory contexts, beyond the visual-auditory domain, for instance, to visuo-haptic interactions.

Visuo-haptic interaction is particularly significant in environments where one sensory modality alone may provide incomplete or ambiguous information: specifically, vision offers precise spatial details, while haptic feedback provides rich tactile and force-related cues. Together, these inputs create a more robust representation of objects, textures, and surfaces (Lederman & Klatzky, 2009).

A good candidate feature where cross-modal serial dependence may exist is the estimation of size. In size discrimination tasks, each modality provides unique information and engages distinct yet overlapping neural pathways. Vision provides a distal view of the object, allowing for quick size estimation based on overall shape and contextual information (Kaiser et al., 2019); in contrast, touch provides proximal, detailed information through direct exploration (Lederman & Klatzky, 1987), offering precise measurements of dimensions (Helbig & Ernst, 2007). The brain often uses both visual and tactile information for more accurate size perception, using cross-modal processing where visual information can influence tactile perception and vice versa (Ernst & Banks, 2002). Therefore, we may expect that the brain combines current sensory inputs with lingering traces of previous visuo-haptic experiences, resulting in systematic biases that reflect both the reliability of each modality and the temporal coherence of past and present stimuli (Bensmaïa et al., 2006).

In this final experimental chapter, we examined the visual and haptic contributions to perceptual decisions about object size and their respective roles in shaping serial dependence effects, to characterize both their individual influence and their cross-modal interactions. To this end, we employed mixed reality (MR), a hybrid technology that integrates virtual objects within real-world environments. This technology enables the exploration of interactive, semi-immersive environments and the execution of tasks within a three-dimensional space. A key

advantage of MR lies in the possibility of interacting with 3D virtual content while maintaining contact with the real world, thereby reducing the motion sickness often associated with virtual reality and enhancing ecological validity. Notwithstanding that, the effectiveness of this technology critically depends on the accuracy and reliability of the hand-tracking systems employed (B. H. Thomas, 2020).

Before proceeding with the serial dependence experiment, we run a preliminary phase focused on the technical validation of the equipment. Specifically, the device used for MR rendering was the Microsoft HoloLens 2 (HL2). This initial phase addressed two critical aspects: first, we assessed the quality of the rendering and the reliability of the hand-tracking system provided by the device; second, we evaluated whether the perception of virtual objects was comparable to that of real objects, in order to guarantee that measurements obtained in mixed reality were valid and interpretable in relation to the physical environment.

The following sections provide a detailed description of the two validation techniques employed. Subsequently, the results of the experiment investigating serial dependence in cross-sensory visuo-haptic size discrimination will be presented.

5.2 Validation of HoloLens 2 hand tracking system

HoloLens 2 (HL2) has been evaluated across multiple studies for its motion tracking performance. Around these, Chaconas and Höllerer (Chaconas & Höllerer, 2018) found that two-handed gestures for object manipulation performed similarly to one-handed methods, despite field-of-view limitations, while Vassallo and colleagues (Vassallo et al., 2017) confirmed HL2's ability to anchor holograms in real-world space, supporting its clinical potential. Some works additionally compared HL2 performance to other devices, such as Magic Leap One augmented reality headset, in a shape-tracing task, finding a better accuracy of HL2 (15 mm) rather than Magic Leap (40 mm) (Schneider et al., 2021). In a study from Hübner and colleagues (Hübner et al., 2020), they first evaluated the performance of the HL2's depth sensor and tracking system, followed by its capability to map indoor environments, revealing a tracking accuracy of approximately 17 mm. A similar result was reported by Soares and colleagues (Soares et al., 2021), who found an accuracy of approximately 20 mm in experiments involving hand and head movements, using the OptiTrack optical tracking

system as the ground-truth measurement system. Overall, all those studies reported high finger tracking accuracy of HL2, and the variations in the results reported may be attributed to the tracking method or validation system used.

What should be noted is that none of these studies examined HL2's tracking capabilities in tasks involving pinching or grasping real objects, which are generally performed in activities of daily living, and also mixed reality applications (Guinet et al., 2019; Smeragliuolo et al., 2016; Soares et al., 2021). In this first study, we evaluated the accuracy of the HL2 hand-tracking system and its reliability in providing kinematic measurements. HL2 was tested not only during free-hand movements but also in realistic interaction scenarios, such as object grasping. Unlike previous studies, we used the Vicon motion capture system (VM) as a *gold standard* reference, a marker-based system that provides high-precision, low-latency tracking in real time.

Three representative tasks were designed to simulate common mixed-reality interactions: (i) finger tracking along a 2D pattern in 3D space to assess fingertip accuracy; (ii) object grasping to evaluate the accuracy of joint angle measurements; and (iii) lateral pinching of objects of various sizes to assess the precision of pinch span estimation. Data from HL2 and VM were collected and compared to determine the spatial accuracy and kinematic measurement capability of HL2.

5.2.1 Materials and methods

5.2.1.1 Participants

A total of 12 healthy adults (age 32.3 ± 5.6 years) were recruited from the general population. Ten participants (age 32.1 ± 5.7 years) completed Task 1 (2D pattern tracing in 3D space) and Task 2 (grasping common objects). Four participants (age 35.0 ± 7.2 years) completed Task 3 (lateral pinching of objects of varying sizes). Inclusion criteria required no history of significant upper limb injury. All participants provided written informed consent. The study was approved by the ethics committee of the local health service (Comitato Etico, ASL3 Genovese, Italy) and conducted in accordance with the Declaration of Helsinki.

5.2.1.2 Apparatus: HoloLens 2 and VICON Nexus motion capture system

Microsoft HoloLens 2

HL2 (Microsoft, Redmond, WA, USA) is an augmented reality headset designed for multi-purpose use (Figure 5.1 panel A). HL2 recognizes hand gestures within a vertical field ranging from +10° to -60° relative to the eye line, with optimal tracking between 0° and -35°. The horizontal tracking range automatically adjusts as the user moves their head, ensuring that gesture recognition always remains aligned with the user's current line of sight.

Hand-tracking data were captured at 100 Hz. During each task, time-stamped joint position data were collected and saved in CSV format for post-processing and comparison.

Vicon Motion Capture System

Vicon Motion capture system (VM; Oxford, UK) allows for the collection of high-precision hand-tracking data. The VM system enables accurate estimation of motion parameters, including speed, acceleration, and jerk. Seven Vero v2.2 infrared cameras (2048×1088 resolution) were arranged to form a capture volume of approximately 2×1×1 meters (Figure 5.1 panel B). Before starting the data collections, system calibration followed standard procedures outlined in the VM user manual, and it was accepted if the mean 3D residual error was below 0.8 mm; the final average calibration error was 0.5 ± 0.2 mm.

Data were recorded at 100 Hz, matching the acquisition rate of the HL2 for the sake of synchronization.

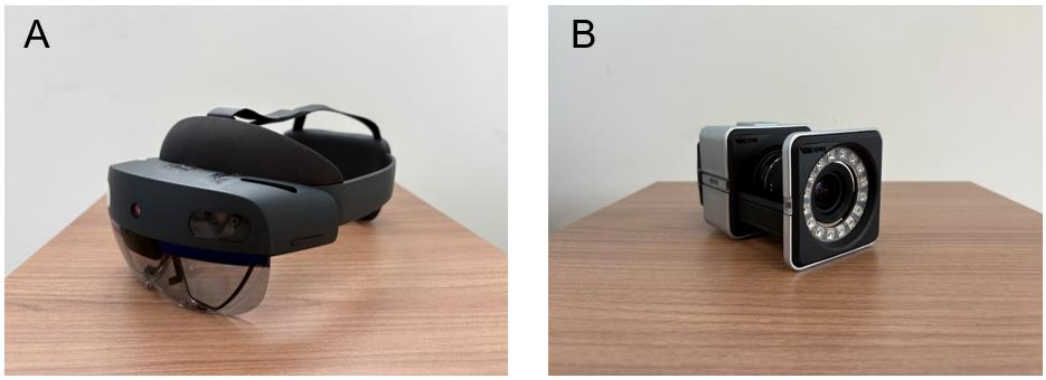

Figure 5.1 – Photograph of HoloLens 2 (A) and Vicon Motion capture Vevo camera (B).

Participants wore lightweight, retroreflective spherical markers (6.5 mm diameter) placed on their hand. Marker placement corresponded to HL2-tracked joints, based on the Mixed Reality Toolkit (MRTK) 2 and guided by recommendations from Cook and colleagues (Cook et al., 2007). For Task 1 (2D pattern tracing), six markers were used (Figure 5.2 panel A). For Tasks 2 and 3 (object grasping and lateral pinching), 14 markers were used (Figure 5.2 panel B). Each marker was labeled and its 3D position recorded for analysis.

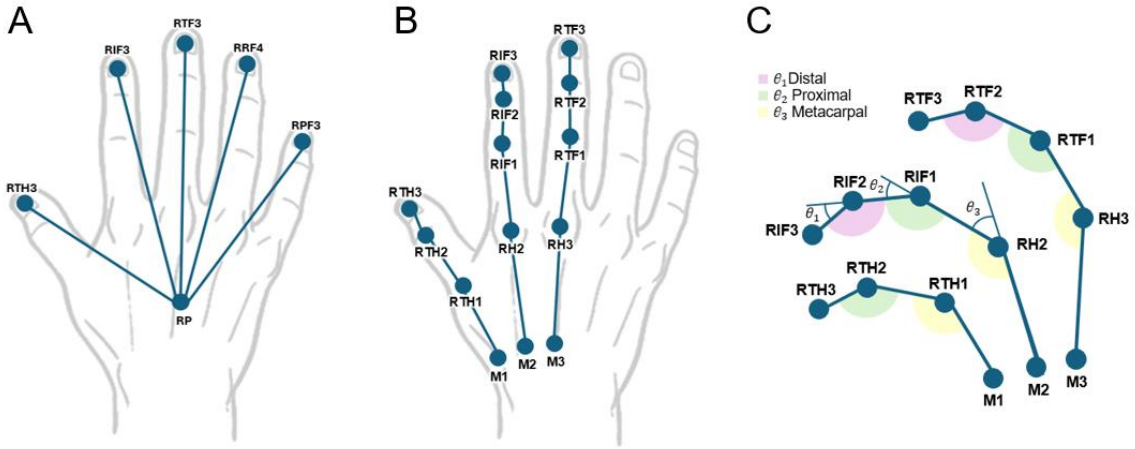

Figure 5.2 – Marker placement and tracking reference for each task. (A) Task 1 (tracing a 2D pattern in 3D space with a finger) marker placement; the RP marker was included only to improve VM reconstruction and was not analyzed. (B) Task 2 (grasping everyday objects) and Task 3 (performing lateral pinch on objects of different sizes) marker placement; for Task 2, markers were applied to the entire hand, while in Task 3, only the thumb and index finger were monitored. (C) Joint angle calculated for Task 2, derived from the distal, proximal, and metacarpophalangeal joints.

5.2.1.3 Experimental tasks

Three tasks were designed to evaluate HL2's hand-tracking performance during realistic interactions. All tasks were performed by participants in a seated position, with the chair placed 40 cm from the table and the right armrest aligned to a fixed calibration mark.

For each task, data collection started by remotely launching the HL2 recording application, followed immediately by activating the VM recording. Data from HL2 and VM were synchronized offline, aligning the tracks using a reference point – that is, a distinct upward index finger movement at the start of each trial, visible in both systems' recordings.

During Tasks 2 and 3, HL2's hand mesh was visible to participants to ensure proper hand positioning tracking. A trial was repeated if the participant reported misalignment between the

virtual mesh and their actual hand. Calibration of both HL2 and VM was conducted using the right hand placed on a predefined resting position.

Task 1: 2D pattern tracing in 3D space

This task assessed HL2's fingertip tracking accuracy. Participants traced an infinity symbol (20 cm high × 50 cm wide), displayed through HL2 at a distance of 60 cm from the head and aligned with the right shoulder. Using their right index finger with an open hand, participants freely traced the full pattern once, starting from any point and direction at a natural speed.

Task 2: Grasping common objects

Participants performed static grasps with their right hand on a set of objects designed to represent typical grasp types (Hamon et al., 2021; Yang et al., 2015):

- Cylindrical grasp: Cylinder (13×3 cm);
- Spherical grasps: Spheres (8 cm and 12 cm in diameter);
- Pinch grasps: Cube (3×3×1 cm) and plug (3 cm in diameter).

To minimize viewing occlusion, some objects were transparent to facilitate tracking, as opaque or colored objects could occlude parts of the hand.

The task consisted of picking up each object from the table, holding it about 20 cm in front of the face for 5 seconds, and then returning it to its original spot. This sequence was repeated five times for every object, always starting from the same initial position. The objects were presented and grasped in a fixed order across all repetitions, as the main goal was to capture consistent hand postures. For each object, a single data file was generated, containing the recordings of all five trials. Figure 5.3 panel A shows how the objects were grasped and positioned in front of the participant's face.

Task 3: Lateral pinching with both hands

To evaluate lateral pinch span tracking, participants pinched five rectangular objects of increasing thickness (from 2 cm to 10 cm in 2 cm increments, see Figure 5.3 panel B) using both hands. Due to HL2's difficulty tracking marker-covered hands, markers were applied only to one hand (randomly assigned), while HL2 tracked the other unmarked hand. Markers were placed on the index and thumb. Each object was held statically in front of the participant's head for 10 seconds, allowing both systems to capture the hand configuration.

Figure 5.3 – Objects grasp for Task 2 and Task 3. (A) Hand grasping various objects (cube, plug, cylinder, two spheres) during Task 2, with reflective markers on the hand. Colors are arbitrary; the cylinder is transparent for HL2 marker visibility. (B) Top view of lateral pinching of a rectangular object with varying thickness during Task 3 (one hand tracked with VM while the markerless one tracked via HL2). Thickness increases by 2 cm per added segment; object colors are arbitrary.

5.2.1.4 Data preprocessing and analyses

General Preprocessing

HL2 data were filtered using a 4th-order Butterworth low-pass filter (6 Hz cutoff) to reduce noise. VM data were pre-filtered using the same parameters during acquisition.

Time alignment between HL2 and VM datasets was performed using the initial index finger movement as a temporal landmark, detected via local maxima within the first 5 seconds of recording.

Task 1: Fingertip tracking accuracy

To compare fingertip trajectories, HL2 coordinates were transformed to align with the VM reference frame. Due to HL2's unknown origin, we used the Iterative Closest Point (ICP) algorithm (Besl & McKay, 1992) to estimate the optimal rotation (R) and translation (T), minimizing the Euclidean distance between paired points:

$$E(R,T) = \frac{1}{N}\sum_{i=1}^{N}\left|\left|V_i - RH_i - T\right|\right|^2 \quad (5.1)$$

where H_i and V_i are matched points from HL2 and VM. The final transformation was applied to HL2 data.

Mean distance error was then calculated as:

$$Dist_{error} = \frac{1}{N}\sum_{i=1}^{N}(V_i - H_i) \tag{5.2}$$

Task 2: Joint Angle Accuracy

Joint angles for the index, middle, and thumb fingers were derived from tracked joint (HL2) and marker (VM) positions. After alignment, grasping attempts were segmented using fingertip velocity thresholds (3% of peak). Segments were time-normalized to 200 samples using spline interpolation.

Joint angles were computed using the inverse cosine of the angle between adjacent vectors:

$$\theta = cos^{-1}\left(\frac{u \cdot v}{\|u\|\|v\|}\right) \tag{5.3}$$

Where u and v represent 3D vectors corresponding to points captured from HL2 and the VM, defining the segment between specific anatomical landmarks.

Average angular error was computed as the difference between HL2 and VM angles per joint and finger.

Task 3: Pinch Span Accuracy

Pinch span was calculated as the distance between thumb and index fingertips, adjusted by subtracting the marker size and half the finger pad thickness (measured via caliper) in VM data recorded, to match the tracked position of the HL2 tracking point. The resulting value was compared to the known object thickness to assess HL2's measurement accuracy.

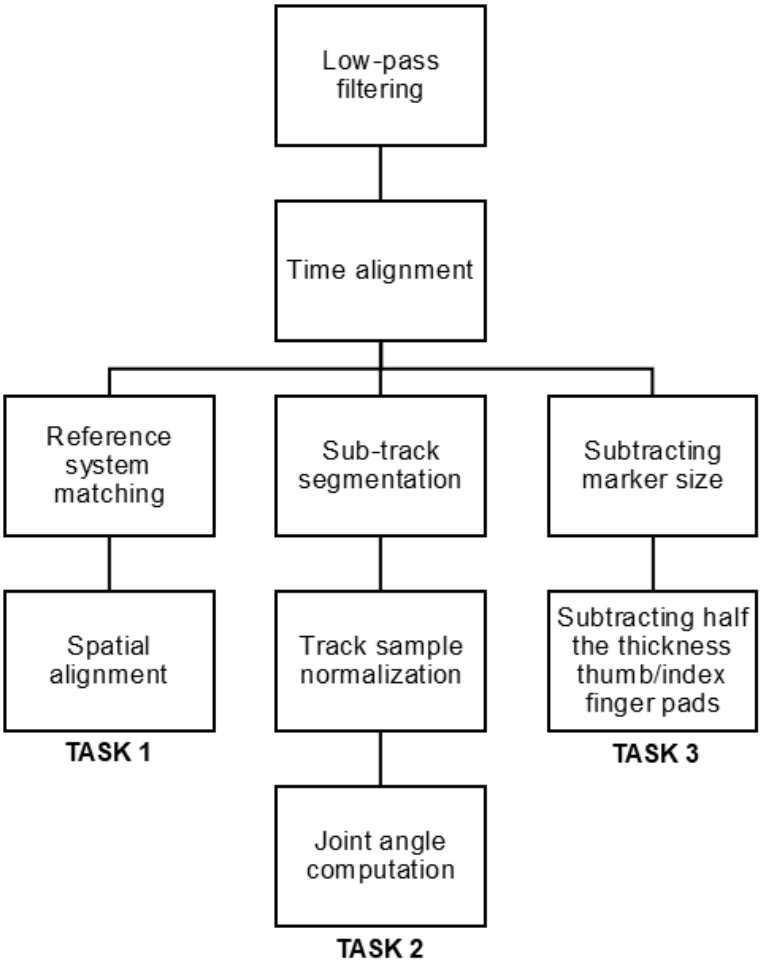

Figure 5.4 – Pipeline for data processing across tasks. Data were first converted to .mat format, low-pass filtered, and temporally aligned using local maximum detection. For Task 1, HL2 axes were corrected to match VM, then trajectories were spatially aligned via ICP. In Task 2, trials were segmented into five repetitions, time-normalized to 200 samples, and joint angles computed from anatomical marker vectors. For Task 3, spatial alignment included compensating for marker and fingertip thickness (6 mm and half fingertip width) in VM data to improve positional error estimation.

Statistical Analysis

First, for all the measures computed, the normality of the data distribution was assessed with the Lilliefors Normality Test.

Then, to evaluate the consistency between the reconstructions obtained from the HL2 and the VM system, the Pearson correlation coefficient (in case of normal distribution) or the Spearman correlation coefficient (in case of non-normal distribution) was calculated for the first and second tasks.

For Task 3, a two-way repeated measures ANOVA assessed the interaction between system (HL2 vs VM) and object size. Additionally, Bayesian repeated-measures ANOVA was conducted to quantify the evidence for the presence or absence of systematic differences between measurement systems. Finally, a frequentist paired sample t-test and a Bayesian paired sample t-test were used to compare pinch span measurements obtained with both systems.

All data processing and frequentist analyses were performed in MATLAB R2022b (The MathWorks Inc., 2022), while Bayesian analyses were performed in JASP version 0.17.1.0 (JASP Team, 2023).

5.2.2 Results and discussion

Task 1: Finger Tracing of a 2D Pattern in 3D Space

Participants traced an infinity-shaped path in 3D space using their right index fingertip while moving their arm, viewed through the HL2. This task aimed to evaluate HL2's fingertip tracking accuracy by comparing its data to that of the VM system.

To account for differences in coordinate systems, the ICP algorithm was applied to find the optimal rotation and translation matrices that aligned HL2 data with VM data, minimizing spatial discrepancies. Figure 5.5 shows the initial trajectories before alignment (left graph), highlighting a noticeable depth-axis (y-axis) mismatch. After applying ICP, the right graph shows a close overlap between the two trajectories, confirming effective correction of the reference frame differences.

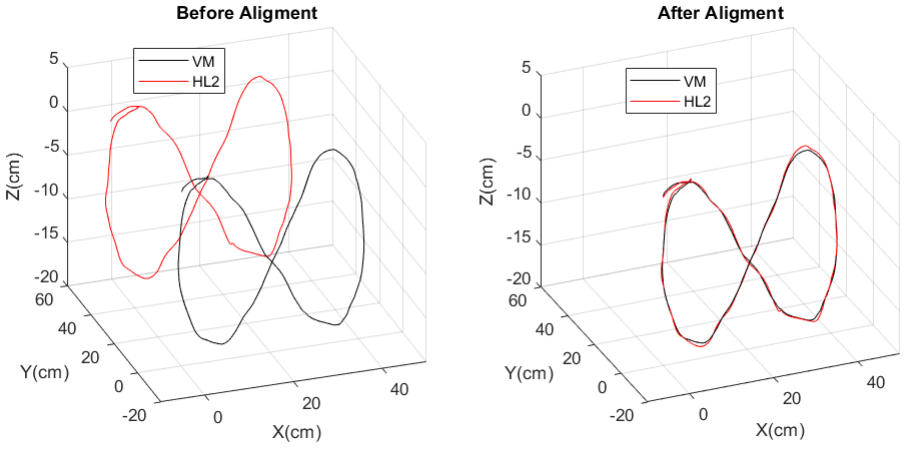

Figure 5.5 – One-participant comparison between the trajectories recorded by the VM (black) and HL2 (red) tracking systems for RIF3 (index tip) marker. The left graph displays the unaligned trajectories, showing an apparent spatial misalignment between the two systems. The right one shows the same trajectories after applying the transformation (R and T) obtained with the ICP algorithm, demonstrating an improved correspondence between the VM and HL2 traces. The enhanced alignment in the fitted trajectories supports the high correlation values reported in the results.

Table 5.1 summarizes the average distance errors between HL2 and VM across participants for each fingertip. Errors for the thumb, middle, ring, and little fingers averaged around 2.8 mm, while the index fingertip error was slightly higher at 3.9 mm – still under 5 mm. Pearson correlation coefficients further supported these findings, with values near 0.99 for all fingertips and all p-values < 0.05, indicating strong, statistically significant correlations. These findings demonstrate HL2's high spatial accuracy in fingertip tracking, considerably outperforming earlier reports of 15-20 mm errors in similar studies (Schneider et al., 2021; Soares et al., 2021).

Table 5.1 – Distance error between HL2 and VM tracking data, expressed as mean ± standard deviation of Euclidean distances, with relative variance and 95% CI. Lower values indicate higher HL2 accuracy, while larger values reflect greater deviation from the VM reference. All fingers showed low variance and narrow CIs, indicating consistent performance across participants.

Finger	Mean ± SD (mm)	Variance (mm^2)	95% CI (mm)
RTH3 (Thumb)	2.77 ± 0.63	0.39	[2.32, 3.22]
RIF3 (Index)	3.94 ± 0.69	0.48	[3.45, 4.44]
RTF3 (Middle)	2.86 ± 0.61	0.37	[2.43, 3.30]
RRF4 (Ring)	2.87 ± 0.59	0.35	[2.44, 3.29]
RPF3 (Little)	2.88 ± 0.58	0.34	[2.46, 3.29]

Minor discrepancies between fingers may be linked to sensor occlusion, inconsistent coverage, or individual anatomical differences such as hand size and finger length, which can affect mesh fitting and tracking precision. Although spatial accuracy is excellent, the current analysis does not address temporal aspects like latency, which could influence real-time interactions. Task design and reference systems also likely contributed to performance differences with prior studies, as this experiment involved 3D hand-tracing with a VM system, unlike 2D touchscreen setups or alternative motion capture platforms used previously (Schneider et al., 2021; Soares et al., 2021).

Task 2: Grasping Common Objects

Participants grasped various objects with their right hand in a static position to evaluate HL2's accuracy in measuring joint angles by comparing HL2 data to VM data. Thumb, index, and middle fingers were involved in most grasps, except for the cube and plug, which used only the thumb and index fingers. Joint angles were measured at the distal (DIP), proximal (PIP), and metacarpophalangeal (MCP) joints for the index and middle fingers, and at the interphalangeal (IP) and MCP joints for the thumb.

Table 5.2 shows angular errors ranging from 0.3° to 22°, with the highest error at the thumb IP joint during the small sphere grasp (21.87 ± 0.62°) and the lowest at the thumb MCP joint during the big sphere grasp (0.28 ± 0.56°). Overall, the average angular error was 5.36 ± 5.31°.

Table 5.2 – Mean angular joint errors (°) between HL and VM systems for each finger and object, reported as mean ± standard deviation.

	Thumb		Index			Middle		
	IP	**MCP**	**DIP**	**PIP**	**MCP**	**DIP**	**PIP**	**MCP**
Small Sphere	21.87°±0.62	7.39°±0.35	0.92°±0.39	0.65°±0.42	3.15°±0.36	9.91°±1.45	4.47°±0.51	1.46°±0.53
Big Sphere	18.11°±0.58	0.28°±0.56	2.64°±0.52	0.79°±0.54	1.37°±0.29	4.43°±0.48	1.38°±0.50	2.39°±0.48
Cylinder	7.18°±0.31	8.03°±0.22	2.72°±0.31	1.14°±0.26	0.53°±0.18	5.35°±0.28	0.68°±0.29	3.91°±0.35
Plug	14.46°±0.53	2.96°±0.47	7.72°±0.57	2.44°±0.44	5.88°±0.29	-	-	-
Cube	12.39°±0.29	2.47°±0.31	14.61°±0.41	1.98°±0.19	6.44°±0.31	-	-	-

Correlation analysis of joint angle distributions between HL2 and VM showed varied results across grasp types. For the small sphere, all joints were significantly correlated ($p < 0.001$), except the thumb MCP ($r = 0.04$, $p = 0.613$), which showed no correlation. For the big sphere, all angles were correlated ($p < 0.005$), except the middle PIP ($r = -0.12$, $p = 0.825$). In the cylindrical grasp, no correlation was found for the thumb IP ($r = 0.09$, $p = 0.211$) and the index PIP ($r = -0.05$, $p = 0.453$). Similarly, for the plug grasp, the thumb IP ($r = 0.01$, $p = 0.892$) and index MCP ($r = 0.10$, $p = 0.163$) showed no significant correlation. In contrast, the cube grasp exhibited strong correlations for all five angles ($p < 0.001$).

Those analyses showed that HL2 is generally reliable for hand kinematic measurements. Average errors were moderate, around 5°, suggesting acceptable accuracy for most objects. Correlation coefficients further confirm strong agreement between systems, particularly for spherical grasps. However, some inconsistencies were observed, such as the absence of

correlation for certain thumb angles in the small sphere grasp and the middle PIP in the big sphere task. These discrepancies may result from variations in finger positioning, individual hand dimensions, or interference from reflective markers, which could disrupt HL2's mesh fitting and reduce tracking precision.

Task 3: Lateral Pinching of Objects

Participants performed lateral pinches on objects of varying thickness using their index finger and thumb. The pinch span – the distance between the fingertip of the index finger and the thumb – was calculated from HL2 and VM data to assess HL2's accuracy.

As shown in Figure 5.6, HL2's pinch span measurements closely matched those from the VM system. The largest difference occurred with the 6 cm thick object (6.77 ± 0.38 mm for HL2 vs. 6.36 ± 0.03 mm for VM), while the smallest difference was observed for the 10 cm object (10.75 ± 0.34 mm for HL2 vs. 10.74 ± 0.01 mm for VM).

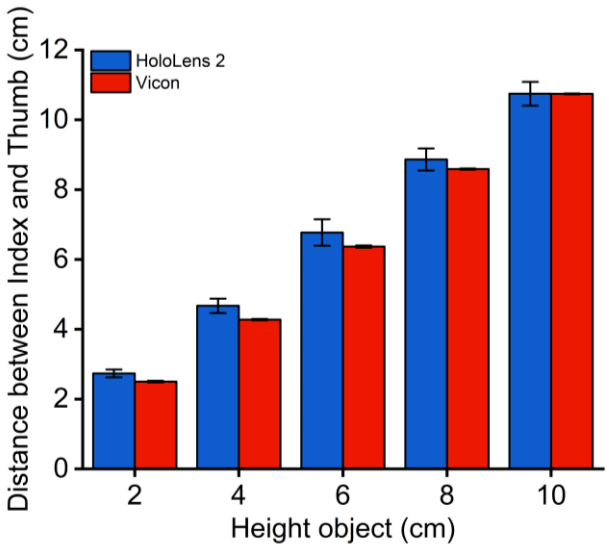

Figure 5.6 – Comparison of pinch span across object thicknesses for HL2 and VM systems. Bars represent mean ± standard deviation.

The accuracy of HL2 does not show a linear improvement with increasing object thickness (see Table 5.3). The average error increases for intermediate thicknesses (4-6 cm) and decreases for larger objects (8-10 cm), suggesting a non-linear trend. However, for greater thicknesses, the confidence intervals include zero, indicating a lack of consistent bias at these thickness levels, caused by HL2 measures.

Table 5.3 – Mean pinch span error (± standard deviation), variance, and 95% CI between HL2 and VM tracking data across different object thicknesses.

Object thickness	Mean ± SD (mm)	Variance (mm^2)	95% CI (mm)
2 cm	0.23 ± 0.09	0.01	[0.09, 0.37]
4 cm	0.40 ± 0.19	0.04	[0.10, 0.69]
6 cm	0.40 ± 0.35	0.12	[-0.15, 0.95]
8 cm	0.28 ± 0.30	0.09	[-0.20, 0.75]
10 cm	0.004 ± 0.33	0.11	[-0.52, 0.53]

The two-way repeated-measures ANOVA revealed a significant interaction between the type of measurement system (HL2 vs. VM) and the size of the grasped object, $F(1, 3) = 644.23$, $p = 0.00013$, $\eta^2_p = 0.995$. Bayesian model comparison indicated that the model including the main effects of *system* (HL2 or VM) and *object thickness* was the most supported by the data ($P(M|data) = 0.42$). Strong evidence was found in favor of the absence of a main effect of *system*, indicating no systematic differences between HL2 and VM. In contrast, the inclusion of the *system* × *thickness* interaction did not improve model evidence, suggesting that the interaction observed in the frequentist analysis was not strongly supported when model complexity was taken into account.

However, no statistically significant differences were found between pinch span measurements obtained with HL2 and VM across all object thicknesses (supporting the null hypothesis): paired-sample t-tests confirmed the absence of systematic differences for each thickness: 2 cm ($t(3) = -1.16 \pm 0.004$, CI [-0.01, 0.004], $p = 0.32$), 4 cm ($t(3) = -1.37 \pm 0.01$, CI [-0.013, 0.005], $p = 0.27$), 6 cm ($t(3) = -1.01 \pm 0.01$, CI [-0.02, 0.01], $p = 0.39$), 8 cm ($t(3) = -2.97 \pm 0.002$, CI [-0.01, 0.00], $p = 0.06$), and 10 cm ($t(3) = -0.02 \pm 0.004$, CI [-0.01, 0.01], $p = 0.99$). Bayesian paired-samples t-tests supported these findings, with Bayes Factors (BF_{10}) consistently below 1 for all thicknesses (2 cm: $BF_{10} = 0.68$; 4 cm: $BF_{10} = 0.78$; 6 cm: $BF_{10} = 0.62$; 8 cm: $BF_{10} = 2.13$; 10 cm: $B_{10} = 7.8 \times 10^{-4}$).

Those results indicated that HL2 achieves performance comparable to VM, with pinch span accuracy improving as object thickness increases. This suggests that HL2 performs better with larger objects, likely due to clearer spatial references and reduced occlusion errors. However, performance remains dependent on grasp type and object characteristics. These results

underscore the need for enhanced tracking algorithms capable of handling finger overlap and accommodating individual hand size variations to improve MR interaction fidelity.

5.3 Validation of HoloLens 2 as a psychophysics instrument

Building on the findings presented in the previous paragraph, which demonstrated the accuracy and reliability of HL2's hand-tracking system when benchmarked against a high-precision marker-based setup, it is essential to extend the analysis beyond tracking performance and consider other factors that influence interaction quality in MR environments.

Hand-tracking accuracy represents only one component of a successful MR experience; equally critical is the user's ability to perceive virtual objects in a way that is consistent with real-world perception. If virtual objects are not perceived with the same fidelity as their physical counterparts, even highly accurate tracking may not guarantee effective interaction.

Accurate perception of virtual object features, particularly size and distance, is fundamental for tasks that require fine motor control and spatial reasoning, such as psychophysics experiments. While these perceptual aspects have been extensively studied in immersive virtual reality systems (Hornsey et al., 2020; Rzepka et al., 2022; B. H. Thomas, 2020), the body of research focusing on optical see-through MR devices such as HL2 remains limited (L. Wang et al., 2023): the optical blending of real and virtual elements, combined with the fixed focal plane of these devices, introduces unique challenges that can potentially affect depth cues and size estimation, leading to discrepancies between real and virtual object perception.

To address this gap, the present study investigates whether the size perception of virtual objects rendered through HL2 is comparable to that of real objects.

5.3.1 Stimuli and experimental design

For this task, we used nineteen spheres of diameters 74, 75, 76, 77, 77.5, 78, 78.5, 79, 79.5, 80, 80.5, 81, 81.5, 82, 82.5, 83, 84, 85, and 86 mm, both in physical and virtual conditions.

Physical spheres were fabricated via selective laser sintering 3D printing (ProX 6100, 3D Systems) using NYLON PA material, offering nominal dimensional accuracy of ±0.1 mm. Given the minimal step size between stimuli (0.5 mm), all printed spheres were measured and confirmed to be within ±0.05 mm of their intended diameters.

Virtual spheres – as well as the whole experimental application – were generated in Unity (version 2022.3.30f1) using C# and Microsoft's Mixed Reality Toolkit (MRTK) and rendered via Microsoft HoloLens 2 through the Holographic Remoting Player app.

The application served three primary functions: (i) calibrating the spatial positions on the table where virtual spheres would be displayed, (ii) initiating trials, and (iii) recording participant responses.

Calibration involved instructing participants to position their right index fingertip on two predetermined table markers, locations corresponding to the sphere placements. The HL2 captured fingertip positions using its internal coordinate system, ensuring that virtual spheres appeared at equivalent real-world positions.

Trial initiation and response recording were controlled by the experimenter via keyboard inputs: pressing "Enter" started a trial, and entering "0" or "1" indicated participant's answer.

5.3.1.1 Experimental protocol

Prior to the experiment, participants were instructed about the experimental procedure and seated facing a table with the chair positioned 40 cm from the table edge.

The study assessed participants' visual size perception accuracy by comparing virtual objects rendered by the HL2 perception against real physical spheres perception using a two-alternative forced choice (2AFC) task. Participants judged which of two spheres appeared larger: a fixed reference sphere (80 mm diameter) or a test sphere (ranging from 74 mm to 86 mm).

In each trial, participants were sequentially presented with the reference first and then the test sphere. For the virtual spheres condition, participants observed the stimuli through the HL2; for the real spheres condition, the experimenter manually placed and removed the spheres on the table. Each sphere was visible for approximately 2 seconds, separated by a 1-second inter-

stimuli interval. Participants verbally indicated which sphere appeared larger (the reference or the test).

Two viewing distances were tested (25 cm and 85 cm from the table edge), chosen based on prior research (Gori, Giuliana, et al., 2012) and reflecting typical interaction distances for real and virtual objects.

Each test sphere was presented four times, resulting in 76 trials per experimental condition. The experiment had a 2×2 design, totaling 304 trials per participant. The order of the viewing distance (25 cm or 85 cm) and the condition (virtual or real) was randomly selected. Each experimental condition lasted approximately 10 minutes.

5.3.1.2 Participants

10 adults (age 28.7 ± 2.5 years) with normal or corrected to normal vision were recruited internally from the Italian Institute of Technology laboratories. All participants gave written informed consent. The study was approved by the local health service ethics committee (Comitato Etico, ASL3 Genovese, Italy) and conducted in line with the Declaration of Helsinki.

5.3.2 Data analysis

To quantify perceptual thresholds, the proportion of trials in which the test sphere was judged larger than the reference was computed for each test size. These data were fitted with cumulative Gaussian psychometric functions to extract two key metrics: the point of subjective equality (PSE) as the size at which the test and reference spheres were perceived as equal, and the just noticeable difference (JND), as the minimal size difference reliably detected by participants, indicating perceptual sensitivity. These measures provide a quantitative representation of perceptual precision.

For both PSE and JND, we conducted both frequentist and Bayesian repeated-measures ANOVA with *modality* (haptic vs. virtual) and *distance* (25 cm vs. 85 cm) as factors. This approach allowed us to evaluate the main effects of each factor and the interactions between them.

Data processing was performed using MATLAB R2022b (The MathWorks Inc., 2022), while Bayesian and frequentist analyses were conducted in JASP version 0.17.1.0 (JASP Team, 2023).

5.3.3 Results and discussion

The PSE and JND were computed for both the real and virtual conditions at viewing distances of 25 cm and 85 cm (see Figure 5.7 for exemplificative psychometric curves).

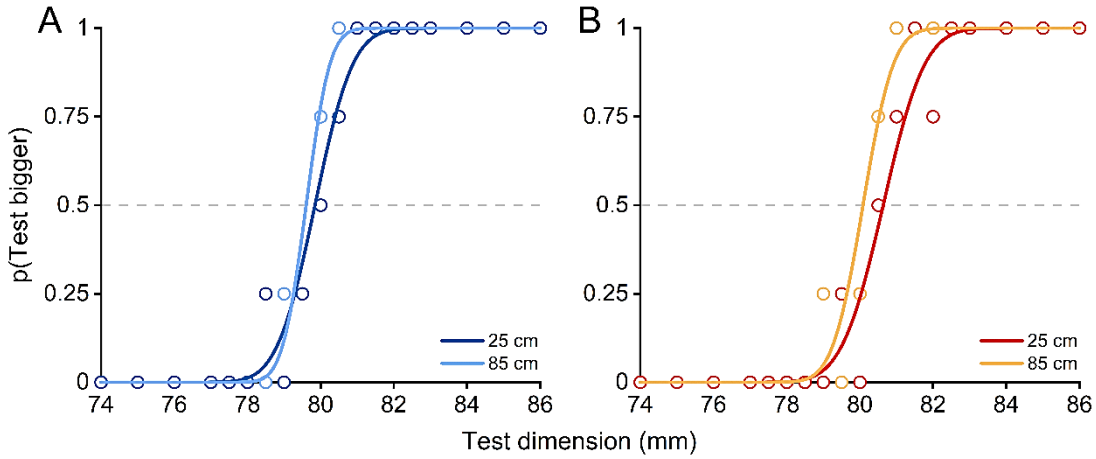

Figure 5.7 – Psychometric functions from a representative participant, illustrating performance at both viewing distances (25 cm and 85 cm) under (A) virtual and (B) real conditions.

In the real condition at 25 cm, the PSE was 80.20 ± 0.33 mm, and the JND was 1.12 ± 0.30 mm, indicating high sensitivity to size differences. At 85 cm, the real condition showed a slight decrease in PSE (79.50 ± 0.34 mm) and a modest increase in JND (1.18 ± 0.23 mm), suggesting stable perceptual performance across distances.

For the virtual condition, the PSE at 25 cm was 79.70 ± 0.39 mm, slightly lower than the real condition, with a JND of 1.38 ± 0.31 mm, suggesting a marginally reduced sensitivity. At 85 cm, the virtual PSE was 80.05 ± 0.34 mm, closely matching the real condition at this distance, and the JND was 1.13 ± 0.25 mm, comparable to the real counterpart (see Figure 5.8).

These values demonstrate a strong consistency in size perception between real and virtual spheres, with differences well below perceptual relevance.

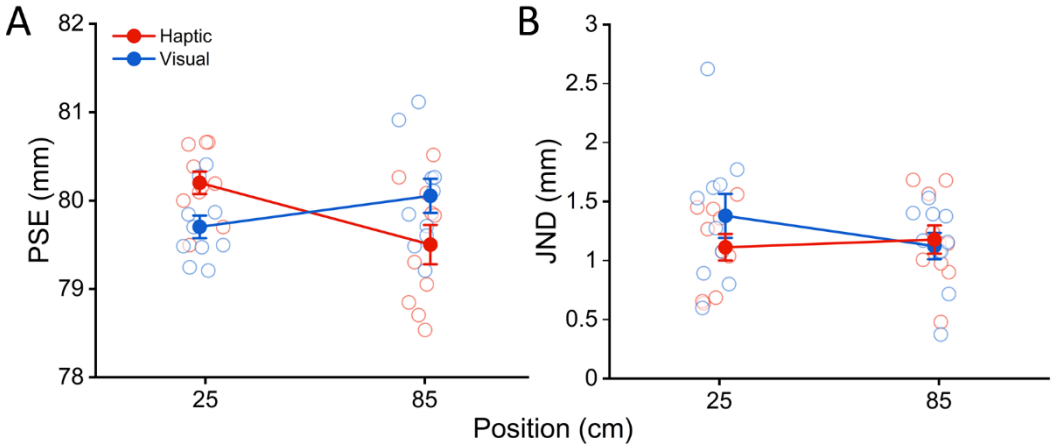

Figure 5.8 – PSE and JND (threshold) for real and virtual conditions at 25 cm and 85 cm. Haptic PSE and JND at 25 cm show large size sensitivity, with a slight PSE decrease at 85 cm. In the virtual condition, PSE is slightly lower and JND slightly higher at 25 cm; at 85 cm, PSE aligns with haptic values, and JND remains similar. Error bars represent the standard error.

The repeated-measures ANOVA examined the effects of *modality* (haptic vs. virtual), *distance* (25 cm vs. 85 cm), and their interaction on participants' PSE and JND.

For what concerns the PSE, neither *modality* ($F(1,9) = 0.03$, $p = 0.867$, $\eta^2 = 8.12\times10^{-4}$) nor *distance* ($F(1,9) = 1.59$, $p = 0.240$, $\eta^2 = 0.04$) showed significant effects. However, the *modality* × *distance* interaction was significant ($F(1,9) = 14.65$, $p = 0.004$, $\eta^2 = 0.32$), suggesting that differences between modalities depend on distance. Bayesian analysis supported these results. The model that includes the *modality* × *distance* interaction received a high Bayes Factor compared to the null model ($BF_{10} = 108.74$). In contrast, models containing only main effects showed Bayes Factors close to 1 (*modality*: $BF_{10} = 1.938$; *distance*: $BF_{10} = 2.59$). This implies that participants' perceptual strategies adapt differently depending on distance and modality.

For JND, the frequentist results did not indicate a significant effect of *modality* ($F(1,9) = 2.761$, $p = 0.13$, $\eta^2 = 0.04$), *distance* ($F(1,9) = 0.65$, $p = 0.440$, $\eta^2 = 0.03$), or the interaction *modality* × *distance* ($F(1,9) = 3.59$, $p = 0.091$, $\eta^2 = 0.10$). Bayesian analysis confirmed these results, providing moderate or weak evidence in favor of the null hypothesis for all effects considered (*modality*: $BF_{10} = 0.56$; *distance*: $BF_{10} = 0.53$; *modality* × *distance*: $BF_{10} = 0.29$). This pattern indicates that individual perceptual performance was preserved across modalities,

showing that participants maintained similar discrimination performance in both real and mixed reality contexts.

These findings reinforce the conclusion that HL2 can reproduce size perception with a fidelity approaching that of real-world vision, even when spatial depth changes.

5.4 Serial dependence in visuo-haptic feedback

These initial validation phases allowed us to conclude that HL2 provides not only reliable hand-tracking but also a visual perception of virtual objects comparable to that of real objects.

This ability is critical for the experiment presented in this section, which aims to selectively investigate the effect of serial dependence by isolating the contributions of visual and haptic information to size perception. In particular, the use of HL2 enables the delivery of a purely visual stimulus, in which the object is visible but not tangible, maintaining the same spatial position relative to the body and eliminating potential interference from object movement.

To date, no works have investigated serial dependence in *haptic* size perception, while only two works have observed the effect in *visual* size perception. In particular, an initial study focused on body size perception (Alexi et al., 2018), and through a reproduction task, they observed that participants' estimates of body size were systematically attracted to the preceding body, with the strongest effect when the size difference was two categorical units and then diminishing for larger differences. In a second study, the size of a stimulus was manipulated not as a main variable, but to shift participants' attention (Fritsche & de Lange, 2019). In each trial, participants were first shown a reference disc, followed by a grating slightly larger or smaller than the reference. They had to judge whether the grating was larger or smaller than the disc, ignoring the orientation. Next, a second grating appeared, whose orientation had to be reproduced with a response bar. By focusing on the size of the first stimulus, the attractive effect of serial dependence on the orientation of the second grating was significantly reduced. Overall, this suggests that serial dependence in the perception of size is still under-explored and requires further investigation.

Based on these evidences, in this section we present an experiment divided into four distinct conditions, designed to investigate how serial dependence influences purely visual and purely

haptic perception, and whether similar effects also emerge in cross-sensory contexts during an object size discrimination task.

5.4.1 Materials and methods

5.4.1.1 Participants

12 healthy volunteers (age 26.3 ± 1.8 years) with normal or corrected-to-normal vision and no history of neurological disorders participated in the study. All participants provided written informed consent prior to their involvement. The experimental protocol was approved by the ASL3 Genovese ethics committee and adhered to the principles outlined in the Declaration of Helsinki.

5.4.1.2 Apparatus, stimuli, and procedure

In this experiment, the nineteen spheres adopted in the previous section (with diameters ranging from 74 mm to 86 mm) were used: the real ones were fabricated using 3D printing technology, while the virtual ones were developed in Unity using MRTK and rendered via the HL2 headset through the Holographic Remoting Player app. As in the previous experiment, the experimenter managed trial initiation and response logging using keyboard inputs.

Participants were seated in a quiet, dimly lit room with their chair back at 40 cm from the table and their right hand positioned up-palm.

Each trial consisted of sequential presentation of three spheres: the first reference sphere (80 mm), an *inducer* sphere (77 mm or 83 mm diameter), followed by a test sphere (one of nineteen diameter spheres). Each sphere was presented for 1.5 seconds, with a 1-second inter-stimulus interval. No response time limit was imposed. Participants performed a 2AFC size discrimination task where they compared the reference sphere with the test sphere for each trial and indicated which appeared larger (see Figure 5.9 for experimental design depiction).

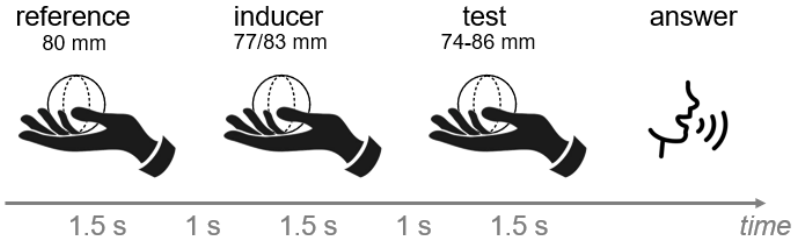

Figure 5.9 – Experimental design. Participants judged whether the first or third sphere appeared larger, with the middle sphere acting as the *inducer* to elicit serial dependence.

Two types of stimulus presentation were defined: in the haptic one (H) the sphere was real, physically grasped by participants with their eyes closed, while in the visual one (V) the sphere was virtual, rendered on participant's hand via HL2 to be viewed but not physically manipulated (so, they were not allowed to perform any physical movement with the hand).

We employed a 2×2 experimental design based on the modality of inducer and test stimuli presentation, with reference stimuli being the same modality of the test one: we defined one condition where both the inducer and the test spheres were haptically perceived (HHH), one with virtual inducer and virtual test sphere (VVV), one with real inducer sphere and virtual test sphere (VHV), and lastly one with virtual inducer sphere and real test sphere (HVH). This allowed us to see both unisensory and cross-sensory modality contributions.

Each combination of inducer and test spheres was presented across four blocks, resulting in a total of 152 trials per experimental condition. The order of experimental conditions was randomized across participants. Short breaks were allowed between blocks, and the entire session lasted approximately 2.5 hours.

5.4.1.3 Data analysis

To assess the influence of serial dependence on size perception within visual and haptic contributions, participants' responses were analyzed by fitting a cumulative Gaussian function to the proportion of trials in which the test sphere was judged as 'larger' than the reference, plotted against the size of the test spheres. This psychometric modeling was performed separately for each participant and each inducer size. From the fitted function, we extracted the point of subjective equality (PSE), defined as the stimulus size at which participants were equally likely (50%) to report the test sphere as larger or smaller than the reference. The PSE served as an index of perceptual bias induced by the preceding stimulus.

The magnitude of the serial dependence effect for each experimental condition was computed as the difference in PSE between the two inducer curves (ΔPSE), reflecting the degree to which prior context influenced current size judgments.

To judge the effect of the inducer dimension and the spheres' nature (V or H) on the PSE, we computed a Bayesian repeated-measures ANOVA using the *BayesFactor* package. We included the main terms of *inducer* (77 mm vs. 83 mm), *test type* (H vs. V), and *inducer type* (unisensory vs. cross-sensory conditions), and all possible interactions, considering subjects (ID) as a random factor. To identify the best model, the inclusion probability of each term was evaluated: for each main term or interaction, the ratio between the sum of the Bayes Factors (BF) of the models that included the term and those that did not include it was calculated. Terms with an inclusion Bayes Factor greater than 3 were considered to have substantial evidential support and were included in the subsequent Bayesian post-hoc paired t-tests. To preserve the within-subject structure of the data, PSE values were averaged within each participant and condition under analysis.

In addition, a targeted post-hoc analysis was performed to directly compare the magnitude of the *inducer* effect across levels of *inducer type*.

Data pre-processing and PSE extraction were performed in MATLAB R2022b (The MathWorks Inc., 2022), while model and post-hoc analysis were conducted in R version 4.5.2 (R Core Team, 2021).

5.4.2 Results

The PSE was computed separately for each inducer in all the experimental conditions (based on the real or virtual nature of the spheres) to assess the influence of serial dependence on size perception in unisensory and cross-sensory contributions.

The serial dependence effect (ΔPSE) for each condition is shown in Table 5.4 and Figure 5.10. As can be seen, in unisensory conditions, the PSE increases consistently with larger inducer (H: 1.26 ± 0.01 mm; V: 1.86 ± 0.02 mm), while in the cross-sensory conditions, the increase in PSE with larger inducer is more modest (HVH: 0.45 ± -0.01 mm; VHV: 0.44 ± -0.05 mm).

Table 5.4 – PSE for 77 mm and 83 mm inducers, and serial dependence effect (ΔPSE) for each condition. PSE values are reported as mean ± standard error of the mean (SEM).

Condition	Inducer 77 mm	Inducer 83 mm	ΔPSE
Unisensory H	80.14 ± 0.23 mm	81.40 ± 0.24 mm	1.26 ± 0.01 mm
Unisensory V	78.62 ± 0.23 mm	80.48 ± 0.26 mm	1.86 ± 0.02 mm
Cross-sensory: Inducer V, Test H	80.29 ± 0.25 mm	80.74 ± 0.24 mm	0.45 ± -0.01 mm
Cross-sensory: Inducer H, Test V	79.66 ± 0.20 mm	80.10 ± 0.15 mm	0.44 ± -0.05 mm

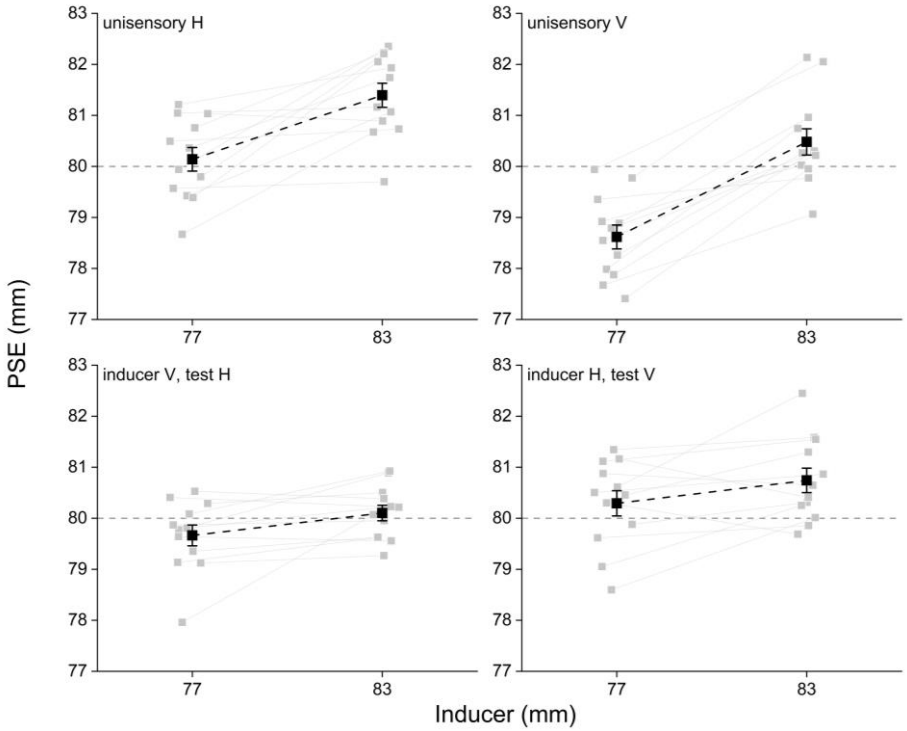

Figure 5.10 – Average PSE values as a function of the inducer (77 mm and 83 mm) for the four experimental conditions. The squares represent the average PSE values, while the error bars indicate the standard error of the mean.

The Bayesian repeated-measures ANOVA analysis showed selective effects of the main factors and interactions on the perception of the size of the test spheres.

The analysis of inclusion Bayes Factors (Table 5.5) showed that the *inducer* dimension (77 mm vs. 83 mm) had a strong effect on test perception. The *inducer type* (same vs. opposite with respect to the test/reference) and *test type* (H vs. V) also showed significant evidence, as did the *test type* × *inducer type* interaction and the *inducer* × *inducer type* interaction. In contrast, the interaction *inducer* × *test type* showed inconclusive evidence, and the interaction *inducer* × *test type* × *inducer type* showed evidence in favor of exclusion from the model.

Table 5.5 – Inclusive Bayes Factors for each term of the Bayesian repeated-measures ANOVA. The values indicate the evidence in favor of including each main factor or interaction in the model, with higher numbers representing stronger evidence.

Term	BF inclusion
Inducer (77 mm vs. 83 mm)	3.16×10^{11}
Inducer type (same as test vs. opposite to test)	2.56×10^{6}
Test type (H vs. V)	1.02×10^{6}
Test type × Inducer type	5.17×10^{5}
Inducer × Inducer type	122
Inducer × Test type	0.799
Inducer × Test type × Inducer type	0.186

This allowed us to conclude that the model that best explains our data is defined by $PSE \sim Inducer + Inducer_{type} + Test_{type} + Test_{type} * Inducer_{type} + Inducer * Inducer_{type}$.

Subsequently, Bayesian post-hoc analyses provided a detailed picture of the observed interaction (Table 5.6).

Table 5.6 – Results of post-hoc analyses conducted using Bayesian t-tests for paired measures. The table shows the Bayes Factors (BF) associated with each comparison between experimental conditions (i.e., each interaction term in our model).

Comparison	BF
Inducer H Test H vs. Inducer V Test V (HHH vs. VVV)	23.28
Inducer V Test H vs. Inducer H Test V (HVH vs. VHV)	2.67
Inducer H Test H vs. Inducer V Test H (HHH vs. HVH)	39.01
Inducer V Test V vs. Inducer H Test V (VVV vs. VHV)	3.75
Inducer 77 mm unimodal vs. Inducer 83 mm unimodal (HHH and VVV)	2253.20
Inducer 77 mm cross-modal vs. Inducer 83 mm cross-modal (HVH and VHV)	13.05

The direct comparison between the two unisensory conditions (HHH vs. VVV) showed strong evidence (BF = 23.28), indicating that the size estimation bias has a different direction between the haptic condition and the visual condition. The comparison between the two cross-sensory conditions (HVH vs. VHV) provided inconclusive evidence regarding their difference (BF = 2.67).

Comparisons between unimodal and cross-modal conditions revealed systematic differences in bias estimates, with cross-modal conditions showing more than moderate evidence in favor of reduced deviations relative to unimodal conditions (HHH vs. HVH, BF = 39.01; VVV vs. VHV, BF = 3.75). Overall, these results suggest that participants are more accurate in the cross-sensory rather than in the unisensory condition.

Finally, direct comparison between small and large inducers (so the inducer-related shift in PSE), both within unimodal (HHH and VVV, BF = 2253.20) and within cross-modal (HVH and VHV, BF = 13.05) conditions, revealed strong evidence, confirming that the size of the inducer shifts the PSE, in both the unimodal and cross-modal conditions. Additionally, a direct comparison of the size of serial dependence effects between unisensory and cross-sensory conditions showed strong evidence that the effect of dimension (77 mm or 83 mm) of the inducer was greater in the unisensory than in the cross-sensory condition (BF = 149.37).

5.4.3 Discussion

This study aimed to investigate how visual and haptic cues can influence the perception of an object's size, with a particular focus on the effect of serial dependence. To do this, we used a mixed reality setup, where real spheres allowed us to obtain purely haptic cues, while virtual spheres, rendered using HL2, allowed us to see the contribution of pure visual perception in a realistic context.

The study builds upon the studies presented in the previous sections of this chapter, where we demonstrated how HL2 allows for highly realistic rendering of virtual objects, to the point that their perception is comparable to that of real objects. This approach not only allows for precise manipulation of the dimensions and visual characteristics of stimuli but also allows this to be done in a realistic three-dimensional context, preserving the natural visual cues that influence perception. In this way, we can isolate the visual contribution from the haptic one without having to resort to simple two-dimensional or artificial stimuli, ensuring more ecological and generalizable results.

Typical biases in visual and haptic size perception

Our findings about the estimation bias in the haptic domain and visual domain are consistent with the literature documenting the existence of systematic biases in the perception of size

within individual sensory modalities, biases that are nevertheless highly dependent on context, task, and stimulus nature.

Literature shows that visual perception of size, especially in peripersonal space, can be relatively accurate but frequently tends towards overestimation, particularly for distant objects or specific visual configurations (Daneyko et al., 2025; Gori, Giuliana, et al., 2012). These effects have been interpreted as a consequence of the visual system's reliance on contextual cues, which can bias metric judgments toward recently encountered or expected stimulus values.

Similarly, although haptic perception supports reliable information for object recognition and size discrimination, it is also subject to systematic metric distortions (Katzakis et al., 2020). In particular, haptic judgments often exhibit a central tendency effect, characterized by overestimation of smaller objects and underestimation of larger ones relative to a reference size (Newlin et al., 1978; D. R. Thomas et al., 1974; Watson, 1957). Such distortions have frequently been interpreted within the framework of adaptation level theory, where perceptual judgments are made relative to an internal reference that reflects the mean of the stimulus distribution rather than an absolute physical scale (Eysenck, 1966, 1966; Helson, 1964).

In line with the literature, the unisensory conditions of our experiment showed a consistent bias in size estimation (haptic underestimation and visual overestimation): importantly, this bias is reduced in cross-sensory conditions, suggesting that the availability of information from another modality constrains size estimations and limits the magnitude of systematic distortions (Katzakis et al., 2020).

Overall, our findings confirm that size perception in both visual and haptic domains is shaped by modality-specific biases that systematically deviate from physical truth.

Serial dependence in unisensory and cross-sensory contexts

In addition to the specific perceptual biases of the individual modalities, our results show a clear serial dependence effect in the estimation of size, highlighted by the systematic shift of the PSE as a function of the size of the inducer stimulus. This pattern is consistent with previous evidence, both from this thesis work and from the literature, showing that perceptual estimates are attracted toward recent sensory input across a variety of features and tasks (Cicchini et al., 2017; J. Fischer & Whitney, 2014; Manassi & Whitney, 2022).

Crucially, the magnitude of this effect depends on the sensory relationship between the inducer and the test stimulus: in unisensory conditions, serial dependence effects were robust, with larger inducer producing consistent increases in PSE and smaller inducer producing consistent reductions, both in the visual and in the haptic modality; in cross-sensory conditions, serial dependence effects were still present but significantly attenuated, and this reduction was observed across both cross-modal configurations.

Importantly, the present findings should also be considered in relation to previous studies on perceptual adaptation and haptic aftereffects. In classical adaptation paradigms, prolonged exposure to a stimulus typically produces repulsive perceptual biases, enhancing sensitivity to changes in incoming sensory information. In the haptic domain, adaptation-like effects have been reported for several object properties, including roughness and size perception (Kahrimanovic et al., 2009; Kappers & Bergmann Tiest, 2013, 2014). In particular, Kappers and Bergmann Tiest (2014) demonstrated a haptic size aftereffect in which prolonged interaction with an object altered the perceived size of subsequently explored stimuli. These findings suggest that recent sensory history can systematically influence haptic perceptual judgments through mechanisms related to sensory recalibration and contextual coding.

The effects observed in the present study differ from classical adaptation effects in at least two important aspects. First, the inducer stimuli were presented only briefly, rather than through prolonged exposure typically used in adaptation paradigms. Second, the observed biases were predominantly attractive rather than repulsive, with perceptual estimates shifting toward the recently experienced stimulus. This attractive pattern is more consistent with accounts of serial dependence proposing a stabilizing mechanism that promotes perceptual continuity over time. However, the relationship between serial dependence and adaptation is unlikely to be strictly dichotomous. Instead, both phenomena may reflect partially overlapping effects of recent sensory history operating at different temporal scales and serving complementary functional roles, such as perceptual stability on the one hand and change sensitivity or efficient coding on the other.

These results fit into the debate on the nature of serial dependence in a structured way. Previous studies have provided strong evidence in favor of serial dependence being predominantly specific to sensory modality. In particular, Fornaciai and Park (Fornaciai & Park, 2019) showed that serial dependence generalizes between different stimulus formats

within the visual modality, but not between different sensory modalities, suggesting a mechanism anchored to specific sensory representations. Partially divergent results were then reported by Hashimoto and Makioka (Hashimoto & Makioka, 2025a), who observed cross-modal serial dependence effects in a sequential numerical comparison task, indicating that transfer between modalities may emerge in the presence of the same stimulus format.

In this context, our results show an intermediate pattern: serial dependence is robust in unisensory conditions but also remains present in cross-sensory conditions. This trend suggests that, in the domain of size perception, the influence of the previous stimulus (*inducer*) on the current one (*test*) is reduced when they belong to different modalities. These results are consistent with the idea that serial dependence could reflect a mechanism that combines specific sensory components and more abstract representations shared between modalities.

Overall, our results help clarify that serial dependence in size perception is not a strictly unisensory or completely amodal phenomenon, but is a flexible process modulated by the availability and consistency of sensory information.

General considerations and limitations of the study

The serial dependence experiment we conducted enabled us to exploit mixed reality technology to create a novel experimental configuration: isolating the visual contribution of an object held in one's hand during a size discrimination task. By using a hologram, we provided visual feedback without any accompanying haptic information. This approach allowed us to investigate serial dependence within these two sensory modalities in isolation and the cross-sensory influence, contributing to deepen the literature on cross-modal serial dependence.

Our results indicate the presence of systematic over- and under-estimation biases in both visual and haptic size perception, and size judgments are consistently modulated by the dimension of the preceding stimulus. Additionally, the magnitude of the serial dependence effect differed between sensory conditions, being larger in unisensory than in cross-sensory configurations.

A possible limitation of this study concerns the relatively small sample size, which may have limited the statistical power of the analyses and, consequently, the ability to detect more subtle contributions of certain factors or interactions, such as the *inducer* × *test type* interaction.

Although the Bayesian approach allows for a direct evaluation of the evidence for or against the inclusion of terms in the model, a larger sample would allow for more accurate estimation of these effects and more robust conclusions. Therefore, a key next step will be to expand the experimental sample in order to strengthen the reliability of the results and clarify the role of any marginal interactions.

Chapter 6

General Discussion

This chapter aims to integrate and critically discuss the main results that emerged in the various experimental chapters, relating them to the research questions that guided the work. The main contributions offered by this thesis regarding the understanding of serial dependence will be highlighted, both in terms of the generality of the phenomenon in the different sensory modalities and in terms of the underlying mechanisms. Finally, future directions for research will be outlined.

6.1 Summary

This thesis investigated the phenomenon of serial dependence as a general mechanism of temporal integration, exploring its extension beyond classical visual features and evaluating its role in the perception of time, audition, touch, and cross-sensory contexts, as well as the influence of visual experience.

The first experimental chapter examined serial dependence in visual temporal perception, comparing temporal discrimination and reproduction tasks to clarify whether the observed biases reflect shared perceptual mechanisms or distinct processes. The results showed that serial dependence emerges in both tasks, but with different characteristics, suggesting a

differential role of serial dependence in the integration of past and present stimuli. Additionally, the serial dependence effect that emerged in the two experiments does not appear to be related to working memory effects, suggesting that the different experimental structures involve distinct memory mechanisms.

The following chapter extended the analysis to auditory temporal perception, demonstrating that serial dependence in this domain critically depends on the temporal structure of stimuli but not on their physical structure, highlighting specific constraints of the auditory modality.

The third experimental chapter investigated serial dependence in the tactile perception of motion direction, introducing dedicated haptic tools and comparing sighted and visually impaired participants, revealing that the effect is present in touch and is also present in the absence of visual experience, suggesting a common mechanism underlying the serial dependence effect in tactile motion direction perception in both sighted and visually impaired populations.

The final chapter addressed cross-sensory serial dependence in the visuo-haptic domain, using mixed reality technology to separately control the contributions of visual and tactile information in the perception of object size, showing that serial dependence can emerge specifically within individual modalities as well as in cross-modal settings.

Overall, the results of this thesis indicate that serial dependence is not a unitary and invariable mechanism, but rather a flexible process that depends on sensory modality and temporal context, contributing to a more nuanced understanding of the computational principles underlying perceptual stability over time.

6.2 The push-pull dynamics of serial dependence

The results presented in the studies in Chapters 2 and 4 reinforce the idea that serial dependence is not a unitary phenomenon attributable to a single mechanism, but rather the expression of a push-pull dynamic in which distinct and opposing processes interact in shaping perceptual behavior (Pascucci et al., 2019; Sadil et al., 2024). More specifically, the presented findings support the idea that recent sensory history can influence perception through at least two partially dissociable mechanisms: an attractive component linked to

perceptual stabilization and history, and a repulsive component more closely related to sensory adaptation and change detection.

This pattern, already documented in the visual domain and presented in the previous chapters, has been interpreted as the result of two functionally distinct mechanisms (Cicchini et al., 2017; J. Fischer & Whitney, 2014; Pascucci et al., 2019). From a functional point of view, the repulsive component associated with the previous stimulus can be understood as a mechanism of *perceptual differentiation* (Blondé et al., 2023; Sheehan & Serences, 2022): distancing the representation of the current stimulus from the recent one allows the perceptual system to maximize sensitivity to changes, preventing neural saturation phenomena and reducing sensory information redundancy. This type of repulsion is consistent with the classic effects of sensory adaptation observed in multiple perceptual domains and appears particularly relevant in the temporal and tactile contexts, where the repetition of similar stimuli can rapidly degrade discriminability (Clifford et al., 2000; Kohn, 2007). Our findings extend this perspective by showing that similar history-dependent influences can also emerge under much shorter stimulation conditions. On the contrary, the attractive component linked to the previous response can be interpreted as a form of decision-making inertia or continuity of action, which helps to stabilize behavior over time, reducing variability and uncertainty in response production (Cicchini et al., 2017; Fritsche et al., 2017).

The observation that the same dynamic also emerges in the tactile domain and in participants with visual impairments provides further evidence in favor of its general nature. In visually impaired subjects, in fact, the simultaneous presence of repulsion towards the stimulus and attraction towards the response suggests that serial dependence does not critically depend on visual experience, but can be supported by internal sensory and motor representations. The cortical reorganization associated with blindness, which also involves the typically visual areas (Coelho et al., 2025; Sadato et al., 2002; Wanet-Defalque et al., 1988), could enhance both sensory adaptation processes and memory and action planning processes, promoting a balance between behavioral stability and flexibility.

To conclude, this ambivalent dynamic of serial dependence can be interpreted as the result of a functional compromise between two fundamental requirements of the perceptual system: on the one hand, the need to remain sensitive to changes in the environment; on the other, the need to maintain continuity and stability in representations and actions. The coexistence of

sensory repulsion and decision-making attraction, therefore, represents an adaptive strategy that allows the brain to integrate past experience without sacrificing the ability to respond flexibly to new information.

6.3 Serial dependence in time perception

The results of the studies presented in Chapters 2 and 3 highlight how serial dependence is a phenomenon present also in the perception of time, extending across both the visual and auditory domains.

In visual temporal discrimination tasks, the presence of an inducer stimulus was sufficient to generate an attractive effect on the subsequent target, confirming what has been observed in the literature (Togoli et al., 2021). At the same time, in visual temporal reproduction tasks, serial dependence shows a dual nature, with repulsive effects linked to the previous stimulus and attractive effects linked to the previous response, consistent with the push-pull model illustrated in the previous paragraph. These two findings suggest that serial dependence in visual temporal perception is not a unitary phenomenon, but reflects the interaction of distinct mechanisms operating at different levels of processing (Ceylan et al., 2021; Cicchini et al., 2017; Pascucci et al., 2019): visual time estimation does not appear to be the product of a single stage of encoding, but rather emerges from a multilevel dynamic in which sensory and decision-making components contribute in different ways to the temporal experience (Himberger et al., 2018; Marti & Dehaene, 2017).

Serial dependence in auditory temporal perception confirms and expands on these results. In this case, we observed how the effect emerges from a temporal discrimination task based on the visual one, and again, the inducer stimulus acts by altering the perception of the following stimulus. However, although auditory temporal perception also exhibited reliable serial dependence, the effect was strongly modulated by the inter-stimulus interval (ISI) between the inducer stimulus and the target stimulus: short ISIs (4 ms) favor the emergence of the effect, while longer ISIs (300 ms) cancel its influence.

This difference from visual temporal perception suggests that, while temporal serial dependence may rely on a general integration principle, its effective temporal window is

modality-dependent. Auditory timing mechanisms, which are often characterized by high temporal precision and rapid updating (Näätänen et al., 2004; Rammsayer et al., 2015; Thibault et al., 2023), may operate on shorter integration scales compared to visual timing processes, which are known to tolerate longer temporal correlations.

These results support the hypothesis that serial dependence in time perception cannot be considered purely amodal nor purely modality-specific. Rather, it appears to reflect a general stabilizing mechanism whose temporal dynamics are constrained by the intrinsic processing characteristics of each sensory modality. The fact that the effect persists across vision and audition supports the hypothesis of a shared adaptive function – namely, the reduction of perceptual variability and the promotion of temporal continuity (Cicchini et al., 2017; J. Fischer & Whitney, 2014) – while the divergence in temporal tuning highlights the role of modality-dependent encoding constraints.

6.4 The role of vision in serial dependence effect

Within the various experimental chapters, specifically in Chapters 2, 4, and 5, vision played a crucial role, either directly or indirectly, in modulating the emergence and characteristics of the serial dependence effect. Overall, the results presented in these studies suggest that vision is not a necessary prerequisite for the emergence of serial dependence, but it is a crucial factor in shaping its amplitude, direction, and level of representation at which the effect emerges.

In purely visual tasks, such as those presented in Chapter 2 on temporal perception, serial dependence emerges in a robust and systematic manner. In particular, in both temporal discrimination and reproduction tasks, previous visual experience significantly influences current estimation. These results are part of a vast literature that identifies vision as the privileged domain for the study of serial dependence (Cicchini et al., 2024; Manassi et al., 2023; Pascucci et al., 2023), probably since vision is the dominant sensory modality in humans and offers a well-known and accessible model for studying perception and sensory processing, as well as naturally involving predictive and temporal integration mechanisms (Deodato & Melcher, 2024).

In Chapter 5, the role of vision is explored in a more subtle way through a mixed reality paradigm that allows visual information to be dissociated from haptic information in the perception of dimension. The results show that, although serial dependence is present in both unisensory and cross-sensory conditions, its amplitude is significantly greater when the inducer and test stimuli belong to the same modality. In particular, the presence of a pure visual component is associated with more pronounced serial dependence effects, while cross-modal interaction seems to attenuate the influence of the previous stimulus. This pattern suggests that vision may serve as a privileged reference system for the encoding of information, helping to stabilize perception over time, but also constraining the emergence of systematic distortions when the disruptive information (so, the *inducer* stimulus) is consistent within the same modality (Heller, 1983; Power, 1980).

A particularly relevant contribution to the understanding of the role of vision emerges from the results of Chapter 4, in which serial dependence is studied in the tactile motion direction perception, both in sighted and visually impaired participants. The results show that the serial dependence effect is present even in the absence of visual input, and that the push-pull dynamic between the perceptual component (ΔS) and the response-related component (ΔR) is consistent in both populations. This evidence suggests that the mechanisms underlying serial dependence do not depend exclusively on visual experience but reflect more general computational principles of the perceptual system, shared between different sensory modalities.

Although serial dependence also emerges in conditions without visual information, the data suggest that vision can play a role in calibrating temporal integration mechanisms. In sighted participants, the availability of visual feedback during the execution of the response can reduce perceptual uncertainty and limit dependence on the recent history of responses. On the contrary, in visually impaired participants, the absence of such feedback could reinforce the weight of the decision-making and mnemonic component, amplifying the attractive effect linked to the previous response. In this sense, vision does not appear to be the origin of serial dependence, but a factor that modulates the balance between sensory adaptation and cognitive stabilization.

Overall, the findings of this thesis suggest that serial dependence is not a mechanism related to a single sensory modality but emerges from the interaction between modality-specific

perceptual processes and more abstract-level representations. In light of this, vision constitutes an important reference system for perceptual stabilization, but it does not represent a necessary condition for serial dependence to manifest itself.

6.5 From unimodal to cross-modal interactions

The results presented in the various chapters of this thesis show how serial dependence emerges consistently within individual sensory modalities. Overall, this suggests that serial dependence is not a phenomenon rigidly anchored to a single mode but reflects a dynamic process that can operate at different levels of representation, from specific sensory contexts to cross-modal contexts.

In Chapters 2 and 3, serial dependence emerges robustly within individual sensory modalities, both in visual and auditory perception of time, confirming that the previous stimulus systematically influences the current estimate. However, the amplitude and persistence of the effect are strongly constrained by the computational characteristics of the specific modality: in particular, in the auditory domain, serial dependence occurs only for very short time intervals, suggesting an origin linked to rapid and transient sensory mechanisms (Näätänen et al., 2004; Rammsayer et al., 2015; Thibault et al., 2023). A more articulated picture emerges when the task requires a reproduction of the stimulus, as in the reproduction experiments proposed in Chapters 2 and in Chapter 4. In these cases, serial dependence does not exclusively reflect the influence of the previous stimulus, but results from the interaction between perceptual and decision-making components, with repulsive effects related to the stimulus and attractive effects related to the response. These results indicate that, under unimodal conditions, serial dependence may reflect mechanisms closely related to the sensory coding of the specific sensory modality.

However, this does not imply that the phenomenon is limited to such levels of representation. In particular, when the relevant feature is a property that allows a shared representation between modalities, such as the size of objects, the influence of perceptual history can persist even when the inducer and stimulus test belong to different sensory systems. Chapter 5 provides direct evidence of how serial dependence behaves in this case: the results from our experiment show that the effect persists even in cross-sensory conditions, but with a

significantly reduced amplitude compared to unimodal conditions. This intermediate pattern suggests that serial dependence is neither completely specific to the modality nor completely amodal.

The attenuation of the effect in cross-modal conditions may reflect a reduction in coherence between the sensory representations involved: when information comes from different modalities, the perceptual system may weigh current information more heavily than recent history, limiting the influence of the previous stimulus. However, the persistence of the effect indicates the existence of shared representations, probably related to more abstract properties of the stimulus, such as size or duration. This is also confirmed by the fact that the serial dependence effect in cross-sensory conditions persists whether one switches from an inducer in visual modality to a test in haptic modality, or vice versa.

6.6 Conclusion and future directions

The purpose of this thesis was to investigate the effect of serial dependence across different sensory modalities, perceptual characteristics, and task types, in order to clarify the mechanisms through which recent sensory history influences current perception. Combining visual, auditory, tactile, and cross-sensory paradigms, this work provides a comprehensive view of serial dependence as a flexible and multi-level phenomenon, rather than as a mechanism confined to a single sensory system or a specific computational stage.

In all experiments, serial dependence manifested as a systematic bias toward recent experience, confirming its robustness across different perceptual domains. However, the characteristics of the effect vary significantly depending on the sensory modality, the perceptual feature analyzed, and the structure of the task.

These results support the interpretation of serial dependence as a multi-level mechanism, capable of operating at different stages of processing. At an early sensory level, the effect may reflect rapid and modality-specific processes aimed at increasing sensitivity to changes and reducing redundancy. At higher levels, serial dependence seems to promote perceptual stability by integrating recent information over time, especially when the feature of interest has amodal or modality-shared representations. In this framework, serial dependence is

neither rigidly unisensory nor completely amodal, but a flexible process whose expression depends on the interaction between sensory precision, feature representation, and task characteristics. This perspective allows for merging previously conflicting results and explaining both the presence and attenuation of the effect across different modalities.

Future research should systematically manipulate the level at which perceptual features are represented to separate modality-specific contributions from amodal ones. A promising extension involves cross-sensory paradigms on other features, such as temporal duration or direction of movement, to verify whether the attenuation observed for size perception generalizes to other perceptual properties. Moreover, combining behavioral paradigms with neuroimaging or neurostimulation techniques could help identify the neural loci where serial dependence emerges and clarify whether different levels of processing contribute in parallel or in sequence. Finally, investigating serial dependence in more ecological and interactive contexts, such as active exploration or natural multisensory environments, could provide further insights into the functional role of the phenomenon in stabilizing perception in daily life.

References

Akaishi, R., Umeda, K., Nagase, A., & Sakai, K. (2014). Autonomous Mechanism of Internal Choice Estimate Underlies Decision Inertia. *Neuron*, *81*(1), 195–206. https://doi.org/10.1016/j.neuron.2013.10.018

Alais, D., Kong, G., Palmer, C., & Clifford, C. (2018). Eye gaze direction shows a positive serial dependency. *Journal of Vision*, *18*(4), 11. https://doi.org/10.1167/18.4.11

Alais, D., Leung, J., & Van Der Burg, E. (2017). Linear Summation of Repulsive and Attractive Serial Dependencies: Orientation and Motion Dependencies Sum in Motion Perception. *The Journal of Neuroscience*, *37*(16), 4381–4390. https://doi.org/10.1523/JNEUROSCI.4601-15.2017

Alexi, J., Cleary, D., Dommisse, K., Palermo, R., Kloth, N., Burr, D., & Bell, J. (2018). Past visual experiences weigh in on body size estimation. *Scientific Reports*, *8*(1), 215. https://doi.org/10.1038/s41598-017-18418-3

Amadeo, M. B., Campus, C., & Gori, M. (2020). Visual representations of time elicit early responses in human temporal cortex. *NeuroImage*, *217*, 116912. https://doi.org/10.1016/j.neuroimage.2020.116912

Anstis, S., Verstraten, F. A., & Mather, G. (1998). The motion aftereffect. *Trends in Cognitive Sciences*, *2*(3), 111–117. https://doi.org/10.1016/s1364-6613(98)01142-5

Arzounian, D., de Kerangal, M., & de Cheveigné, A. (2017). Sequential dependencies in pitch judgments. *Journal of the Acoustical Society of America*, *142*(5), 3047–3057. https://doi.org/10.1121/1.5009938

Balsdon, T., Wyart, V., & Mamassian, P. (2020). Confidence controls perceptual evidence accumulation. *Nature Communications*, *11*(1), 1753. https://doi.org/10.1038/s41467-020-15561-w

Barbosa, J., & Compte, A. (2020). Build-up of serial dependence in color working memory. *Scientific Reports*, *10*(1), 10959. https://doi.org/10.1038/s41598-020-67861-2

Bensmaïa, S. J., Killebrew, J. H., & Craig, J. C. (2006). Influence of Visual Motion on Tactile Motion Perception. *Journal of Neurophysiology*, *96*(3), 1625–1637. https://doi.org/10.1152/jn.00192.2006

Bertonati, G., Tonelli, A., Cuturi, L. F., Setti, W., & Gori, M. (2020). Assessment of spatial reasoning in blind individuals using a haptic version of the Kohs Block Design Test. *Current Research in Behavioral Sciences*, *1*, 100004. https://doi.org/10.1016/j.crbeha.2020.100004

Besl, P. J., & McKay, N. D. (1992). A method for registration of 3-D shapes. *IEEE Transactions on Pattern Analysis and Machine Intelligence*, *14*(2), 239–256. https://doi.org/10.1109/34.121791

Bilacchi, C. M., Sirius, E. V. P., Cravo, A. M., & de Azevedo Neto, R. M. (2022). Temporal dynamics of implicit memory underlying serial dependence. *Memory & Cognition*, *50*(2), 449–458. https://doi.org/10.3758/s13421-021-01221-x

Bliss, D. P., Sun, J. J., & D'Esposito, M. (2017). Serial dependence is absent at the time of perception but increases in visual working memory. *Scientific Reports*, *7*(1), 14739. https://doi.org/10.1038/s41598-017-15199-7

Blondé, P., Kristjánsson, Á., & Pascucci, D. (2023). Tuning perception and decisions to temporal context. *iScience*, *26*(10). https://doi.org/10.1016/j.isci.2023.108008

Boven, R. W. V., Hamilton, R. H., Kauffman, T., Keenan, J. P., & Pascual–Leone, A. (2000). Tactile spatial resolution in blind Braille readers. *Neurology*, *54*(12), 2230–2236. https://doi.org/10.1212/WNL.54.12.2230

Brainard, D. H. (1997). The Psychophysics Toolbox. *Spatial Vision*, *10*(4), 433–436. https://doi.org/10.1163/156856897X00357

Brock, A., & Jouffrais, C. (2015). Interactive audio-tactile maps for visually impaired people. *SIGACCESS Access. Comput.*, (113), 3–12. https://doi.org/10.1145/2850440.2850441

Buckthought, A., Kim, J., & Wilson, H. R. (2008). Hysteresis effects in stereopsis and binocular rivalry. *Vision Research*, *48*(6), 819–830. https://doi.org/10.1016/j.visres.2007.12.013

Buhusi, C. V., & Meck, W. H. (2009). Relativity Theory and Time Perception: Single or Multiple Clocks? *PLoS ONE*, *4*(7), e6268. https://doi.org/10.1371/journal.pone.0006268

Burg, E. V. der, Toet, A., Brouwer, A.-M., & Erp, J. B. F. V. (2021). Serial Dependence of Emotion Within and Between Stimulus Sensory Modalities. *Multisensory Research*, *35*(2), 151–172. https://doi.org/10.1163/22134808-bja10064

Burr, D., Banks, M. S., & Morrone, M. C. (2009). Auditory dominance over vision in the perception of interval duration. *Experimental Brain Research*, *198*(1), 49–57. https://doi.org/10.1007/s00221-009-1933-z

Burr, D., Rocca, E. D., & Morrone, M. C. (2013). Contextual effects in interval-duration judgements in vision, audition and touch. *Experimental Brain Research*, *230*(1), 87–98. https://doi.org/10.1007/s00221-013-3632-z

Ceylan, G., Herzog, M. H., & Pascucci, D. (2021). Serial dependence does not originate from low-level visual processing. *Cognition*, *212*, 104709. https://doi.org/10.1016/j.cognition.2021.104709

Ceylan, G., & Pascucci, D. (2023). Attractive and repulsive serial dependence: The role of task relevance, the passage of time, and the number of stimuli. *Journal of Vision*, *23*(6), 8. https://doi.org/10.1167/jov.23.6.8

Chaconas, N., & Höllerer, T. (2018). An Evaluation of Bimanual Gestures on the Microsoft HoloLens. *2018 IEEE Conference on Virtual Reality and 3D User Interfaces (VR)*, 1–8. https://doi.org/10.1109/VR.2018.8446320

Chaney, W., Liberman, A., & Whitney, D. (2016). Serial dependence in perception of biological motion. *Journal of Vision*, *16*(12), 274–274. https://doi.org/10.1167/16.12.274

Cicchini, G. M., Anobile, G., & Burr, D. C. (2014). Compressive mapping of number to space reflects dynamic encoding mechanisms, not static logarithmic transform. *Proceedings of the National Academy of Sciences*, *111*(21), 7867–7872. https://doi.org/10.1073/pnas.1402785111

Cicchini, G. M., Arrighi, R., Cecchetti, L., Giusti, M., & Burr, D. C. (2012). Optimal Encoding of Interval Timing in Expert Percussionists. *Journal of Neuroscience*, *32*(3), 1056–1060. https://doi.org/10.1523/JNEUROSCI.3411-11.2012

Cicchini, G. M., Benedetto, A., & Burr, D. C. (2021). Perceptual history propagates down to early levels of sensory analysis. *Current Biology*, *31*(6), 1245-1250.e2. https://doi.org/10.1016/j.cub.2020.12.004

Cicchini, G. M., Mikellidou, K., & Burr, D. (2017). Serial dependencies act directly on perception. *Journal of Vision*, *17*(14), 6. https://doi.org/10.1167/17.14.6

Cicchini, G. M., Mikellidou, K., & Burr, D. C. (2018). The functional role of serial dependence. *Proceedings. Biological Sciences*, *285*(1890), 20181722. https://doi.org/10.1098/rspb.2018.1722

Cicchini, G. M., Mikellidou, K., & Burr, D. C. (2024). Serial Dependence in Perception. *Annual Review of Psychology*, *75*(Volume 75, 2024), 129–154. https://doi.org/10.1146/annurev-psych-021523-104939

Clark, A. (2013). Whatever next? Predictive brains, situated agents, and the future of cognitive science. *Behavioral and Brain Sciences*, *36*(3), 181–204. https://doi.org/10.1017/S0140525X12000477

Clifford, C. W., Wenderoth, P., & Spehar, B. (2000). A functional angle on some after-effects in cortical vision. *Proceedings of the Royal Society B: Biological Sciences*, *267*(1454), 1705–1710. https://doi.org/10.1098/rspb.2000.1198

Coelho, L. A., Ramirez, D. E. A., Basta, S., Guarischi, M., Gonzalez, C. L. R., & Gori, M. (2025). The role of visual experience in haptic spatial perception: Evidence from early blind, late blind, and sighted individuals. *Biology of Sex Differences*, *16*(1), 64. https://doi.org/10.1186/s13293-025-00747-y

Cohen, L. G., Celnik, P., Pascual-Leone, A., Corwell, B., Faiz, L., Dambrosia, J., Honda, M., Sadato, N., Gerloff, C., Catala´, M. D., & Hallett, M. (1997). Functional relevance of cross-modal plasticity in blind humans. *Nature*, *389*(6647), 180–183. https://doi.org/10.1038/38278

Collins, T. (2022a). Serial dependence occurs at the level of both features and integrated object representations. *Journal of Experimental Psychology: General*, *151*(8), 1821–1832. https://doi.org/10.1037/xge0001159

Collins, T. (2022b). Serial dependence tracks objects and scenes in parallel and independently. *Journal of Vision*, *22*(7), 4. https://doi.org/10.1167/jov.22.7.4

Comstock, D. C., Hove, M. J., & Balasubramaniam, R. (2018). Sensorimotor Synchronization With Auditory and Visual Modalities: Behavioral and Neural Differences. *Frontiers in Computational Neuroscience*, *12*. https://doi.org/10.3389/fncom.2018.00053

Cook, J. R., Baker, N. A., Cham, R., Hale, E., & Redfern, M. S. (2007). Measurements of Wrist and Finger Postures: A Comparison of Goniometric and Motion Capture Techniques. *Journal of Applied Biomechanics*, *23*(1), 70–78. https://doi.org/10.1123/jab.23.1.70

Corbett, J. E., Fischer, J., & Whitney, D. (2011). Facilitating Stable Representations: Serial Dependence in Vision. *PLOS ONE*, *6*(1), e16701. https://doi.org/10.1371/journal.pone.0016701

Coull, J. T., & Nobre, A. C. (1998). Where and When to Pay Attention: The Neural Systems for Directing Attention to Spatial Locations and to Time Intervals as Revealed by Both PET and fMRI. *Journal of Neuroscience*, *18*(18), 7426–7435. https://doi.org/10.1523/JNEUROSCI.18-18-07426.1998

Cuturi, L. F., & Gori, M. (2017). The Effect of Visual Experience on Perceived Haptic Verticality When Tilted in the Roll Plane. *Frontiers in Neuroscience*, *11*. https://doi.org/10.3389/fnins.2017.00687

Cuturi, L. F., & Gori, M. (2019). Biases in the Visual and Haptic Subjective Vertical Reveal the Role of Proprioceptive/Vestibular Priors in Child Development. *Frontiers in Neurology*, *9*. https://doi.org/10.3389/fneur.2018.01151

Czoschke, S., Fischer, C., Beitner, J., Kaiser, J., & Bledowski, C. (2019). Two types of serial dependence in visual working memory. *British Journal of Psychology*, *110*(2), 256–267. https://doi.org/10.1111/bjop.12349

Daneyko, O., Frisco, F., Maravita, A., & Zavagno, D. (2025). 'See what you feel': The impact of visual scale distance in haptic-to-visual crossmodal matching. *I-Perception*, *16*(1), 20416695251318591. https://doi.org/10.1177/20416695251318591

Deodato, M., & Melcher, D. (2024). Continuous temporal integration in the human visual system. *Journal of Vision*, *24*(13), 5. https://doi.org/10.1167/jov.24.13.5

Domenici, N., & Mamassian, P. (2025). *Confidence judgements from fused multisensory percepts* (p. 2025.09.05.674507). bioRxiv. https://doi.org/10.1101/2025.09.05.674507

Ernst, M. O., & Banks, M. S. (2002). Humans integrate visual and haptic information in a statistically optimal fashion. *Nature*, *415*(6870), 429–433. https://doi.org/10.1038/415429a

Eysenck, H. J. (1966). Adaptation-level theory: An experimental and systematic approach to behavior. *Behaviour Research and Therapy*, *4*(1–2), 69. https://doi.org/10.1016/0005-7967(66)90044-1

Faul, F., Erdfelder, E., Buchner, A., & Lang, A.-G. (2009). Statistical power analyses using G*Power 3.1: Tests for correlation and regression analyses. *Behavior Research Methods*, *41*(4), 1149–1160. https://doi.org/10.3758/BRM.41.4.1149

Fecteau, J. H., & Munoz, D. P. (2003). Exploring the consequences of the previous trial. *Nature Reviews Neuroscience*, *4*(6), 435–443. https://doi.org/10.1038/nrn1114

Feigin, H., Baror, S., Bar, M., & Zaidel, A. (2021). Perceptual decisions are biased toward relevant prior choices. *Scientific Reports*, *11*(1), 648. https://doi.org/10.1038/s41598-020-80128-0

Fischer, C., Czoschke, S., Peters, B., Rahm, B., Kaiser, J., & Bledowski, C. (2020). Context information supports serial dependence of multiple visual objects across memory episodes. *Nature Communications*, *11*(1), 1932. https://doi.org/10.1038/s41467-020-15874-w

Fischer, C., Kaiser, J., & Bledowski, C. (2022). Neural signatures of serial dependence emerge during cued selection in working memory. *Journal of Vision*, *22*(14), 3893–3893. https://doi.org/10.1167/jov.22.14.3893

Fischer, C., Kaiser, J., & Bledowski, C. (2025). A direct neural signature of serial dependence in working memory. *eLife*, *13*, RP99478. https://doi.org/10.7554/eLife.99478.3

Fischer, J., & Whitney, D. (2014). Serial dependence in visual perception. *Nature Neuroscience*, *17*(5), 738–743. https://doi.org/10.1038/nn.3689

Fitzgibbons, P. J. (1984). Temporal gap resolution in narrow-band noises with center frequencies from 6000–14000 Hz. *The Journal of the Acoustical Society of America*, *75*(2), 566–569. https://doi.org/10.1121/1.390529

Fornaciai, M., & Park, J. (2018a). Attractive Serial Dependence in the Absence of an Explicit Task. *Psychological Science*, *29*(3), 437–446. https://doi.org/10.1177/0956797617737385

Fornaciai, M., & Park, J. (2018b). Serial dependence in numerosity perception. *Journal of Vision*, *18*(9), 15. https://doi.org/10.1167/18.9.15

Fornaciai, M., & Park, J. (2019). Serial dependence generalizes across different stimulus formats, but not different sensory modalities. *Vision Research*, *160*, 108–115. https://doi.org/10.1016/j.visres.2019.04.011

Fornaciai, M., & Park, J. (2020). Neural Dynamics of Serial Dependence in Numerosity Perception. *Journal of Cognitive Neuroscience*, *32*(1), 141–154. https://doi.org/10.1162/jocn_a_01474

Fritsche, M., & de Lange, F. P. (2019). The role of feature-based attention in visual serial dependence. *Journal of Vision*, *19*(13), 21. https://doi.org/10.1167/19.13.21

Fritsche, M., Mostert, P., & de Lange, F. P. (2017). Opposite Effects of Recent History on Perception and Decision. *Current Biology: CB*, *27*(4), 590–595. https://doi.org/10.1016/j.cub.2017.01.006

Fritsche, M., Spaak, E., & de Lange, F. P. (2020). A Bayesian and efficient observer model explains concurrent attractive and repulsive history biases in visual perception. *eLife*, *9*, e55389. https://doi.org/10.7554/eLife.55389

Gallagher, G. K., & Benton, C. P. (2024). Characterizing serial dependence as an attraction to prior response. *Journal of Vision*, *24*(9), 16. https://doi.org/10.1167/jov.24.9.16

Gekas, N., McDermott, K. C., & Mamassian, P. (2019). Disambiguating serial effects of multiple timescales. *Journal of Vision*, *19*(6), 24. https://doi.org/10.1167/19.6.24

Gentaz, E., Baud-Bovy, G., & Luyat, M. (2008). The haptic perception of spatial orientations. *Experimental Brain Research*, *187*(3), 331–348. https://doi.org/10.1007/s00221-008-1382-0

Gibbon, J. (1977). Scalar expectancy theory and Weber's law in animal timing. *Psychological Review*, *84*(3), 279–325. https://doi.org/10.1037/0033-295X.84.3.279

Gibbon, J., Church, R. M., & Meck, W. H. (1984). Scalar Timing in Memory. *Annals of the New York Academy of Sciences*, *423*(1), 52–77. https://doi.org/10.1111/j.1749-6632.1984.tb23417.x

Gibson, J. J. (1937). Adaptation with negative after-effect. *Psychological Review*, *44*(3), 222–244. https://doi.org/10.1037/h0061358

Goldreich, D., & Kanics, I. M. (2003). Tactile Acuity is Enhanced in Blindness. *The Journal of Neuroscience*, *23*(8), 3439–3445. https://doi.org/10.1523/JNEUROSCI.23-08-03439.2003

Goldstone, S., & Lhamon, W. T. (1974). Studies of Auditory-Visual Differences in Human Time Judgment: 1. Sounds are Judged Longer than Lights. *Perceptual and Motor Skills*, *39*(1), 63–82. https://doi.org/10.2466/pms.1974.39.1.63

Gori, M., Crepaldi, M., Orciari, L., Campus, C., Merello, A., Dellepiane, D., & Parmiggiani, A. (2021). RoMAT: Robot for Multisensory Analysis and Testing of visual-tactile perceptual functions. *2021 43rd Annual International Conference of the IEEE Engineering in Medicine & Biology Society (EMBC)*, 4781–4786. https://doi.org/10.1109/EMBC46164.2021.9630479

Gori, M., Giuliana, L., Sandini, G., & Burr, D. (2012). Visual size perception and haptic calibration during development. *Developmental Science*, *15*(6), 854–862. https://doi.org/10.1111/j.1467-7687.2012.01183.x

Gori, M., Sandini, G., & Burr, D. (2012). Development of Visuo-Auditory Integration in Space and Time. *Frontiers in Integrative Neuroscience*, *6*. https://doi.org/10.3389/fnint.2012.00077

Gori, M., Sandini, G., Martinoli, C., & Burr, D. (2010). Poor Haptic Orientation Discrimination in Nonsighted Children May Reflect Disruption of Cross-Sensory Calibration. *Current Biology*, *20*(3), 223–225. https://doi.org/10.1016/j.cub.2009.11.069

Gori, M., Sandini, G., Martinoli, C., & Burr, D. C. (2014). Impairment of auditory spatial localization in congenitally blind human subjects. *Brain*, *137*(1), 288–293. https://doi.org/10.1093/brain/awt311

Grondin, S. (1993). Duration discrimination of empty and filled intervals marked by auditory and visual signals. *Perception & Psychophysics*, *54*(3), 383–394. https://doi.org/10.3758/BF03205274

Grondin, S., Meilleur-Wells, G., Ouellette, C., & Macar, F. (1998). Sensory effects on judgments of short time-intervals. *Psychological Research*, *61*(4), 261–268. https://doi.org/10.1007/s004260050030

Guan, S., & Goettker, A. (2024). Individual differences reveal similarities in serial dependence effects across perceptual tasks, but not to oculomotor tasks. *Journal of Vision*, *24*(12), 2. https://doi.org/10.1167/jov.24.12.2

Guinet, A. L., Bouyer, G., Otmane, S., & Desailly, E. (2019). Reliability of the head tracking measured by Microsoft Hololens during different walking conditions. *Computer Methods in Biomechanics and Biomedical Engineering*, *22*(sup1), S169–S171. https://doi.org/10.1080/10255842.2020.1714228

Hamon, P., Chablat, D., & Plestan, F. (2021, November 17). *A New Robotic Hand Based on the Design of Fingers With Spatial Motions*. ASME 2021 International Design Engineering Technical Conferences and Computers and Information in Engineering Conference. https://doi.org/10.1115/DETC2021-70233

Hashimoto, T., & Makioka, S. (2025a). Cross-modal serial dependence emerges in sequential numerosity comparison task. *Proceedings of the Annual Meeting of the Cognitive Science Society*, *47*(0). https://escholarship.org/uc/item/2235s4xm

Hashimoto, T., & Makioka, S. (2025b). *Serial dependence in numerosity perception generalizes across different sensory modalities: Evidence from sequential numerosity comparison* (7f5qu_v1). PsyArXiv. https://doi.org/10.31234/osf.io/7f5qu_v1

Heeley, D. W., Buchanan-Smith, H. M., Cromwell, J. A., & Wright, J. S. (1997). The oblique effect in orientation acuity. *Vision Research*, *37*(2), 235–242. https://doi.org/10.1016/S0042-6989(96)00097-1

Helbig, H. B., & Ernst, M. O. (2007). Optimal integration of shape information from vision and touch. *Experimental Brain Research*, *179*(4), 595–606. https://doi.org/10.1007/s00221-006-0814-y

Heller, M. A. (1983). Haptic dominance in form perception with blurred vision. *Perception*, *12*(5), 607–613. https://doi.org/10.1068/p120607

Helson, H. (1964). Current trends and issues in adaptation-level theory. *American Psychologist*, *19*(1), 26–38. https://doi.org/10.1037/h0040013

Heron, J., Aaen-Stockdale, C., Hotchkiss, J., Roach, N. W., McGraw, P. V., & Whitaker, D. (2012). Duration channels mediate human time perception. *Proceedings of the Royal Society B: Biological Sciences*, *279*(1729), 690–698. https://doi.org/10.1098/rspb.2011.1131

Hildebrandt, A., Grießbach, E., & Cañal-Bruland, R. (2022). Auditory perception dominates in motor rhythm reproduction. *Perception*, *51*(6), 403–416. https://doi.org/10.1177/03010066221093604

Himberger, K. D., Chien, H.-Y., & Honey, C. J. (2018). Principles of Temporal Processing Across the Cortical Hierarchy. *Neuroscience*, *389*, 161–174. https://doi.org/10.1016/j.neuroscience.2018.04.030

Ho, P. K., & Newell, F. N. (2020). Changes in perceptual category affects serial dependence in judgements of attractiveness. *Visual Cognition*, *28*(10), 557–580. https://doi.org/10.1080/13506285.2020.1841867

Hock, H. S., Kelso, J. S., & Schöner, G. (1993). Bistability and hysteresis in the organization of apparent motion patterns. *Journal of Experimental Psychology: Human Perception and Performance*, *19*(1), 63–80. https://doi.org/10.1037/0096-1523.19.1.63

Hollingworth, H. L. (1910). The Central Tendency of Judgment. *The Journal of Philosophy, Psychology and Scientific Methods*, *7*(17), 461–469. https://doi.org/10.2307/2012819

Hong, B., Chen, J., Huang, W., & Li, L. (2024). Serial Dependence in Smooth Pursuit Eye Movements of Preadolescent Children and Adults. *Investigative Ophthalmology & Visual Science*, *65*(14), 37. https://doi.org/10.1167/iovs.65.14.37

Hornsey, R. L., Hibbard, P. B., & Scarfe, P. (2020). Size and shape constancy in consumer virtual reality. *Behavior Research Methods*, *52*(4), 1587–1598. https://doi.org/10.3758/s13428-019-01336-9

Hübner, P., Clintworth, K., Liu, Q., Weinmann, M., & Wursthorn, S. (2020). Evaluation of HoloLens Tracking and Depth Sensing for Indoor Mapping Applications. *Sensors*, *20*(4), 1021. https://doi.org/10.3390/s20041021

Ivry, R. B., & Hazeltine, R. E. (1995). Perception and production of temporal intervals across a range of durations: Evidence for a common timing mechanism. *Journal of Experimental Psychology: Human Perception and Performance*, *21*(1), 3–18. https://doi.org/10.1037/0096-1523.21.1.3

James, G., Witten, D., Hastie, T., Tibshirani, R., & Taylor, J. (2023). *An Introduction to Statistical Learning: With Applications in Python*. Springer International Publishing. https://doi.org/10.1007/978-3-031-38747-0

Jasmin, K., Sun, H., & Tierney, A. T. (2021). Effects of language experience on domain-general perceptual strategies. *Cognition*, *206*, 104481. https://doi.org/10.1016/j.cognition.2020.104481

JASP Team. (2023). *JASP version 0.17.1.0* [Computer software]. https://jasp-stats.org/

Jazayeri, M., & Shadlen, M. N. (2010). Temporal context calibrates interval timing. *Nature Neuroscience*, *13*(8), 1020–1026. https://doi.org/10.1038/nn.2590

Jin, D. Z., Dragoi, V., Sur, M., & Seung, H. S. (2005). Tilt Aftereffect and Adaptation-Induced Changes in Orientation Tuning in Visual Cortex. *Journal of Neurophysiology*, *94*(6), 4038–4050. https://doi.org/10.1152/jn.00571.2004

John-Saaltink, E. S., Kok, P., Lau, H. C., & Lange, F. P. de. (2016). Serial Dependence in Perceptual Decisions Is Reflected in Activity Patterns in Primary Visual Cortex. *Journal of Neuroscience*, *36*(23), 6186–6192. https://doi.org/10.1523/JNEUROSCI.4390-15.2016

Jones, M. R., & Mcauley, J. D. (2005). Time judgments in global temporal contexts. *Perception & Psychophysics*, *67*(3), 398–417. https://doi.org/10.3758/BF03193320

Jones, P. R., & Dekker, T. M. (2018). The development of perceptual averaging: Learning what to do, not just how to do it. *Developmental Science*, *21*(3), e12584. https://doi.org/10.1111/desc.12584

Kahrimanovic, M., Bergmann Tiest, W. M., & Kappers, A. M. L. (2009). Context effects in haptic perception of roughness. *Experimental Brain Research*, *194*(2), 287–297. https://doi.org/10.1007/s00221-008-1697-x

Kaiser, D., Quek, G. L., Cichy, R. M., & Peelen, M. V. (2019). Object Vision in a Structured World. *Trends in Cognitive Sciences*, *23*(8), 672–685. https://doi.org/10.1016/j.tics.2019.04.013

Kappers, A. M. L., & Bergmann Tiest, W. M. (2013). Haptic perception. *WIREs Cognitive Science*, *4*(4), 357–374. https://doi.org/10.1002/wcs.1238

Kappers, A. M. L., & Bergmann Tiest, W. M. (2014). Influence of Shape on the Haptic Size Aftereffect. *PLoS ONE*, *9*(2), e88729. https://doi.org/10.1371/journal.pone.0088729

Karmarkar, U. R., & Buonomano, D. V. (2007). Timing in the Absence of Clocks: Encoding Time in Neural Network States. *Neuron*, *53*(3), 427–438. https://doi.org/10.1016/j.neuron.2007.01.006

Katzakis, N., Chen, L., & Steinicke, F. (2020). Visual-Haptic Size Estimation in Peripersonal Space. *Frontiers in Neurorobotics*, *14*. https://doi.org/10.3389/fnbot.2020.00018

Kessels, R. P. C., Van Den Berg, E., Ruis, C., & Brands, A. M. A. (2008). The Backward Span of the Corsi Block-Tapping Task and Its Association With the WAIS-III Digit Span. *Assessment*, *15*(4), 426–434. https://doi.org/10.1177/1073191108315611

Kim, S., Burr, D., & Alais, D. (2019). Attraction to the recent past in aesthetic judgments: A positive serial dependence for rating artwork. *Journal of Vision*, *19*(12), 19. https://doi.org/10.1167/19.12.19

Kohn, A. (2007). Visual adaptation: Physiology, mechanisms, and functional benefits. *Journal of Neurophysiology*, *97*(5), 3155–3164. https://doi.org/10.1152/jn.00086.2007

Lak, A., Hueske, E., Hirokawa, J., Masset, P., Ott, T., Urai, A. E., Donner, T. H., Carandini, M., Tonegawa, S., Uchida, N., & Kepecs, A. (2020). Reinforcement biases subsequent perceptual decisions when confidence is low, a widespread behavioral phenomenon. *eLife*, *9*, e49834. https://doi.org/10.7554/eLife.49834

Large, E. W., & Jones, M. R. (1999). The dynamics of attending: How people track time-varying events. *Psychological Review*, *106*(1), 119–159. https://doi.org/10.1037/0033-295X.106.1.119

Lau, W. K., & Maus, G. W. (2019). Visual serial dependence in an audiovisual stimulus. *Journal of Vision*, *19*(13), 20. https://doi.org/10.1167/19.13.20

Lederman, S. J., & Klatzky, R. L. (1987). Hand movements: A window into haptic object recognition. *Cognitive Psychology*, *19*(3), 342–368. https://doi.org/10.1016/0010-0285(87)90008-9

Lederman, S. J., & Klatzky, R. L. (2009). Haptic perception: A tutorial. *Attention, Perception, & Psychophysics*, *71*(7), 1439–1459. https://doi.org/10.3758/APP.71.7.1439

Lewis, T. L., & Maurer, D. (2005). Multiple sensitive periods in human visual development: Evidence from visually deprived children. *Developmental Psychobiology*, *46*(3), 163–183. https://doi.org/10.1002/dev.20055

Li, B., Wang, B., & Zaidel, A. (2023). Modality-specific sensory and decisional carryover effects in duration perception. *BMC Biology*, *21*(1), 48. https://doi.org/10.1186/s12915-023-01547-9

Li, B., Wang, B., & ZAIDEL, A. (2024). *Serial Dependence in Perception of Temporal Dynamics* (Pfgv5_v1). OSF Preprints. https://doi.org/10.31219/osf.io/pfgv5

Li, Y., Ding, X., Qian, J., Su, Z., & Ji, H. (2021). Serial dependence in biological motion perception. *Journal of Vision*, *21*(9), 2962–2962. https://doi.org/10.1167/jov.21.9.2962

Liberman, A., Kosovicheva, A., & Whitney, D. (2014). Serial Dependence of Position Perception. *Journal of Vision*, *14*(10), 1186–1186. https://doi.org/10.1167/14.10.1186

Lidström, A. (2023). Serial dependence in facial identity perception and visual working memory. *Attention, Perception, & Psychophysics*, *85*(7), 2226–2241. https://doi.org/10.3758/s13414-023-02799-x

Manassi, M., Kristjánsson, Á., & Whitney, D. (2019). Serial dependence in a simulated clinical visual search task. *Scientific Reports*, *9*(1), 19937. https://doi.org/10.1038/s41598-019-56315-z

Manassi, M., Liberman, A., Kosovicheva, A., Zhang, K., & Whitney, D. (2018). Serial dependence in position occurs at the time of perception. *Psychonomic Bulletin & Review*, *25*(6), 2245–2253. https://doi.org/10.3758/s13423-018-1454-5

Manassi, M., Marini, F., & Ramon, M. (2022). Serial dependence as a stable attribute in Super-Recognizers. *Journal of Vision*, *22*(14), 3881–3881. https://doi.org/10.1167/jov.22.14.3881

Manassi, M., Murai, Y., & Whitney, D. (2023). Serial dependence in visual perception: A meta-analysis and review. *Journal of Vision*, *23*(8), 18. https://doi.org/10.1167/jov.23.8.18

Manassi, M., & Whitney, D. (2022). Illusion of visual stability through active perceptual serial dependence. *Science Advances*, *8*(2), eabk2480. https://doi.org/10.1126/sciadv.abk2480

Marti, S., & Dehaene, S. (2017). Discrete and continuous mechanisms of temporal selection in rapid visual streams. *Nature Communications*, *8*(1), 1955. https://doi.org/10.1038/s41467-017-02079-x

Mascetti, S., Bernareggi, C., & Belotti, M. (2011). TypeInBraille: A braille-based typing application for touchscreen devices. *The Proceedings of the 13th International ACM SIGACCESS Conference on Computers and Accessibility, ASSETS '11*, 295–296. https://doi.org/10.1145/2049536.2049614

Mattheiss, E., Regal, G., Schrammel, J., Garschall, M., & Tscheligi, M. (2015). EdgeBraille: Braille-based text input for touch devices. *Journal of Assistive Technologies*, *9*(3), 147–158. https://doi.org/10.1108/JAT-10-2014-0028

McAuley, J. D., & Jones, M. R. (2003). Modeling Effects of Rhythmic Context on Perceived Duration: A Comparison of Interval and Entrainment Approaches to Short-Interval Timing. *Journal of Experimental Psychology: Human Perception and Performance*, *29*(6), 1102–1125. https://doi.org/10.1037/0096-1523.29.6.1102

Mei, G., Chen, S., & Dong, B. (2019). Working Memory Maintenance Modulates Serial Dependence Effects of Perceived Emotional Expression. *Frontiers in Psychology*, *10*. https://doi.org/10.3389/fpsyg.2019.01610

Merchant, H., Harrington, D. L., & Meck, W. H. (2013). Neural Basis of the Perception and Estimation of Time. *Annual Review of Neuroscience*, *36*(1), 313–336. https://doi.org/10.1146/annurev-neuro-062012-170349

Morimoto, Y., & Makioka, S. (2024). Response boosts serial dependence in the numerosity estimation task. *Scientific Reports*, *14*(1), 2059. https://doi.org/10.1038/s41598-024-52470-0

Motala, A., Zhang, H., & Alais, D. (2020). Auditory Rate Perception Displays a Positive Serial Dependence. *I-Perception*, *11*(6), 2041669520982311. https://doi.org/10.1177/2041669520982311

Mueller, S. T., & Piper, B. J. (2014). The Psychology Experiment Building Language (PEBL) and PEBL Test Battery. *Journal of Neuroscience Methods*, *222*, 250–259. https://doi.org/10.1016/j.jneumeth.2013.10.024

Murai, Y., & Whitney, D. (2021). Spatial and feature tuning of serial dependence in audiovisual timing perception. *Journal of Vision*, *21*(9), 2233–2233. https://doi.org/10.1167/jov.21.9.2233

Näätänen, R., Syssoeva, O., & Takegata, R. (2004). Automatic time perception in the human brain for intervals ranging from milliseconds to seconds. *Psychophysiology*, *41*(4), 660–663. https://doi.org/10.1111/j.1469-8986.2004.00182.x

Neto, R. M. de A., & Bartels, A. (2021). Disrupting Short-Term Memory Maintenance in Premotor Cortex Affects Serial Dependence in Visuomotor Integration. *Journal of Neuroscience*, *41*(45), 9392–9402. https://doi.org/10.1523/JNEUROSCI.0380-21.2021

Newlin, R. J., Rodgers, J. P., Dickson, J. F., Strub, H., & Thomas, D. R. (1978). The central tendency effect in stimulus generalization: Effects of establishing a "preexperimental" frame of reference. *Perception & Psychophysics*, *24*(2), 161–167. https://doi.org/10.3758/BF03199543

Owens, D. M., & Lumpkin, E. A. (2014). Diversification and Specialization of Touch Receptors in Skin. *Cold Spring Harbor Perspectives in Medicine*, *4*(6), a013656. https://doi.org/10.1101/cshperspect.a013656

Pascual-Leone, A., Amedi, A., Fregni, F., & Merabet, L. B. (2005). THE PLASTIC HUMAN BRAIN CORTEX. *Annual Review of Neuroscience*, *28*(Volume 28, 2005), 377–401. https://doi.org/10.1146/annurev.neuro.27.070203.144216

Pascucci, D., Mancuso, G., Santandrea, E., Della Libera, C., Plomp, G., & Chelazzi, L. (2019). Laws of concatenated perception: Vision goes for novelty, decisions for perseverance. *PLOS Biology*, *17*(3), e3000144. https://doi.org/10.1371/journal.pbio.3000144

Pascucci, D., & Plomp, G. (2021). Serial dependence and representational momentum in single-trial perceptual decisions. *Scientific Reports*, *11*(1), 9910. https://doi.org/10.1038/s41598-021-89432-9

Pascucci, D., Tanrikulu, Ö. D., Ozkirli, A., Houborg, C., Ceylan, G., Zerr, P., Rafiei, M., & Kristjánsson, Á. (2023). Serial dependence in visual perception: A review. *Journal of Vision*, *23*(1), 9. https://doi.org/10.1167/jov.23.1.9

Pashler, H. (2001). Perception and production of brief durations: Beat-based versus interval-based timing. *Journal of Experimental Psychology: Human Perception and Performance*, *27*(2), 485–493. https://doi.org/10.1037/0096-1523.27.2.485

Postma, A., Zuidhoek, S., Noordzij, M. L., & Kappers, A. M. L. (2008). Haptic orientation perception benefits from visual experience: Evidence from early-blind, late-blind, and sighted people. *Perception & Psychophysics*, *70*(7), 1197–1206. https://doi.org/10.3758/PP.70.7.1197

Power, R. P. (1980). The dominance of touch by vision: Sometimes incomplete. *Perception*, *9*(4), 457–466. https://doi.org/10.1068/p090457

Purkinje, J. (1820). *Beitage zur Naheren Kenntnis des Schwindels nach heautognostischen Daten*. Med. Jahrbücher. Wien.

Quinton, G., & Fellows, B. J. (1975). 'Perceptual' Strategies in the Solving of Three-Term Series Problems. *British Journal of Psychology*, *66*(1), 69–78. https://doi.org/10.1111/j.2044-8295.1975.tb01441.x

R Core Team. (2021). *R: A Language and Environment for Statistical Computing* [Computer software]. R Foundation for Statistical Computing. https://www.R-project.org/

Rafiei, M., Hansmann-Roth, S., Whitney, D., Kristjánsson, Á., & Chetverikov, A. (2021). Optimizing perception: Attended and ignored stimuli create opposing perceptual biases. *Attention, Perception, & Psychophysics*, *83*(3), 1230–1239. https://doi.org/10.3758/s13414-020-02030-1

Rammsayer, T. H., Borter, N., & Troche, S. J. (2015). Visual-auditory differences in duration discrimination of intervals in the subsecond and second range. *Frontiers in Psychology*, *6*. https://doi.org/10.3389/fpsyg.2015.01626

Recanzone, G. H. (2003). Auditory Influences on Visual Temporal Rate Perception. *Journal of Neurophysiology*, *89*(2), 1078–1093. https://doi.org/10.1152/jn.00706.2002

Roseboom, W. (2019). Serial dependence in timing perception. *Journal of Experimental Psychology. Human Perception and Performance*, *45*(1), 100–110. https://doi.org/10.1037/xhp0000591

Ryan, C. P., Bettelani, G. C., Ciotti, S., Parise, C., Moscatelli, A., & Bianchi, M. (2021). The interaction between motion and texture in the sense of touch. *Journal of Neurophysiology*, *126*(4), 1375–1390. https://doi.org/10.1152/jn.00583.2020

Rzepka, A. M., Hussey, K. J., Maltz, M. V., Babin, K., Wilcox, L. M., & Culham, J. C. (2022). Familiar size affects perception differently in virtual reality and the real world.

Philosophical Transactions of the Royal Society B: Biological Sciences, *378*(1869), 20210464. https://doi.org/10.1098/rstb.2021.0464

Sacharin, V., Sander, D., & Scherer, K. R. (2012). The perception of changing emotion expressions. *Cognition and Emotion*, *26*(7), 1273–1300. https://doi.org/10.1080/02699931.2012.656583

Sadato, N., Okada, T., Honda, M., & Yonekura, Y. (2002). Critical period for cross-modal plasticity in blind humans: A functional MRI study. *NeuroImage*, *16*(2), 389–400. https://doi.org/10.1006/nimg.2002.1111

Sadato, N., Pascual-Leone, A., Grafman, J., Deiber, M. P., Ibañez, V., & Hallett, M. (1998). Neural networks for Braille reading by the blind. *Brain*, *121*(7), 1213–1229. https://doi.org/10.1093/brain/121.7.1213

Sadato, N., Pascual-Leone, A., Grafman, J., Ibañez, V., Deiber, M.-P., Dold, G., & Hallett, M. (1996). Activation of the primary visual cortex by Braille reading in blind subjects. *Nature*, *380*(6574), 526–528. https://doi.org/10.1038/380526a0

Sadil, P., Cowell, R. A., & Huber, D. E. (2024). The push–pull of serial dependence effects: Attraction to the prior response and repulsion from the prior stimulus. *Psychonomic Bulletin & Review*, *31*(1), 259–273. https://doi.org/10.3758/s13423-023-02320-3

Saluja, S., Croy, I., & Stevenson, R. J. (2024). The Functions of Human Touch: An Integrative Review. *Journal of Nonverbal Behavior*, *48*(3), 387–417. https://doi.org/10.1007/s10919-024-00464-x

Schneider, D., Biener, V., Otte, A., Gesslein, T., Gagel, P., Campos, C., Pucihar, K. Č., Kljun, M., Ofek, E., Pahud, M., Kristensson, P. O., & Grubert, J. (2021). *Accuracy Evaluation of Touch Tasks in Commodity Virtual and Augmented Reality Head-Mounted Displays* (arXiv:2109.10607). arXiv. https://doi.org/10.48550/arXiv.2109.10607

Schwiedrzik, C. M., Ruff, C. C., Lazar, A., Leitner, F. C., Singer, W., & Melloni, L. (2014). Untangling Perceptual Memory: Hysteresis and Adaptation Map into Separate Cortical Networks. *Cerebral Cortex*, *24*(5), 1152–1164. https://doi.org/10.1093/cercor/bhs396

Sheehan, T. C., & Serences, J. T. (2022). Attractive serial dependence overcomes repulsive neuronal adaptation. *PLOS Biology*, *20*(9), e3001711. https://doi.org/10.1371/journal.pbio.3001711

Smeragliuolo, A. H., Hill, N. J., Disla, L., & Putrino, D. (2016). Validation of the Leap Motion Controller using markered motion capture technology. *Journal of Biomechanics*, *49*(9), 1742–1750. https://doi.org/10.1016/j.jbiomech.2016.04.006

Soares, I., B. Sousa, R., Petry, M., & Moreira, A. P. (2021). Accuracy and Repeatability Tests on HoloLens 2 and HTC Vive. *Multimodal Technologies and Interaction*, *5*(8), 47. https://doi.org/10.3390/mti5080047

Stevens, J. C., Foulke, E., & Patterson, M. Q. (1996). Tactile acuity, aging, and braille reading in long-term blindness. *Journal of Experimental Psychology: Applied*, *2*(2), 91–106. https://doi.org/10.1037/1076-898X.2.2.91

The MathWorks Inc. (2022). *MATLAB version: 9.13.0 (R2022b)* [Computer software]. https://www.mathworks.com

Thibault, N., Albouy, P., & Grondin, S. (2023). Distinct brain dynamics and networks for processing short and long auditory time intervals. *Scientific Reports*, *13*(1), 22018. https://doi.org/10.1038/s41598-023-49562-8

Thomas, B. H. (2020). Examining User Perception of the Size of Multiple Objects in Virtual Reality. *Applied Sciences*, *10*(11), 4049. https://doi.org/10.3390/app10114049

Thomas, D. R., Strub, H., & Dickson, J. F. (1974). Adaptation level and the central tendency effect in stimulus generalization. *Journal of Experimental Psychology*, *103*(3), 466–474. https://doi.org/10.1037/h0037184

Tivadar, R. I., Chappaz, C., Anaflous, F., Roche, J., & Murray, M. M. (2020). Mental Rotation of Digitally-Rendered Haptic Objects by the Visually-Impaired. *Frontiers in Neuroscience*, *14*. https://doi.org/10.3389/fnins.2020.00197

Tivadar, R. I., Rouillard, T., Chappaz, C., Knebel, J.-F., Turoman, N., Anaflous, F., Roche, J., Matusz, P. J., & Murray, M. M. (2019). Mental Rotation of Digitally-Rendered Haptic Objects. *Frontiers in Integrative Neuroscience*, *13*. https://doi.org/10.3389/fnint.2019.00007

Togoli, I., Fedele, M., Fornaciai, M., & Bueti, D. (2021). Serial dependence in time and numerosity perception is dimension-specific. *Journal of Vision*, *21*(5), 6. https://doi.org/10.1167/jov.21.5.6

Trapp, S., Pascucci, D., & Chelazzi, L. (2021). Predictive brain: Addressing the level of representation by reviewing perceptual hysteresis. *Cortex*, *141*, 535–540. https://doi.org/10.1016/j.cortex.2021.04.011

Turbett, K., Palermo, R., Bell, J., Burton, J., & Jeffery, L. (2019). Individual Differences in Serial Dependence of Facial Identity are Associated with Face Recognition Abilities. *Scientific Reports*, *9*(1), 18020. https://doi.org/10.1038/s41598-019-53282-3

Turbett, K., Palermo, R., Bell, J., Hanran-Smith, D. A., & Jeffery, L. (2021). Serial dependence of facial identity reflects high-level face coding. *Vision Research*, *182*, 9–19. https://doi.org/10.1016/j.visres.2021.01.004

Van der Burg, E., Alais, D., & Cass, J. (2015). Audiovisual temporal recalibration occurs independently at two different time scales. *Scientific Reports*, *5*(1), 14526. https://doi.org/10.1038/srep14526

Van der Burg, E., Baart, M., Vroomen, J., Zhang, H., & Alais, D. (2024). Opposing serial dependencies revealed for sequences of auditory emotional stimuli. *Perception*, *53*(5–6), 317–334. https://doi.org/10.1177/03010066241235562

Van der Burg, E., Rhodes, G., & Alais, D. (2019). Positive sequential dependency for face attractiveness perception. *Journal of Vision*, *19*(12), 6. https://doi.org/10.1167/19.12.6

Vassallo, R., Rankin, A., Chen, E. C. S., & Peters, T. M. (2017). Hologram stability evaluation for Microsoft HoloLens. *Medical Imaging 2017: Image Perception, Observer Performance, and Technology Assessment*, *10136*, 295–300. https://doi.org/10.1117/12.2255831

Wanet-Defalque, M.-C., Veraart, C., De Volder, A., Metz, R., Michel, C., Dooms, G., & Goffinet, A. (1988). High metabolic activity in the visual cortex of early blind human subjects. *Brain Research*, *446*(2), 369–373. https://doi.org/10.1016/0006-8993(88)90896-7

Wang, G., & Alais, D. (2025a). *Characteristics of Tactile Orientation Perception: Oblique Effect, Active vs Passive Exploration, and Serial Dependence* (p. 2025.03.19.644099). bioRxiv. https://doi.org/10.1101/2025.03.19.644099

Wang, G., & Alais, D. (2025b). *Tactile and Visual Spatial Frequency Perception Follows Optimal Integration but Is Not Affected by Spatial Proximity* (p. 2025.05.27.656312). bioRxiv. https://doi.org/10.1101/2025.05.27.656312

Wang, L., Cai, S., & Sandor, C. (2023). Perceptual thresholds of visual size discrimination in augmented and virtual reality. *Computers & Graphics*, *117*, 105–113. https://doi.org/10.1016/j.cag.2023.10.001

Wang, T., Luo, Y., Ivry, R. B., Tsay, J. S., Pöppel, E., & Bao, Y. (2023). A unitary mechanism underlies adaptation to both local and global environmental statistics in time perception. *PLOS Computational Biology*, *19*(5), e1011116. https://doi.org/10.1371/journal.pcbi.1011116

Watson, W. A. (1957). Contrast, Assimilation, and the Effect of Central Tendency. *The American Journal of Psychology*, *70*(4), 560–568. https://doi.org/10.2307/1419446

Wearden, J. H., & Jones, L. A. (2021). Judgements of the Duration of Auditory and Visual Stimuli. *Timing & Time Perception*, *9*(2), 199–224. https://doi.org/10.1163/22134468-bja10008

Wearden, J. H., Norton, R., Martin, S., & Montford-Bebb, O. (2007). Internal clock processes and the filled-duration illusion. *Journal of Experimental Psychology: Human Perception and Performance*, *33*(3), 716–729. https://doi.org/10.1037/0096-1523.33.3.716

Wiener, M., Thompson, J. C., & Coslett, H. B. (2014). Continuous Carryover of Temporal Context Dissociates Response Bias from Perceptual Influence for Duration. *PLoS ONE*, *9*(6), e100803. https://doi.org/10.1371/journal.pone.0100803

Xia, Y., Leib, A. Y., & Whitney, D. (2016). Serial dependence in the perception of attractiveness. *Journal of Vision*, *16*(15), 28. https://doi.org/10.1167/16.15.28

Yang, Y., Fermüller, C., Li, Y., & Aloimonos, Y. (2015). Grasp type revisited: A modern perspective on a classical feature for vision. *2015 IEEE Conference on Computer Vision and Pattern Recognition (CVPR)*, 400–408. https://doi.org/10.1109/CVPR.2015.7298637

You, F.-H., Gong, X.-M., & Sun, Q. (2023). Serial dependencies between form orientation and motion direction are asymmetric. *Frontiers in Psychology*, *14*. https://doi.org/10.3389/fpsyg.2023.1248307

Yu, J.-M., Yang, W., & Ying, H. (2023). Modeling facial perception in group context from a serial perception perspective. *Journal of Vision*, *23*(3), 4. https://doi.org/10.1167/jov.23.3.4

Zhang, H., & Alais, D. (2020). Individual difference in serial dependence results from opposite influences of perceptual choices and motor responses. *Journal of Vision*, *20*(8), 2. https://doi.org/10.1167/jov.20.8.2

Zhang, H., & Luo, H. (2023). Feature-specific reactivations of past information shift current neural encoding thereby mediating serial bias behaviors. *PLOS Biology*, *21*(3), e3002056. https://doi.org/10.1371/journal.pbio.3002056